NASA Contractor Report 185601

National Aeronautics and Space Administration (NASA)/American Society for Engineering Education (ASEE) Summer Faculty Fellowship Program–1989

Volume 1

William B. Jones, Jr., Editor
Texas A&M University
College Station, Texas

Stanley H. Goldstein, Editor
University Programs Office
Lyndon B. Johnson Space Center
Houston, Texas

Grant NGT 44-001-800
December 1989

PREFACE

The 1989 Johnson Space Center (JSC) National Aeronautics and Space Administration (NASA)/ American Society for Engineering Education (ASEE) Summer Faculty Fellowship Program was conducted by Texas A&M University and JSC. The 10-week program was operated under the auspices of the ASEE. The program at JSC, as well as the programs at other NASA Centers, was funded by the Office of University Affairs, NASA Headquarters, Washington, D.C. The objectives of the program, which began nationally in 1964 and at JSC in 1965, are

1. To further the professional knowledge of qualified engineering and science faculty members
2. To stimulate an exchange of ideas between participants and NASA
3. To enrich and refresh the research and teaching activities of participants' institutions
4. To contribute to the research objective of the NASA Centers

Each faculty fellow spent at least 10 weeks at JSC engaged in a research project commensurate with his/her interests and background and worked in collaboration with a NASA /JSC colleague. This document is a compilation of the final reports on the research projects performed by the faculty fellows during the summer of 1989. Volume 1 contains reports 1 through 11, and Volume 2 contains reports 12 through 26.

CONTENTS

Volume 1

Volume 2

TEMPERATURE DETERMINATION OF SHOCK LAYER USING SPECTROSCOPIC TECHNIQUES

Final Report

NASA/ASEE Summer Faculty Fellowship Program -- 1989

Johnson Space Center

Prepared BY:	Murty A. Akundi, Ph.D.
Academic Rank:	Associate Professor
University & Department:	Xavier University Physics/Engineering Department New Orleans, Louisiana 71245
NASA/JSC	
Directorate:	Engineering
Division:	Structure and Mechanics Division
Branch:	Thermal
JSC Colleague:	John E. Grimaud
Date Submitted:	August 11, 1989
Contract Number:	NGT 44-001-800

ABSTRACT

Shock layer temperature profiles are obtained through analysis of radiation from shock layers produced by a blunt body inserted in an arc jet flow. Spectral measurements of N_2^+ have been made at 0.5", 1.0" and 1.4" from the blunt body. A technique is developed to measure the vibrational and rotational temperatures of N_2^+. Temperature profiles from the radiation layers show a high temperature near the shock front and decreasing temperature near the boundary layer. Precise temperature measurements could not be made using this technique due to the limited resolution. Use of a high resolution grating will help to make a more accurate temperature determination. Laser induced fluorescence technique is much better since it gives the scope for selective excitation and a better spacial resolution.

INTRODUCTION

Temperature determination of the shock layer during the space vehicle reentry conditions is of utmost importance for thermal protection system (TPS). The identification, characterization and temperature determination of different atomic,molecular and ionic species in the shock layer and boundary layers form the basis of the plasma diagnostics program in the atmospheric reentry materials and structures evaluation facility (ARMSEF). Vibrational and rotational temperature determinations were made for N_2 and N_2^+ by Blackwell et. al. (1). Their technique involves calculating the spectrum for a number of cases and obtain integrals over the wavelength regions of the spectrum as functions of temperature. Ratios of these integrals were then related to the temperatures used to generate the spectra. Spectral integrals from measured spectra were then compared with the calculated values to determine the temperature. This technique has some limitations and needs lot of parameters to produce the calculated spectra. In this report I will present a simple technique to find the vibrational and rotational temperatures of molecules in the shock layer which inturn can be related to the temperature of the shock layer.

MEASUREMENTS

Facility:

A lay out of the experimental set up is shown in fig. 1. Mixture of N_2 and O_2 are heated in an arc powered by a variable direct current power supply. The hot discharge products (Plasma) are then expanded through a conical nozzle which gives hypersonic speeds to the plasma. A shock layer is formed when a thermal protection system (TPS), for example a tile, is introduced in this flow. One of the major criteria at the NASA/JSC arc jet facility is to understand the heat transfer process to TPS. Rotational temperature determination of molecular species is one of the major parameters , since this temperature is close to the shock layer temperature. This is achieved by spectroscopic techniques which are non intrusive in nature.

Spectral system:

Light emitted from the shock layer of a blunt body is focused on to an entrance slit of 0.6m SPEX triplemate spectrometer having 1024 linear diode array detector. A 600 lines/mm and 1800 lines/mm gratings were used, yielding a pixel resolution of 0.069nm and 0.023nm respectively.

The spectral data were recorded using an optical multichannel analyzer (OMA) system, on which the wavelength and intensity calibrations are performed and integrations may be made.

N_2^+ spectra between 340 nm and 480 nm at 0.5" from the blunt body using 600 lines/mm grating is shown in fig. 2. This low resolution spectra was used to find the vibrational temperature. Rotation structure of 0-1 band taken on 1800 lines/mm grating at various distances from the blunt body are used for rotational temperature determinations.

RESULTS AND ANALYSIS

Vibrational temperature of a given vibrational state can be obtained theoretically (2) using

$$\ln [I^{v',v''} / \upsilon^4] = c_1 - G'(v') \, hc/kT \qquad (1)$$

where

c_1 = a constant

$G'(v') = w_e'(v'+ .5) - w_e'x_e'(v'+.5)^2$
w_e' and $w_e'x_e'$ values are taken from Huber and Herzberg (3)

h = Planck's constant

c = Speed of light

k = Boltzmann's constant

T = the temperature to be determined.

By plotting a graph of logarithm of the intensities of the progressions against the vibrational term (G(v)), a straight line is obtained. The slope of the line gives hc/kT from which the vibrational temperature of a given electronic state can be determined. This method is used for the spectra taken at 0.5" from the blunt body and is shown in fig.2. The areas under the curves of 0-1, 1-1, 2-1, and 3-1 bands of the N_2^+ were used for vibrational temperature determinations. The graph along with the calculated temperature is shown in fig.3. The temperature determined using this technique is close to the one determined earlier by Blackwell et.al(1) at this distance. Vibrational temperature determinations using other progressions could not be made as sufficient data is not available. This procedure seems to be simple and

comparable to the methods used by earlier workers (1).

During my stay here, more empahasis is given for rotational temperature determinations of N_2^+. The necessary equations for determining the rotational line intensities are shown in Appendix 1. When a graph is plotted using equation (4) between ln [I/(k'+k"+1)] against k'(k'+1), a straight line is obtained. The slope of the line gives B_0hc/kT from which the rotational temperature can be determined.

The rotational structure of the 0-1 band of N_2^+ is shown in fig.4. Due to the limited resolution the spectrum is not well resolved and we could not resolve P and R branches. AS a first order approximation, we tried to treat the observed peak intensity as purely due to the P branch only and rotational temperature determinations are made as per equation (4) shown in Appendix 1. Similarly considering the observed intensity as purely due to the R branch, rotational temperature is determined. As shown in fig.5. the temperatures obtained are not the same and not close to the rotational temperatures determined by earlier methods(4). this is expected because the experimental spectra contains the intensity contributions of both P and R branches. One therefore can not use equation (4) for cases where the spectra are not well resolved.

We have developed a method to determine the rotational temperatures in cases where the P and R branches are not well resolved. The necessary equations have been derived and shown in Appendix 2. Using equations (7) and (8) the observed intensity is corrected for P and R branches at various temperatures(T). Graphs are now plotted; $\ln[I_{Pc}/(K'+K"+1)]$ against $K'(K'+1)$ for P- branch and $\ln[I_{Rc}/(K'+K"+1)$ against $K'(K'+1)$ for R-branch. The temperatures (T_P and T_R) are now calculated using the slopes of the straight lines obtained from the graphs for both P and R branches. The particular set for which the temperature $T_P = T_R = T$ is considered as the temperature of the shock layer.

Using this method, spectra taken at 0.5", 1.0" and 1.4" from the blunt body on October '88 are analyzed for rotational temperature determination. Figs. 6 and 7 show the graphs plotted for the corrected P and R branches at various temperatures for the spectra taken at 0.5" from the body. Temperatures are calculated using the slopes of the lines and are tabulated in Table 1. The best agreement is obtained at 5000 K as can be seen from the % errors shown in Table 1. Fig. 8 is a graph showing the agreement between P and R branches. Similar calculations are carried out for spectra

taken at 1.0" and 1.4" and the corresponding temperatures are found to be 6000 K and 5000 K respectively.

CONCLUSIONS

We have developed a procedure to calculate the vibrational and rotational temperatures of simple molecules. These methods have been tested to determine the shock layer temperatures of N_2^+ and it could be extended to other molecular species present in the shock layer. We encountered some problems of convergence when the rotational temperature procedure was tested on a different data set. This therefore needs further testing with bigger data base. The accuracy of rotational temperature determination could be improved further if the P and R branches could be resolved.

Recommendations: In order to obtain a more accurate temperature determination and to resolve P and R branches the following Suggestions are made.

1. A bigger spectrometer of at least one meter in length with 1800 lines/mm will be able to resolve the spectra.

2. A photodiode array with five times the present photodiode density will basically also resolve the spectra.

3. Laser Induced fluorescence on the other hand will provide selective excitation, spatial as well as high resolution. Therefore this seems to be the ideal approach for the present problem.

ACKNOWLEDGMENTS

I wish to take this opportunity to thank NASA/ASEE summer faculty fellowship program for giving me an opportunity to work at NASA, Johnson Space center. My sincere thanks are to John Grimaud, my NASA colleague, for providing the facilities and for his complete cooperation. My special thanks are to Dr. Sivaram Arepalli of Lockheed with out whose help I might not have been able to complete this work. Last but not the least, I wish to thank all NASA and the Lockheed personnel of the arc jet facility who made my stay here very pleasant and rewarding.

REFERENCES

1. Blackwell, H.E., Wierum, F.A., Arepalli, S.and Scott, C.d., " vibrational measurements of N_2 and N_2^+ shock layer radiation." 27th Aerospace Sciences Meeting, AIAA-89-0248, (1989).

2. Herzberg, G., " Molecular Spectra and Molecular structure, Vol. 1 Spectra of Diatomic Molecules", D. Van Nostrand Co., Inc., New York, N.Y. (1950).

3. Huber, K.P., and Herzberg, G.," Molecular spectra and Molecular structure Vol. IV, Constants of Diatomic Molecules.", D. Van Nostrand Co., Inc., New York, N.Y (1979).

4. Blackwell, H.E., Yuen E., Arepalli, S., and Scott, C.D., " Nonequilibrium shock layer temperature profiles from arc jet radiation measurements." 24th Thermophysics conference, AIAA-89-1679, (1989).

EXPERIMENTAL ARRANGEMENT

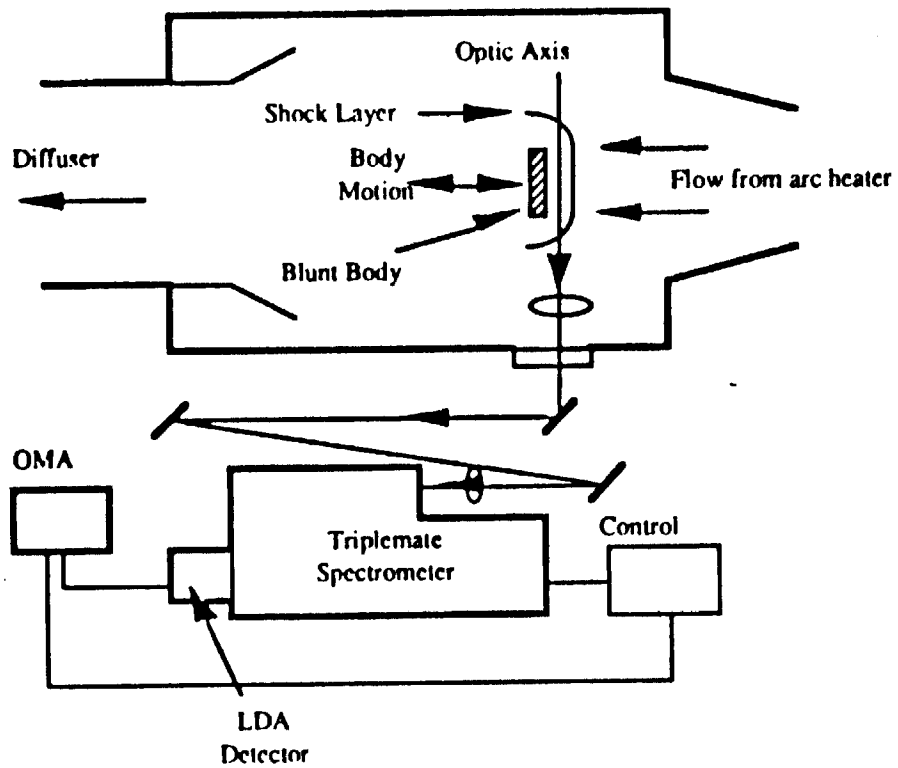

Fig. 1

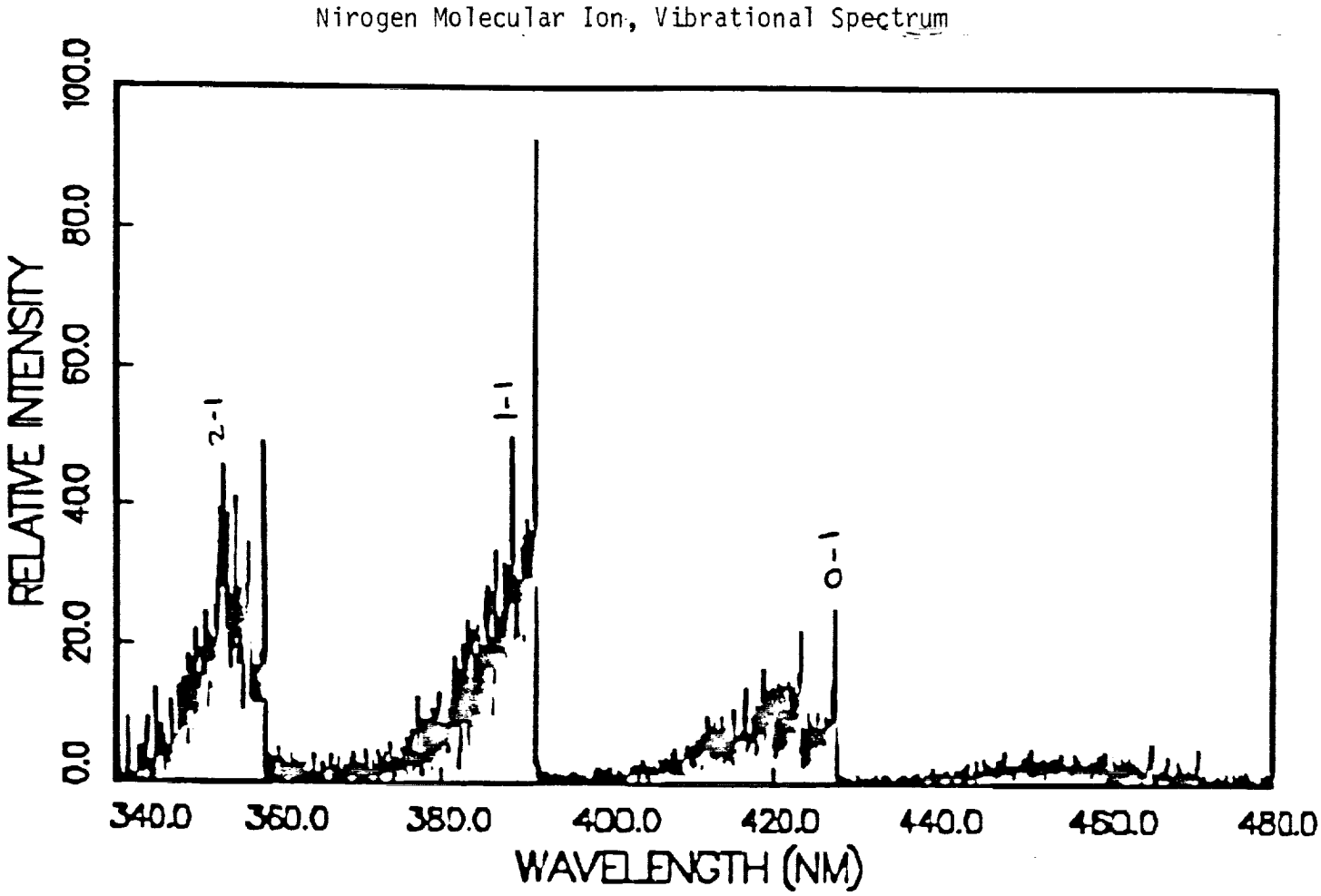
Nirogen Molecular Ion, Vibrational Spectrum
RELATIVE INTENSITY
0.0
20.0
40.0
60.0
80.0
100.0
2-1
1-1
0-1
340.0
360.0
380.0
400.0
420.0
440.0
460.0
480.0
WAVELENGTH (NM)

Fig. 2.

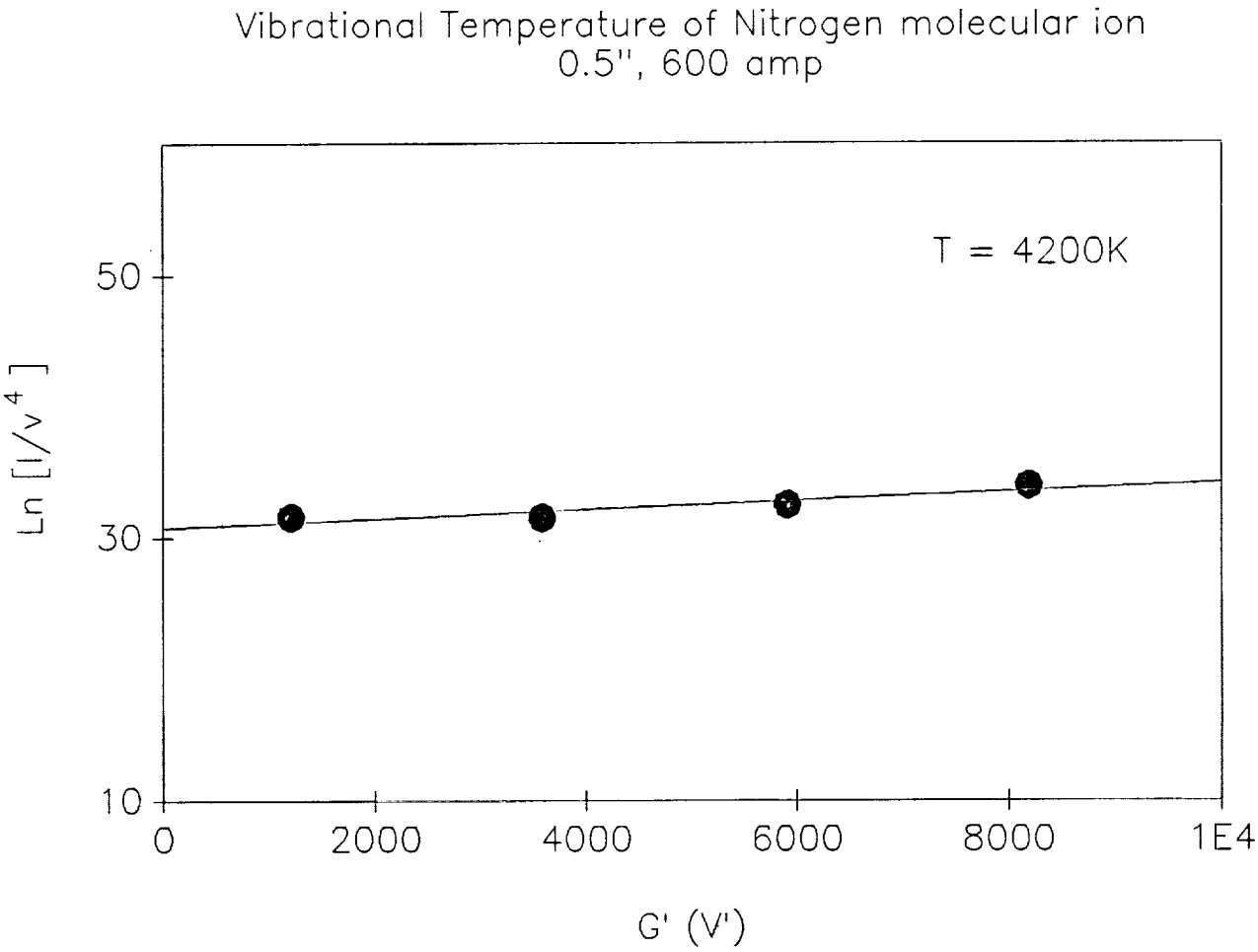
Vibrational Temperature of Nitrogen molecular ion
0.5", 600 amp
T = 4200K
50
30
10
Ln [I/v^4]
0
2000
4000
6000
8000
1E4
G' (V')

Fig. 3

Nitrogen Molecular Ion (0,1) band, Rotational structure

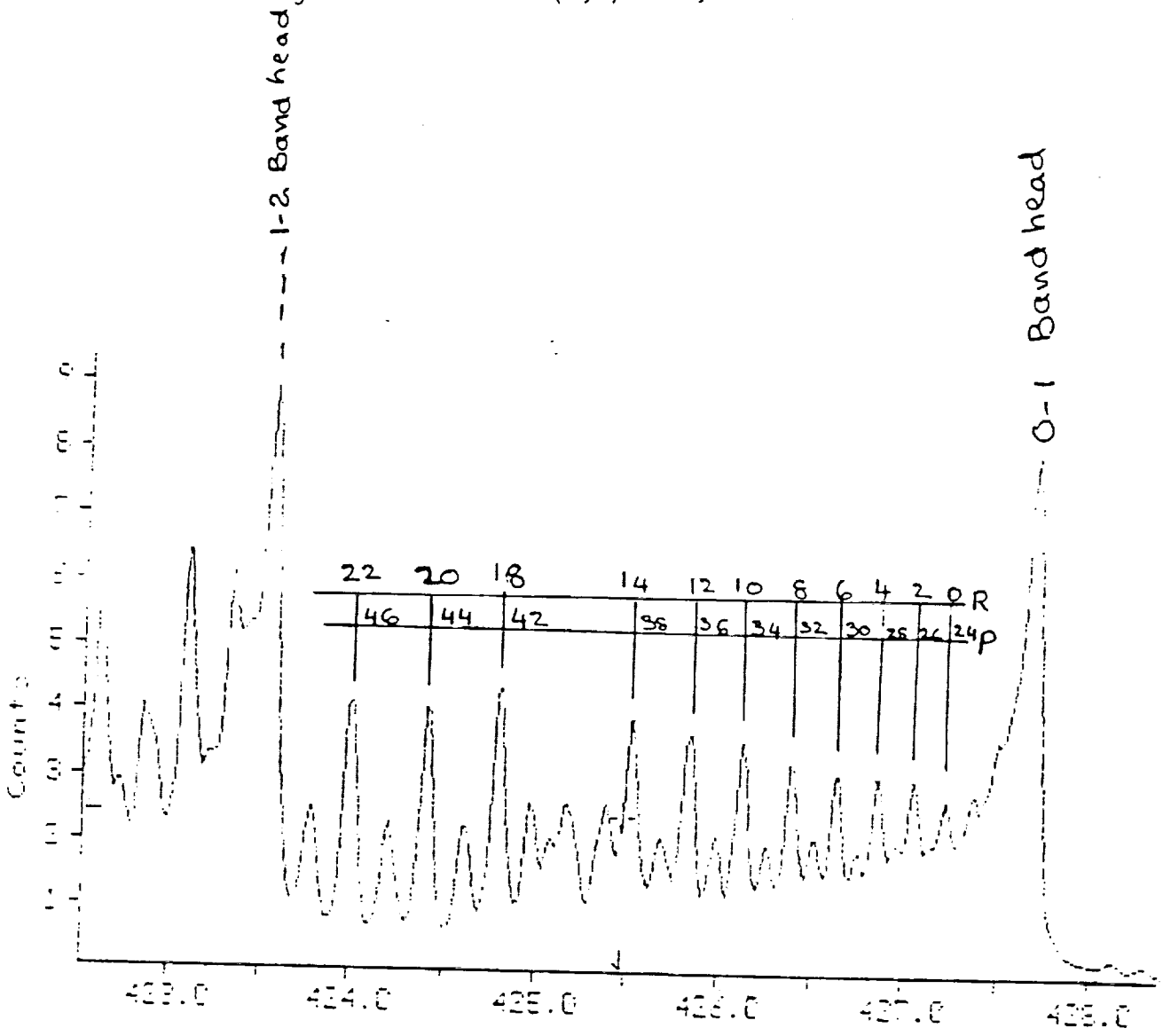

Fig. 4.

Nitrogen Molecular Ion (0,1) band, 0.5", 800amp

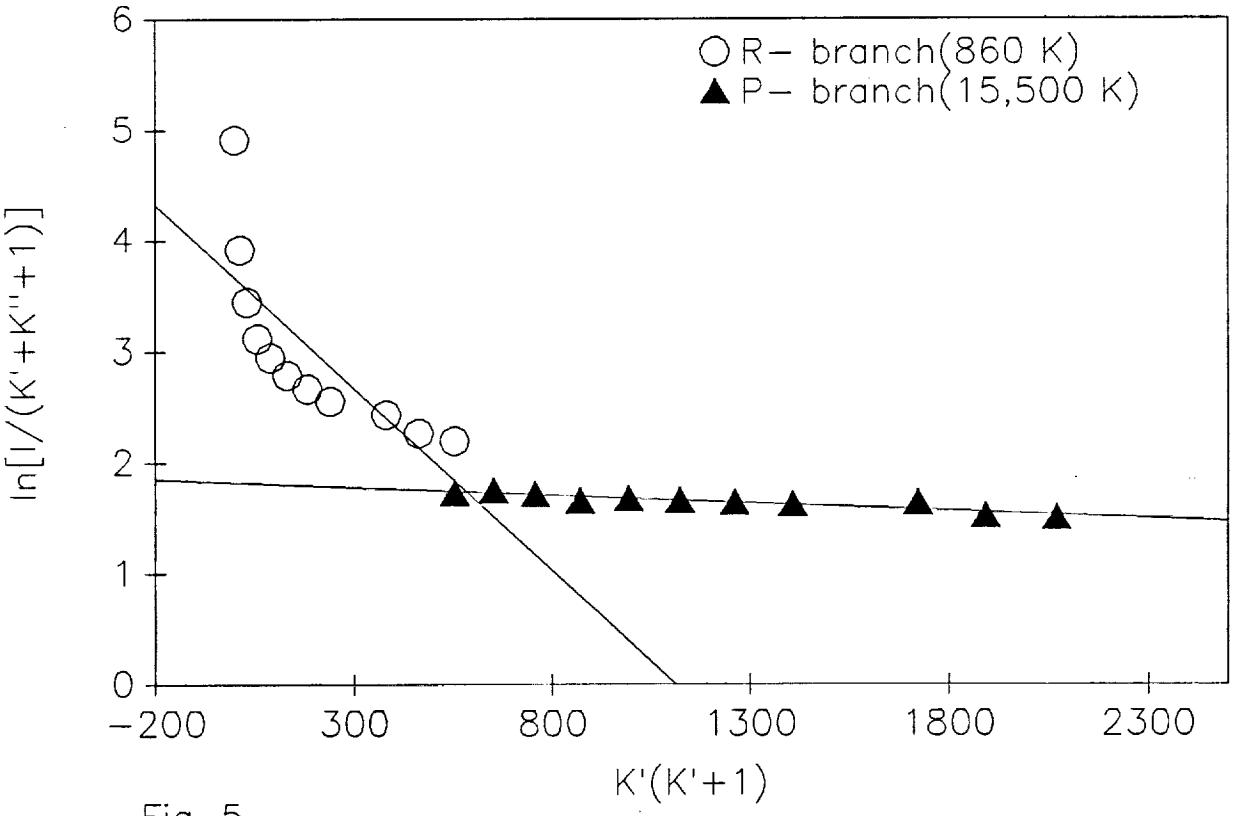

Fig. 5.

10/24/88

Nitrogen Molecular Ion (0,1) band, 0.5", 800 amp
P−branch

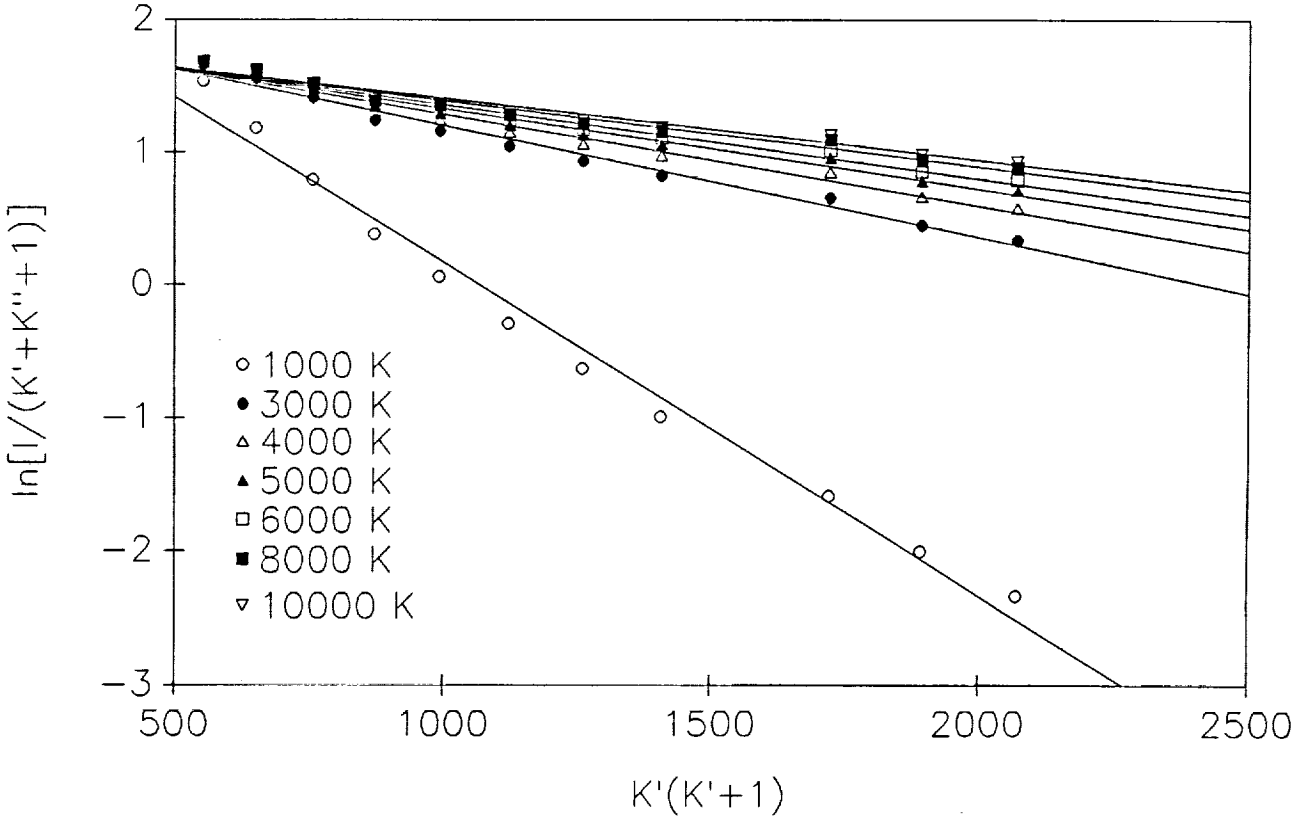

Fig. 6

10/24/88

Nitrogen Molecular Ion (0,1) band, 0.5",800 amp
R–branch

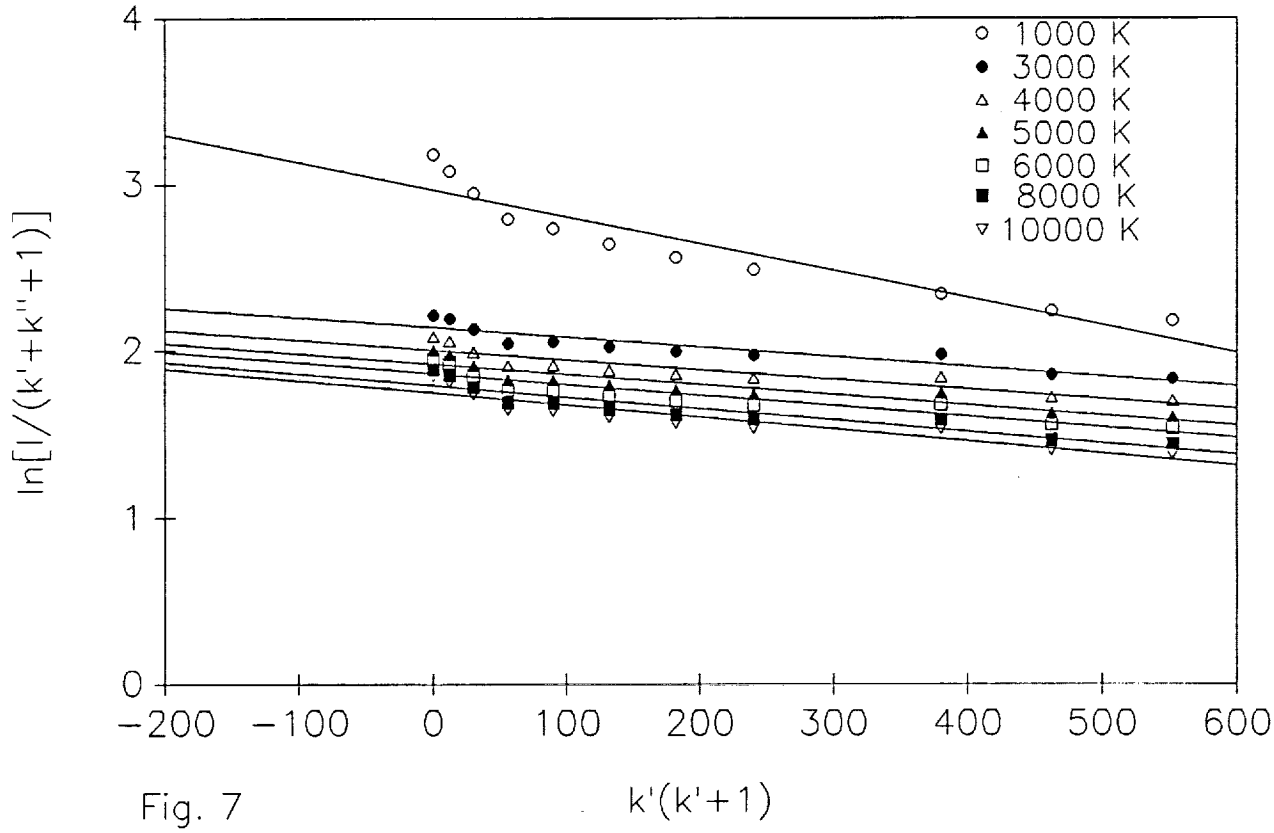

Fig. 7

10/24/88

Nitrogen Molecular Ion (0,1) band; 0.5", 800 amp

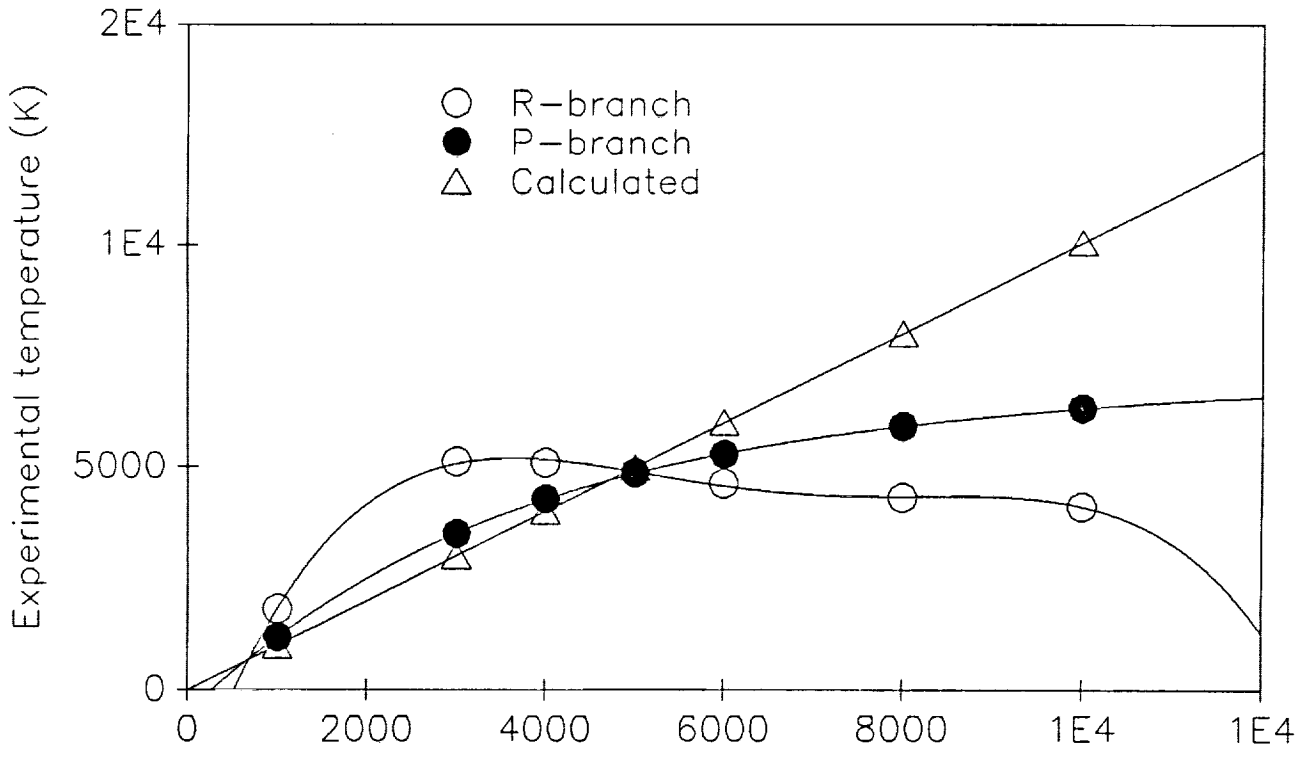

Fig. 8

TABLE I

NITROGEN MOLECULAR ION
(0,1) BAND, 0.5", 800 AMP

Temperature (K) Actual	Temperature (K) R-Branch	% Error	Temperature (K) P-Branch	% Error
1,000	1,820	82	1,188	19
3,000	5,124	71	3,497	17
4,000	5,091	27	4,276	7
5,000	**4,874**	**2.5**	**4,860**	**2.8**
6,000	4,629	22	5,288	12
8,000	4,304	46	5,912	26
10,000	4,104	59	6,307	37

APPENDIX - 1

ROTATIONAL TEMPERATURE EQUATIONS

$$I(P - Branch) = A - 2Je^{-\frac{B_0 J(J-1)hc}{kT}} \quad (1)$$

$$I(R - branch) = A - 2(J+1)e^{-\frac{B_0 (J+1)(J+2)hc}{kT}} \quad (2)$$

Rearranging equations (1) and (2)

$$\ln\left[\frac{I_p}{2J}\right] = \ln A - \frac{B'_0 J(J-1)hc}{kT}$$

$$\ln\left[\frac{I_p}{2J}\right] = A' - \frac{B'_0 J(J-1)hc}{kT} \quad (3)$$

Similarly for R Branch

$$\ln\left[\frac{I_R}{2(J+1)}\right] = A' - \frac{B'_0 (J+1)(J+2)hc}{kT} \quad (4)$$

Equation (3) and (4) can general be written for either case as

$$\ln\left[\frac{I}{k' + k'' + 1}\right] = A - \frac{B' K'(k'+1)hc}{kT}$$

where k' - upper rotational state quantum number
k'' - lower rotational state quantum number

CORRECTED INTENSITIES

$$I_{EXP} = I_P + I_R \tag{5}$$

$$\frac{I_{EXP}}{I_R} = \frac{I_P}{I_R} + 1 \tag{6}$$

Let $\frac{I_P}{I_R} = B$ where I_P and I_R are the intensities calculated for any temperature using equations (1) and (2)

$$I_{Rc} = I_{EXP}\left[\frac{1}{1+B}\right] \tag{7}$$

$$I_{Pc} = I_{EXP}\left[\frac{1}{1+\frac{1}{B}}\right] \tag{8}$$

I_{Rc} and I_{Pc} are the intensity contributions of P and R branches in the observed spectra

N90-24974

A BAYESIAN APPROACH TO RELIABILITY AND CONFIDENCE

Final Report

NASA/ASEE Summer Faculty Fellowship Program 1989

Johnson Space Center

Prepared By:	Ron Barnes, Ph.D.
Academic Rank:	Associate Professor
University & Department:	University of Houston-Downtown Department of Applied Mathematical Sciences One Main Street Houston, Texas 77002
NASA/JSC Directorate:	Safety, Reliability, and Quality Assurance
Division:	Reliability and Maintainability
JSC Colleague:	Richard Heydorn
Date Submitted:	August 4, 1989
Contract Number:	NGT 44-001-800

ABSTRACT

In response to the Challenger accident, NASA has expanded its risk assessment studies from a completely qualitative Failure Modes and Effects Analysis/Critical Items Lists (FMEA/CIL) to include some quantitative investigations like Probability Risk Assessment (PRA).

Dr. Richard Heydorn (Reliability) presented lectures on quantitative methods to the Vehicle Reliability Branch at the request of branch chief, Malcolm Himel. As an outgrowth, the Extended Duration Orbiter - Weakest Link study is being developed. Three avionics subsystems and one with mechanical components, the freon coolant loop, have been identified as posing potential problems to keeping the Orbiter in space for long periods of time. The intent of the study is to devise a standard methodology for constructing system reliability diagrams and identifying what data is needed and/or potentially available. The data will then be utilized in Bayesian probability models to estimate reliabilities and consequently identify any significant problem subsystems.

Classical statistical methods are not suitable for many NASA problems. At NASA, data records are often sparse, incomplete or in a form not amenable to classical confidence estimates. Also, since problem-identification-problem-correction is employed throughout the operating lifetime of many NASA systems, the usefulness of failure history data is greatly compromised. Bayesian analysis addresses such concerns since it allows for the insertion of informed opinions instead of/or in addition to observational data on failures.

Our summer work generalized some of Dr. Heydorn's results for systems with a constant failure rate (exponential model) that is generally applicable to avionic systems, to the case of a variable failure rate (Weibull model) which contains the exponential as a special case. The Weibull model applies to reliability systems with burn in and/or wear out stages including most mechanical systems.

In the exponential case a closed form was obtained for the Bayesian estimate of the reliability function of a single component. The reliability of a system can then be evaluated using the rules of probability. With these estimators it is also possible to calculate the probability that the true reliability of a component lies within a certain interval and estimate the probability that the reliability of a system lies in a certain interval.

Using Bayesian ideas it now becomes possible to handle situations which the classical analysis could not, namely: (1) how to handle problems where no failure data has been observed over a period of time and (2) how to incorporate expert opinions into the probability calculations along with the data on failures.

In the more general Weibull (variable failure rate) model we have obtained a Bayesian estimator for the reliability which reduces to a closed form for special cases. In these cases the rest of the Bayesian analysis can be pursued.

Further investigations will consider the numerical evaluation of the Weibull Bayesian estimator for reliability in the general case. Bayesian estimates for the reliability of single components and systems, and probability statements similar to those described for the exponential model may then be pursued. The results can then be applied to the freon coolant subsystem of the Extended Duration Orbiter - Weakest Link study.

INTRODUCTION

In response to the Challenger accident and subsequent reports by governmental commissions [NRC, House Report] , NASA has expanded its risk assessment studies from a completely qualitative Failure Modes and Effects Analysis/Critical Items List (FMEA/CIL) to some quantitative investigations including Probability Risk Assessment (PRA).

FMEA/CIL is basically a bottom-up approach. Individual components of a system are analyzed. Their individual failure modes are determined and the effects of each type of failure are investigated. On the basis of this analysis, various critical categories are assigned to each failure mode of each component. One shortcoming of the FMEA/CIL approach is that it does not assign priorities. As Charles Harlan, director of the Safety, Reliability, and Quality Assurance Directorate at NASA/JSC has noted, "There are many criticality 1 items in a system like the Shuttle, or in your car for that matter, . . .How do you distinguish the very unlikely failure you can live with from the likely ones you have to fix?" He further stated that "Our present system doesn't assess priorities, and we're going to modify that. We need a relative ranking of the risk associated with each failure mode."[SPECTRUM]

Probability Risk Assessment addresses this shortcoming. In contradistinction to FMEA/CIL, PRA is a top-down method in which possible failure modes of the entire system are first identified. The possible ways this could occur are enumerated and for each fault, chains of faults are traced out until eventually one arrives at the failure of a single component or a human error. A downward branching fault tree is constructed in which probabilities are assigned to the basic faults and then the total probability of various failure paths can be computed. In this way their relative contributions to the total risk are assessed.

NASA's historical preference for a qualitative approach to reliability and shunning of quantitative procedures is documented in the June 1989 special issue on risk analysis in SPECTRUM. As noted by the SPECTRUM editors:

> During the Apollo days NASA contracted with General Electric to do a PRA to determine the chances of landing a man on the moon and safely returning him to earth. When the study indicated the probability of success was less than five percent, NASA decided the study would do "irreparable harm..." and they "studiously stayed away from [numerical risk assessment] as a result.

Will Willoughby, NASA head of Reliability and Safety at the time, added:

> "That's when we threw all that garbage out and got down to work... Statistics don't count for anything . They have no place in engineering anywhere."[SPECTRUM]

As a result, NASA adapted qualitative failure modes and effects analysis (FMEA).

The SPECTRUM article further pointed out that in the 1970's and early 1980's, because of political realities it became necessary for NASA to show that the Shuttle would be "cheap and routine, rather than expensive and risky." Such pressures led to examples where data was disregarded and arbitrary assignments of risk levels were made.

The deliberate decision by NASA to forgo quantitative (probabilistic) risk analyses determined the type of data NASA decided to collect. For example no elapsed times were originally recorded for components on the shuttle. The failure to record various kinds of data, which was recoverable, precluded many forms of statistical analyses from even being considered.

After the Challenger accident the National Research Council (NRC) and the House of Representative committee on Science and Technology issued reports, in addition to the Presidential Commission [Roger's Report]. The Congressional report noted that:

> Without some means of estimating the probability of failure of the various elements, it is not clear how NASA can focus its attention and resources as effectively as possible on the most critical systems.

In a similar vein the NRC noted:

> The Committee views the NASA/CIL waiver decision making process as being subjective with little in the way of formal and consistent criteria for approval or rejection of waivers. Waiver decisions appear to be driven almost exclusively by the design based FMEA/CIL retention rationale rather than being based on an integrated assessment of all inputs to risk management.

In response to the Challenger accident and these reports, NASA is now changing in favor of a "willingness to explore other things" [SPECTRUM]. NASA has contracted two PRA pilot projects and has developed workshops to train engineers and others in quantitative risk assessment techniques.

One Approach

In this spirit, Dr. Richard Heydorn presented lectures on quantitative methods to the Vehicle Reliability Branch at the request of branch chief, Malcolm Himel. As an outgrowth, the Extended Duration Orbiter - Weakest Link study is being developed. Three avionics subsystems and one with mechanical components, the freon coolant loop, have been identified as posing potential problems to keeping the Orbiter in space for long periods of time. The intent of the study is to devise a standard methodology for constructing

system reliability diagrams and identifying what data is needed and/or potentially available. The data will then be utilized in Bayesian probability models to estimate reliabilities and consequently identify any significant problem subsystems.

Classical statistical methods are not suitable for many NASA problems. At NASA, data records are often sparse, incomplete or in a form not amenable to classical confidence estimates. Also, since problem-identification-problem-correction is employed throughout the operating lifetime of many NASA systems, the usefulness of failure history data is greatly compromised. Bayesian analysis addresses such concerns since it allows for the insertion of informed opinions instead of/or in addition to observational data on failures.

PRELIMINARY WORK ON A BAYESIAN APPROACH TO RELIABILITY AND CONFIDENCE

Prior to my arrival to take part in the NASA Summer Faculty Fellow program, Dr. Heydorn had begun Bayesian investigations into reliability by modeling the reliability of a single component (e.g. valve, piston, computer chip, etc...)assuming a constant rate of failure. The reliability of a system of components can then be modeled using the laws of probability.

The Bayesian approach was selected because of the shortcomings of classical statistical analysis with NASA data as pointed out earlier. In particular, in cases with very few data values on failures, classical confidence intervals for the reliability may be larger than the unit interval [0,1] and hence quite meaningless. Similarly since classical estimates of reliability depend on the failure history sample, an extreme but not uncommon situation in which no failures are recorded can lead one to blindly believe that we can conclude a high confidence in high reliability. The Bayesian approach appears to be much more fruitful in that it can address such data difficulties.

In the case where the failure rate λ is constant, under the fairly general assumptions that (a) the number of failures in any two disjoint time intervals are independent and (b) the distribution of the number of failures in any time interval depends only on the interval length, it follows that for $t>0$, $N(t)$ the number of failures from time 0 to t is a random variable defined on a probability space Ω_λ. $N(\omega,t)$ has a Poisson probability distribution with

$$Pr(N(t) = n) = ((\lambda t)^n/n!)e^{-\lambda t} \qquad (1)$$

For this process let $x(\omega,t) = 1$ if $N(\omega,t) = 0$ and let $x(\omega,t) = 0$ if $N(\omega,t)>0$. The reliability function is then defined as:

$$R(t) = Pr(x(t) = 1) = P(N(t) = 0) = e^{-\lambda t} \qquad (2)$$

Note that the reliability is just the probability that the component is still operating after time t (i.e. it has not failed on the interval (0,t]).Note that in this case the reliability function is exponential.

Assuming that a component was observed (or tested) over a period of time length T and was seen to have failed n times, a logical question to ask is

> "What is the probability that after some additional time interval of length t, the component will not have failed again?"

Since we know the component starts in an operating state and since the events $\{x(t) = 1\}$ and $\{N(t) = n\}$ occur in disjoint time intervals, the Poisson assumption (a) shows that

$$Pr[x(t) = 1 \mid N(T) = n] = Pr[x(t) = 1], \tag{3}$$

i.e. the failure history has no direct bearing on the reliability when we assume the component starts in an operating state.

Heydorn has pointed out the inadequacies of classical statistical analysis, as noted earlier in this paper. He has shown that the Bayesian estimator of the reliability, given that n failures were recorded in an earlier time interval of length T, and assuming a uniform prior distribution of λ on $(0,\ell]$ and then letting $\ell \to \infty$, is given by:

$$E(R_\Lambda(t) \mid N(T) = n) = P(x(t) = 1 \mid N(T) = n) = 1/(1 + t/T)^{n+1} \tag{4}$$

The expression

$$E(R_\Lambda(t) \mid N(T) = n) = 1/(1 + t/T)^{n+1} \tag{5}$$

is the key to his discussion and allows him to make probability statements about the reliability of the component. Heydorn also has shown that the Bayesian estimator for the reliability given by expression (4) is a consistent estimator for the true reliability R(t). Exploiting (5) Heydorn has obtained expressions for the probability that the reliability of a component (and of a system of components) lies in specified intervals of values between 0 and 1. He notes that this formulation addresses some of the data problems with classical statistical analysis. For example if no failures were recorded in time T (not an uncommon occurrence when testing highly reliable components) expression (5) gives

$$E(R_\Lambda(t) \mid N(T) = 0) = 1/(1 + t/T) \tag{6}$$

and Heydorn is able to exploit this expression , while in the classical case no such expression is possible! Heydorn also indicates how the Bayesian approach can be used to incorporate expert opinion into the probabilistic process even when no historical data may be available. Essentially the uniform prior on $(0,\infty)$ is in some sense the "least informative" prior since it assumes that every positive value of λ is equally likely of being the "true"

value of the constant rate λ. Given additional expert opinion, it is often possible to incorporate that opinion into the choice of an alternate prior distribution for λ. Heydorn illustrates this with an example and shows how a system containing a mixture of components, some with failure data and others will only expert opinions on the failure mechanisms, can be probabilistically analyzed.

DISCUSSION

For these summer investigations, the first objective was to extend the results to the more general case where the failure rate (hazard function) is non-constant. A good model for a non-constant hazard function is the Weibull distribution, $W(\lambda,\beta)$, which can model both "break in" and "wear out" failure conditions in a system and contains the constant failure rate model as a special case. The discussion that follows considers the following formulation of the Weibull distribution.

$$f(t,\lambda,\beta) = \lambda \beta t^{\beta-1} e^{-\lambda t^{\beta}}$$

$$R(t,\lambda,\beta) = e^{-\lambda t^{\beta}} \qquad \lambda,\beta,t > 0$$

$$h(t,\lambda,\beta) = \lambda\beta t^{\beta-1} \tag{7}$$

Note that in the special case when $\beta = 1$ the hazard function reduces to the constant λ and the reliability function is the exponential function, i.e. one has the constant failure rate model considered earlier.

In Weibull reliability analysis it is often the case that the value of the shape parameter β is known. In fact the literature sharply divides into the case where β is known and only the scale parameter λ is unknown and the more general case where both parameters are unknown. In the case where β is known considerable analysis has occurred [Martz].

If one assumes a non-constant intensity function $h(t,\lambda,\beta) = \lambda \beta t^{\beta-1}$, it is easy to show under assumptions similar to (a) and (b) given earlier that the probability of n failures occurring by time T is given by

$$P[N(T) = n] = (e^{-\lambda T^{\beta}} (\lambda T^{\beta})^{n})/n! \tag{8}$$

This is usually referred to as the nonhomogeneous Poisson process.

SPECIAL CASE

Now for the Weibull model with β known, the Bayesian estimate for the reliability can be calculated (assuming λ has a uniform prior and the limiting process is carried out as before) and one sees that

$$E(R_{\lambda}(t) \mid N(T)=n) = P[x(t) = 1 \mid N(T)=n] = 1/(1 + (t/T)^{\beta})^{n+1} \tag{9}$$

In this special case the Bayesian estimate is seen to be a consistent estimator of the reliability function (7). With expression (8) one is able to make probability statements about the reliability of a component (and system) as Heydorn did for the exponential case for situations that classical reliability theory can not address. The inclusion of expert opinion into the process can also proceed as was indicated earlier.

GENERAL CASE

In the more general case where both β and λ are unknown, we assume they are unknown values of random variables that must be estimated. We assume prior uniform distribution on $(0,\ell_\lambda]$ and $(0,\ell_\beta]$ and eventually take the limiting values so that λ and β may take on any nonnegative values. In a sense, these are the least informative priors since they assume that every possible value for λ (and β) is equally likely of occurring i.e. we have no additional information on the true values of λ and β.

Preliminary investigations indicated that N(T), the number of failures recorded in time T, is not sufficient to ensure that the corresponding Bayesian estimate of reliability is a consistent estimator of the true reliability.

It is well known [Bain, Finklestein, et al.] that if $T_1,\ldots,T_n$ denote the first n successive times of failure of a Weibull process ($T_1 \leq T_2 \ldots \leq T_n$) then the likelihood function is given by:

$$f(t_1,\ldots t_n,\lambda,\beta) = \lambda^n\beta^n \left(\prod t_i\right)^{\beta-1} e^{-\lambda(t_n)^\beta} \qquad (10)$$

The Bayesian Estimator of reliability is this case (for uniform priors on $(0,\ell_\lambda]$ $(0,\ell_\beta]$ and taking limits) reduces to:

$$E[R_\lambda(t) \mid T_1 = t_1,\ldots T_n=t_n] = P[x(t) = 1 \mid T_1 = t_1,\ldots T_n=t_n]$$
$$= \frac{[\ln[t_n\Pi(t_n/t_i)]]^{n+1}}{n!} \quad \text{limit}_{\ell\to\infty} \int_0^\ell \frac{\beta^n e^{-\beta \ln[t_n \Pi (t_n/t_i)]}\, d\beta}{[1 + (t/t_n)^\beta]^{n+1}} \qquad (11)$$

While expression (11) does not have a closed form in general, a few observations are in order:

(a) The form of (11) indicates that t_n and $\prod t_i$ together carry all the information necessary to obtain the Bayesian estimate of reliability. We note that in the classical analysis t_n and $\prod t_i$ are joint sufficient statistics [Bain].

(b) The Bayesian estimate (11) is a consistent estimator for R(t), the true reliability. In fact, we conjecture that an even more general result holds.

Namely, under some rather general conditions we believe it is possible to show that for any estimator Θ of θ,

$$E[\Theta \mid x_1 \ldots x_n] \to \theta \ (\text{as } n \to \infty) \qquad (12)$$

(c) In the special case that $t = t_n$, i.e. one wants to estimate the reliability after time t in the future that is equal to the total elapsed time for the first n past failures, expression (11) reduces to

$$E[R_\lambda(t) \mid T_1 = t_1 \ldots\ldots T_n = t_n] = (1/2)^{n+1} \qquad (13)$$

With this closed form one can again make probability statements about the reliability of a component, conditioned on the failure times $t_1 \ldots t_n$. In particular the probability that this system has not failed after t units of time given that it failed n times over a period of time t in the past is $(1/2)^{n+1}$. For example if one had data on 1 failure after 10,000 hours of operation then the probability that the component (starting from an operating state) will not fail during the next 10,000 hours is $(1/2)^2 = 1/4 = .25$. Expression (13) suggests that if no failures were encountered in t units of time then the probability that there will be no failures in a future time interval of t units (starting from an operating state) would be $1/2 = .50$. In some sense there is a 50/50 chance of the component failing in the next t units of time if it has not failed in a prior t units of time.

Again with expression (13), using the laws of probability it is possible to obtain expressions for the probability that the reliability of a component (or a system of components) lies in a specified range of values between 0 and 1.

CONCLUSION

This report outlined the historical evolution of NASA's interest is quantitative measures of reliability assessment. The introduction of some quantitative methodologies into the Vehicle Reliability Branch of the SR&QA Division at JSC was noted along with the development of the Extended Orbiter Duration - Weakest Link study which will utilize quantitative tools for a Bayesian statistical analysis.

Extending the earlier work of my NASA sponsor, Richard Heydorn, we have been able to produce a consistent Bayesian estimate for the reliability of a component and hence by a simple extension for a system of components in some cases where the rate of failure is not constant but varies over time. Mechanical systems in general have this property since the reliability usually decreases markedly as the parts degrade over time. While we have been able to reduce the Bayesian estimator to a simple closed form for a large class of such systems, the form for the most general case needs to be attacked by the computer. Once a table is generated for this form, we will have a numerical form for the general solution. With this, the corresponding probability statements about the reliability of a system can be made in the most general setting. Note that the utilization of uniform Bayesian priors represent a "worst case" scenario in the sense that as we incorporate more expert opinion into the model we will be able to improve the strength of the probability calculations.

REFERENCES

1. National Research Council, Aeronautics and Space Engineering Board, Committee on Shuttle Criticality Review and Hazard Analysis audit, "Post-Challenger Evaluation of Space Shuttle Risk Assessment and Management," January 1988.

2. Committee on Science and Technology, U.S. House of Representatives, "Investigation of the Challenger Accident", Ninety - Ninth Congress, October 29, 1986.

3. Bell,Trudy E. and Karl Esch, "Special Report: the Space Shuttle: A Case of Subjective Engineering,' IEEE SPECTRUM,42-46, June 1989.

4. Presidential Commission on the Space Shuttle Challenger Accident, "Report to the President", June 6, 1986.

5. Heydorn, Richard, unpublished lecture notes on quantitative methods for reliability, NASA/JSC, Reliability and Maintainability Division, Spring 1989.

6. Martz, Harry F. and Ray A.Waller, Bayesian Reliability Analyses, John Wiley and Sons, New York, 1982.

7. Bain, Lee J. Statistical Analysis of Reliability and Life-Testing Models, Marcel Dekker Inc., New York , 1978.

8. Finkelstein, J. M., "Confidence Bands on the Parameters of the Weibull Process, ' Technometrics, Vol. 18, No. 1, 115-117, February 1976.

APPENDIX

$$E[R_\lambda(t) \mid T_1 = t_1, \ldots T_n = t_n] = P[x(t) = 1 \mid T_1 = t_1 \ldots T_n = t_n]$$

$$= \lim_{\substack{\ell_\beta \to \infty \\ \ell_\lambda \to \infty}} \frac{\frac{1}{\ell_\beta}\frac{1}{\ell_\lambda}\int_0^{\ell_\beta}\int_0^{\ell_\lambda} \beta^n \lambda^n \left(\prod t_i\right)^{\beta-1} e^{-\lambda(t_n)^\beta} e^{-\lambda t^\beta}\, d\lambda\, d\beta}{\frac{1}{\ell_\beta}\frac{1}{\ell_\lambda}\int_0^{\ell_\beta}\int_0^{\ell_\lambda} \beta^n \lambda^n \left(\prod t_i\right)^{\beta-1} e^{-\lambda(t_n)^\beta}\, d\lambda\, d\beta}$$

EFFECT OF LOW AIR VELOCITIES ON THERMAL HOMEOSTASIS AND COMFORT DURING EXERCISE AT SPACE STATION OPERATIONAL TEMPERATURE AND HUMIDITY

Final Report

NASA/ASEE Summer Faculty Fellowship Program--1989

Johnson Space Center

Prepared By:	Ronald J. Beumer, Ph.D.
Academic Rank:	Associate Professor
University & Department:	Armstrong State College Department of Biology Savannah, Georgia 31419
NASA/JSC	
Directorate:	Space and Life Sciences
Division:	Medical Sciences
Branch:	Space Biomedical Research Institute
JSC Colleague:	James M. Waligora
Date Submitted:	August 14, 1989
Contract Number:	NGT44-001-800

ABSTRACT

This study investigated the effectiveness of different low air velocities in maintaining thermal comfort and homeostasis during exercise at space station operational temperature and humidity. Five male subjects exercised on a treadmill for successive ten minute periods at 60, 71 and 83% of maximum oxygen consumption at each of four air velocities, 30, 50, 80 and 120 ft/min, at 22°C and 62% relative humidity. No consistent trends or statistically significant differences between air velocities were found in body weight loss, sweat accumulation, or changes in rectal, skin and body temperatures. Occurrence of the smallest body weight loss at 120 ft/min, the largest sweat accumulation at 30 ft/min, and the smallest rise in rectal temperature and the greatest drop in skin temperature at 120 ft/min all suggested more efficient evaporative cooling at the highest velocity. Heat storage at all velocities was evidenced by increased rectal and body temperatures; skin temperatures declined or increased only slightly. Body and rectal temperature increases corresponded with increased perception of warmth and slight thermal discomfort as exercise progressed. At all air velocities, mean thermal perception never exceeded "warm" and mean discomfort, greatest at 30 ft/min, was categorized at worst as "uncomfortable"; sensation of thermal neutrality and comfort returned rapidly after cessation of exercise. Suggestions for further elucidation of the effects of low air velocities on thermal comfort and homeostasis include larger numbers of subjects, more extensive skin temperature measurements and more rigorous analysis of the data from this study.

INTRODUCTION

An exercise regimen is being developed to help counter musculoskeletal degeneration during sustained space flight. The thermal environment during this exercise must be sufficient to avoid extensive heat storage and should suffice to maintain thermal comfort, including minimal accumulation of unevaporated sweat. It is not known whether specified space station habitat and exercise station air velocities (15-40 and 80 ft/min), temperatures (65-80^{o}F, 18.5-26.7^{o}C) and dew points (40-60^{o}F, 4.5 - 15.5^{o}C) will accomplish these objectives. The purpose of this study was to investigate the effect of similar air velocities on heat storage and comfort of subjects exercising according to a space station protocol, at space station operational temperature and humidity.

METHODS

Five male subjects exercised on a treadmill at each of four air velocities at approximately 22^{o}C and 62% relative humidity, the mid-range of selectable temperature and near the upper limit of allowable humidity. Each subject exercised at the same time of day over a period of two weeks, July 25 through August 4, 1989. Except for tests on two successive days for two subjects, a minimum of one day rest intervened between successive tests for each subject. The sequence of air velocities was randomized for each subject. All subjects had undergone a stress test within the past year and gave their informed consent to testing, approved by the Johnson Space Center Human Research Policy and Procedures Committee. Subject characteristics at the time of the stress tests are given in table 1.

Tests were conducted in an environmental chamber 1.8x2.7x2.5m high. An open plastic grid 16cm beneath the ceiling diffused light from two 80 watt fluorescent tubes mounted on the ceiling. Environmental temperature was calculated as the mean of air and wall temperatures measured immediately before and after each test. Relative humidity was similarly determined from psychrometric data. Extremes of wall temperature for all tests were 21.4-23.0^{o}, of air temperature 21.0-23.1^{o}, of relative humidity 54-66.5%. Table 2 presents mean temperature and humidity conditions during testing at the different air velocities.

Controlled air flow was provided by two 56x56cm fans on shelves 1.2m behind the exercising subject. Fan air flow was turbulent but primarily parallel to the treadmill. Fan speeds were adjusted so as to provide, in combination with

TABLE 1.- PHYSICAL CHARACTERISTICS OF SUBJECTS

Subject	Weight kg	Height cm	Body Fat %	Age	Maximum oxygen consumption ml/kg/min
1	95.9	184	29	33	45.9
2	67.2	172	9	27	49.1
3	77.8	165	16	27	38.5
4	76.3	180	12	40	38.3
5	75.4	176	24	49	37.0

TABLE 2.- MEAN TEMPERATURE (^{o}C) AND RELATIVE HUMIDITY

Air velocity	Temperature	Humidity
30	21.9	62.4
50	22.2	62.7
80	22.3	61.0
120	22.3	60.4
Mean	22.2	61.6

uncontrolled air flow associated with the temperature and humidity control system, the air flows used during testing.

Nominal air velocities used were the means of at least two replicates of air velocities measured at twelve points in a vertical plane perpendicular to the treadmill and at the approximate location of the exercising subjects. Four measurement points each were used at 0.5, 1.0 and 1.5m above the treadmill. At each point, measured air velocity was taken as the mean of the mid-points of five ten-second ranges of air velocity. Mean air velocities at the three levels are presented in table 3.

TABLE 3.- NOMINAL AND MEASURED AIR VELOCITIES (FT/MIN)

Nominal velocity	30	50	80	120
Meters above treadmill:				
0.5	49	50	93	94
1.0	32	61	81	183
1.5	16	45	67	88
Mean	32	52	80	122
Standard deviation	16	8	13	53

The suggested space station exercise schedule specifies successive ten minute periods at 65, 75 and 85% maximum oxygen consumption. Treadmill speeds and grades needed to achieve these oxygen consumptions for each subject were estimated using the chart and formula of Givoni and Goldman (1971). Small adjustments were made after each subject's first test to more closely approximate targeted values. The range of speeds and grades used was 5.6-6.6km/hr and 5-15%.

Before each test, thermistor probes were attached with porous paper tape to the mid-sternum, anterior left thigh and dorsal left hand of the subject, a rectal thermistor was inserted to 10cm, and EKG electrodes and transmitter were attached; total mass of this apparatus was approximately 430gm. The nude subject was then weighed to the nearest 5gm on an electronic platform balance before donning preweighed shorts, socks and shoes. Within five minutes after completing exercise, clothing and a towel used to remove perspiration after exercise were placed in a plastic bag and nude weight was again determined. Body weight loss was determined as the difference of these two weights; unevaporated sweat accumulation was estimated as the difference in garment and towel weight before and after exercise.

After the first weighing, fans were turned on and the subject stood at rest on the treadmill for 15 minutes in order to establish thermal equilibrium. At the beginning of this period, the beginning of exercise, and at each five minute interval thereafter during exercise and a subsequent 15 minute recovery period, rectal and the three skin temperatures were recorded. Mean skin and body temperatures were computed according to equations modified from Berenson and Robertson (1973):

$$T_{skin}=0.53T_{thigh}+0.33T_{chest}+0.14T_{hand};$$

$$T_{body}=0.67T_{rectal}+0.33T_{skin}.$$

At the same time intervals, subjects categorized perception of temperature and thermal comfort according to temperature and discomfort scales described by Gagge et al. (1967) and illustrated in table 4. Scales were posted in front of the treadmill to facilitate subject response.

During the initial equilibrium period and at the mid-point of each exercise level, oxygen consumption and carbon dioxide production were measured by timed collection of

TABLE 4.- TEMPERATURE SENSATION AND THERMAL COMFORT SCALES

Temperature:		Comfort:	
-3	cold	0	comfortable
-2	cool	1	slightly uncomfortable
-1	slightly cool	2	uncomfortable
0	neutral	3	very uncomfortable
+1	slightly warm	4	intolerable
+2	warm		
+3	hot		

expired gas samples and analysis of gas composition by a mass spectrometer.

RESULTS

Table 5 presents mean percentages of maximum oxygen consumption during the three ten minute periods of exercise at each air velocity. The percentage in each case was lower than the targeted values of 65, 75 and 85%. Analysis of variance (ANOVA) within exercise periods revealed no significant differences between the different air velocities.

TABLE 5.- MEAN PERCENTAGE OF MAXIMUM OXYGEN CONSUMPTION DURING SUCCESSIVE EXERCISE PERIODS ( )=S.D.

Air velocity ft/min	Period First	Second	Third
30	59 (6)	73 (6)	81 (11)
50	60 (6)	71 (6)	82 (10)
80	62 (7)	72 (9)	81 (7)
120	60 (6)	71 (10)	83 (11)

Body weight loss was least at 120 ft/min and sweat recovered was greatest at 30 ft/min (table 6). ANOVA indicated no significant differences between air velocities for any of these parameters.

Figures 1 and 2 show that rectal and body temperatures both rose gradually through the exercise period and declined during the recovery period. The decline in rectal temperature was more gradual than its rise and more immediate and consistent than the decline in body temperature. Air velocity had little effect on the change in rectal temperature at 30 minutes, nor any consistent effect on body temperature. ANOVA indicated no significant differences between air velocities in mean body or rectal

TABLE 6.- MEAN ABSOLUTE AND PERCENTAGE BODY WEIGHT LOSSES, ABSOLUTE WEIGHT OF RECOVERED SWEAT AND WEIGHT OF RECOVERED SWEAT AS PERCENTAGE OF BODY WEIGHT LOSS ( )=S.D.

Air velocity ft/min	Weight loss gm	percent	Sweat recovered gm	percent
30	425 (213)	0.5 (0.2)	85 (95)	16.2 (10.5)
50	421 (174)	0.5 (0.2)	68 (75)	13.5 (9.5)
80	442 (158)	0.6 (0.1)	63 (69)	12.1 (9.6)
120	356 (229)	0.4 (0.2)	64 (72)	14.8 (7.9)

temperature changes at 30 minutes.

All skin temperatures dropped initially and then rose slightly (figure 3). At 80 and 50 ft/min, skin temperature continued to rise through the exercise period, at 30 ft/min it oscillated, and at 120 ft/min it declined until the end of the exercise. At the end of the exercise period, the skin temperatures at 50 and 80 ft/min were approximately the same as at the beginning of the period; the greatest change was at 120 ft/min, slightly greater than that at 30 ft/min. Differences at 30 minutes were not statistically significant.

During recovery, skin temperatures first rose then declined precipitously at all air velocities except 80 ft/min, in which case the opposite occurred. At the end of the recovery period, the greatest change from the start of the exercise was at 120 ft/min and the least at 80 ft/min.

Figure 4 indicates that mean temperature perception at the start of exercise was slightly cool at 80 and 120 ft/min and near neutral at 30 and 50 ft/min. Ranking of perceived temperature rose until the end of exercise, when subjects felt warm at 80 ft/min and between slightly warm and warm at other velocities. Feeling of warmth decreased rapidly at the beginning of the recovery period and thereafter approximated starting values.

Subjects at 120 ft/min were slightly less comfortable than at other velocities at the beginning of exercise (figure 5). Mean discomfort level at 30 ft/min was almost a whole category above that at other velocities at 25 minutes. At 30 minutes, subjects at 30 ft/min gave the highest discomfort ranking, and subjects at 120 ft/min were the most comfortable. After exercise, comfort level at all velocities rapidly returned to "comfortable".

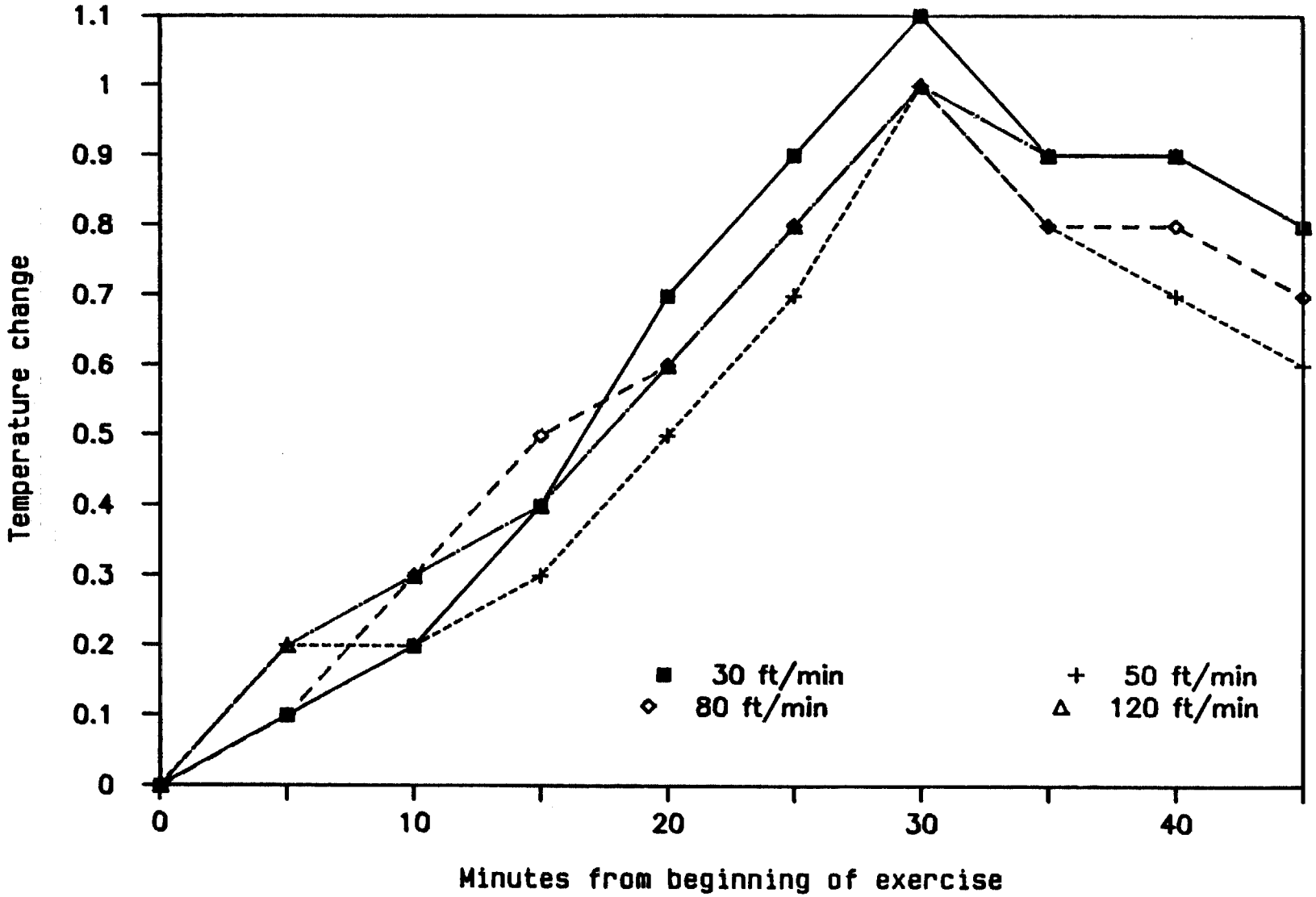

Figure 1.— Change in rectal temperature during and after 30 minute exercise at different air velocities.

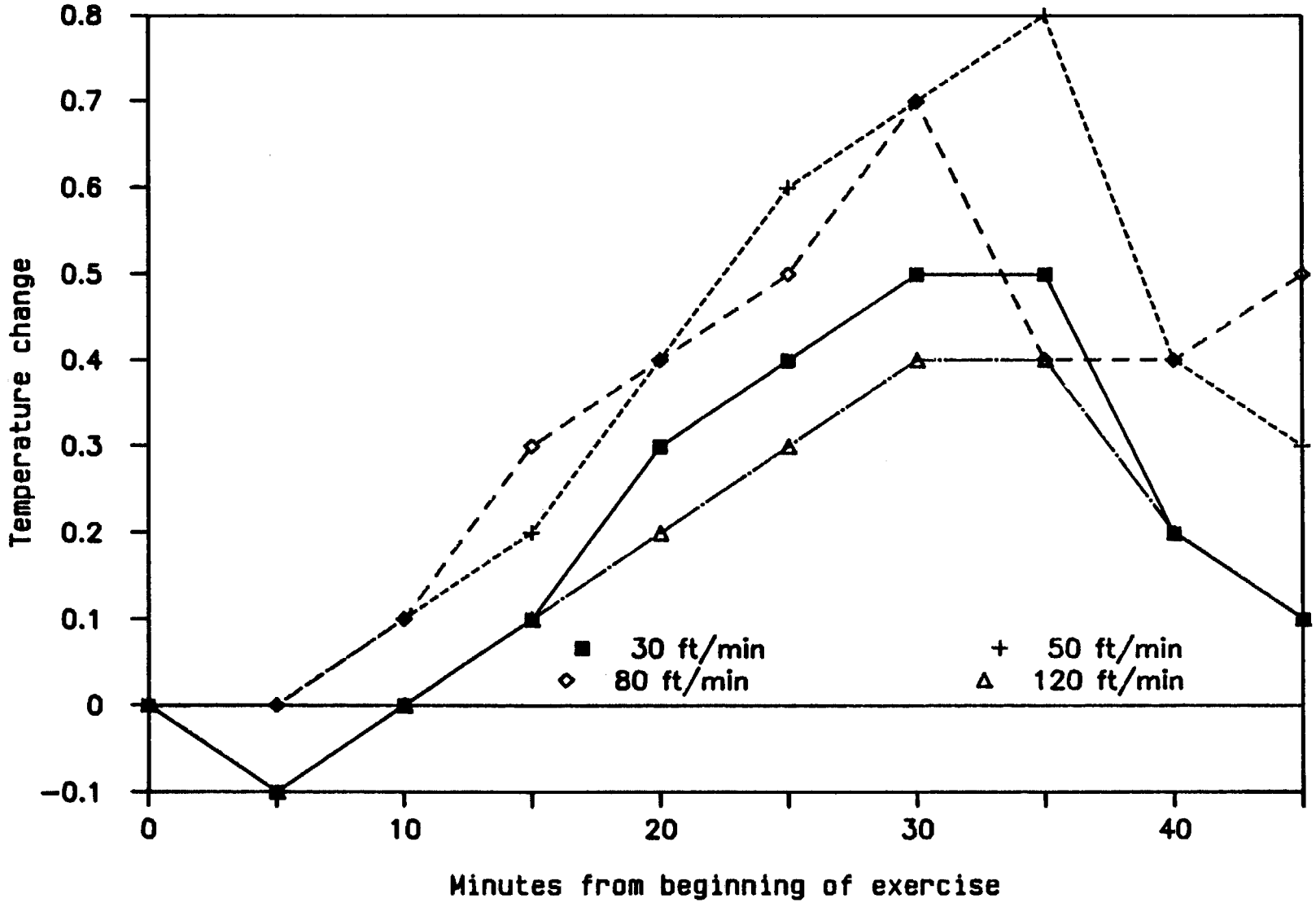

Figure 2.– Change in body temperature during and after 30 minute exercise at different air velocities.

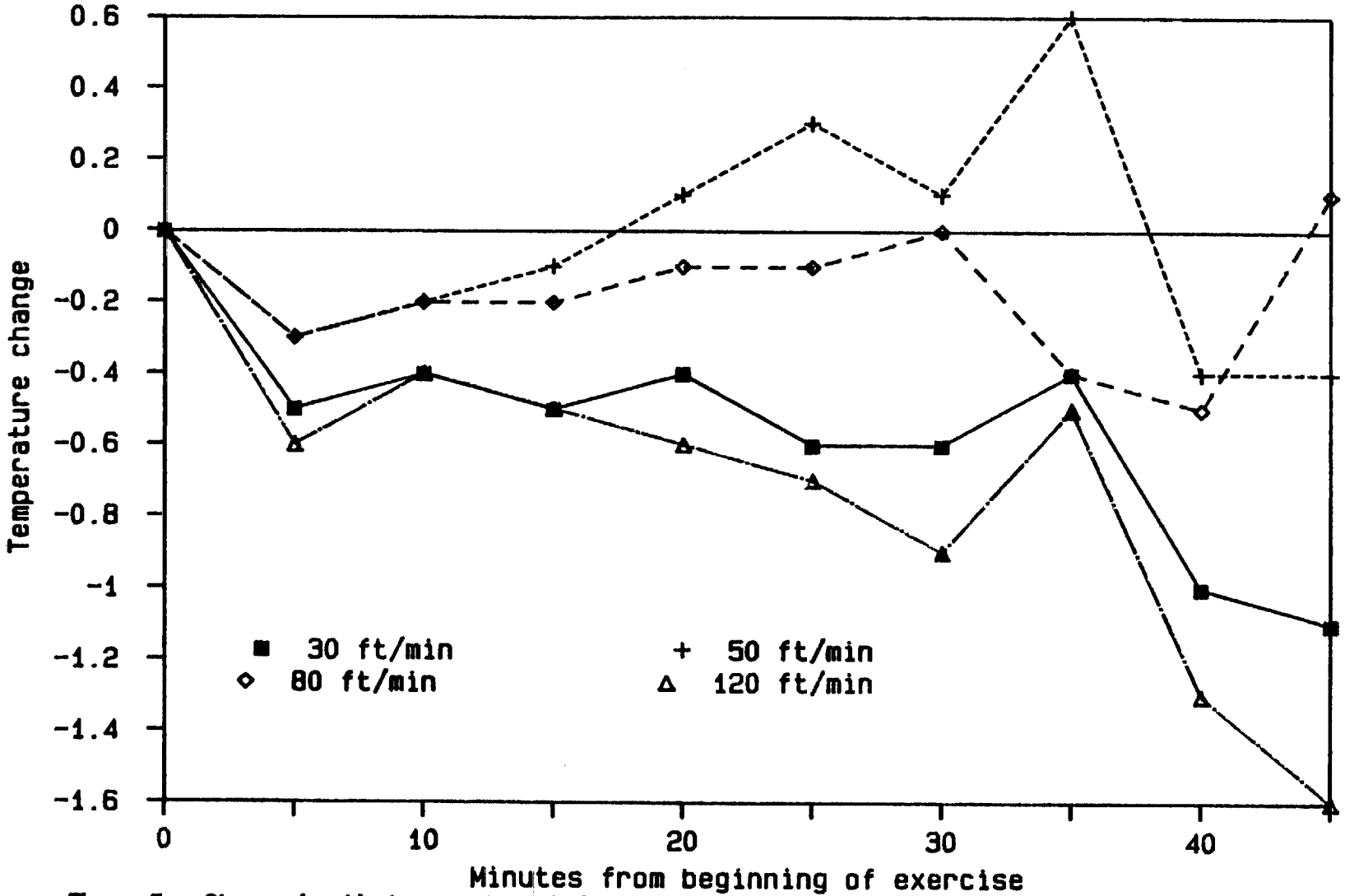

Figure 3.– Change in skin temperature during and after 30 minute exercise at different air velocities.

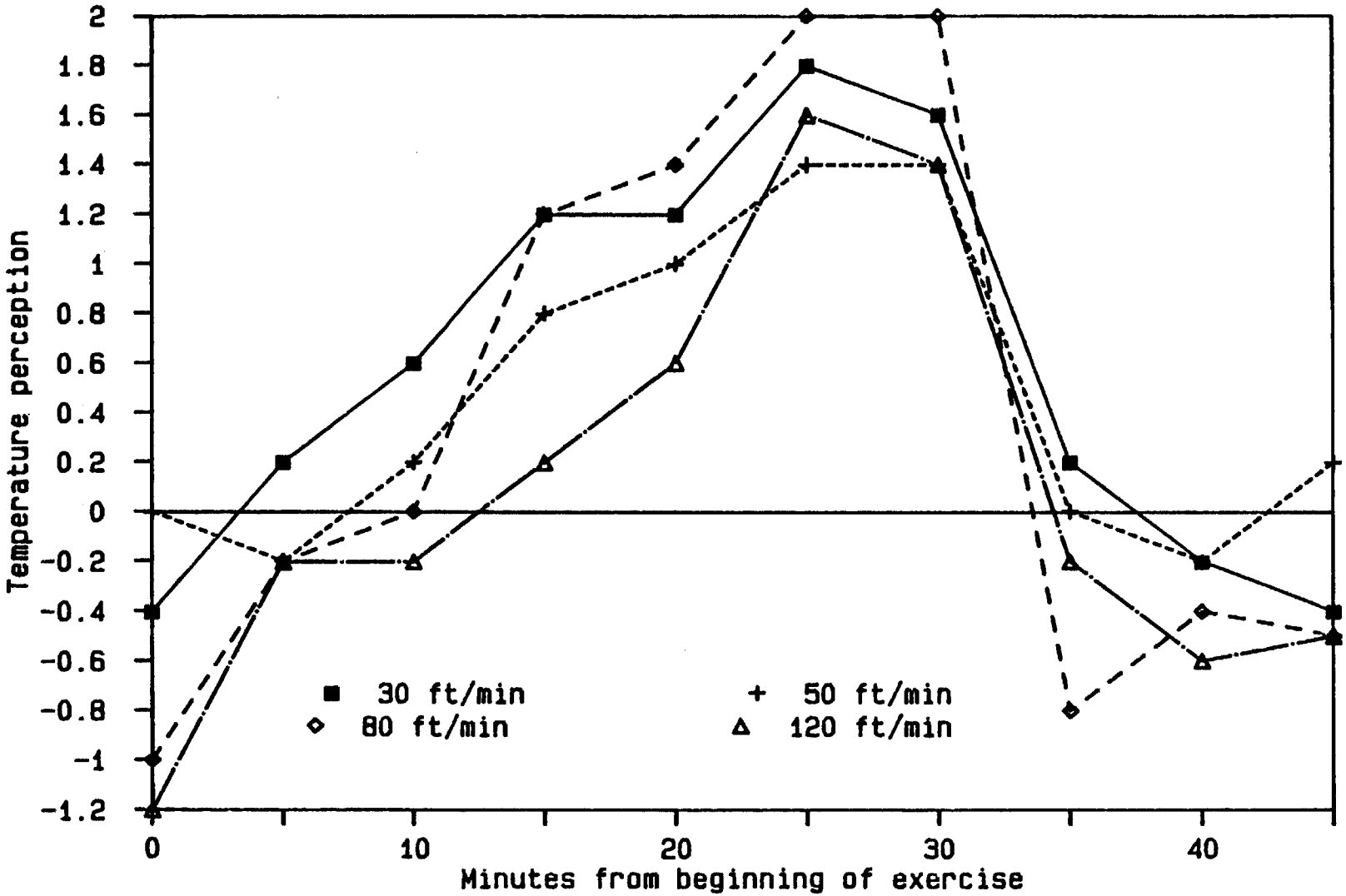

Figure 4.— Mean temperature perception during and after 30 minute exercise at different air velocities.

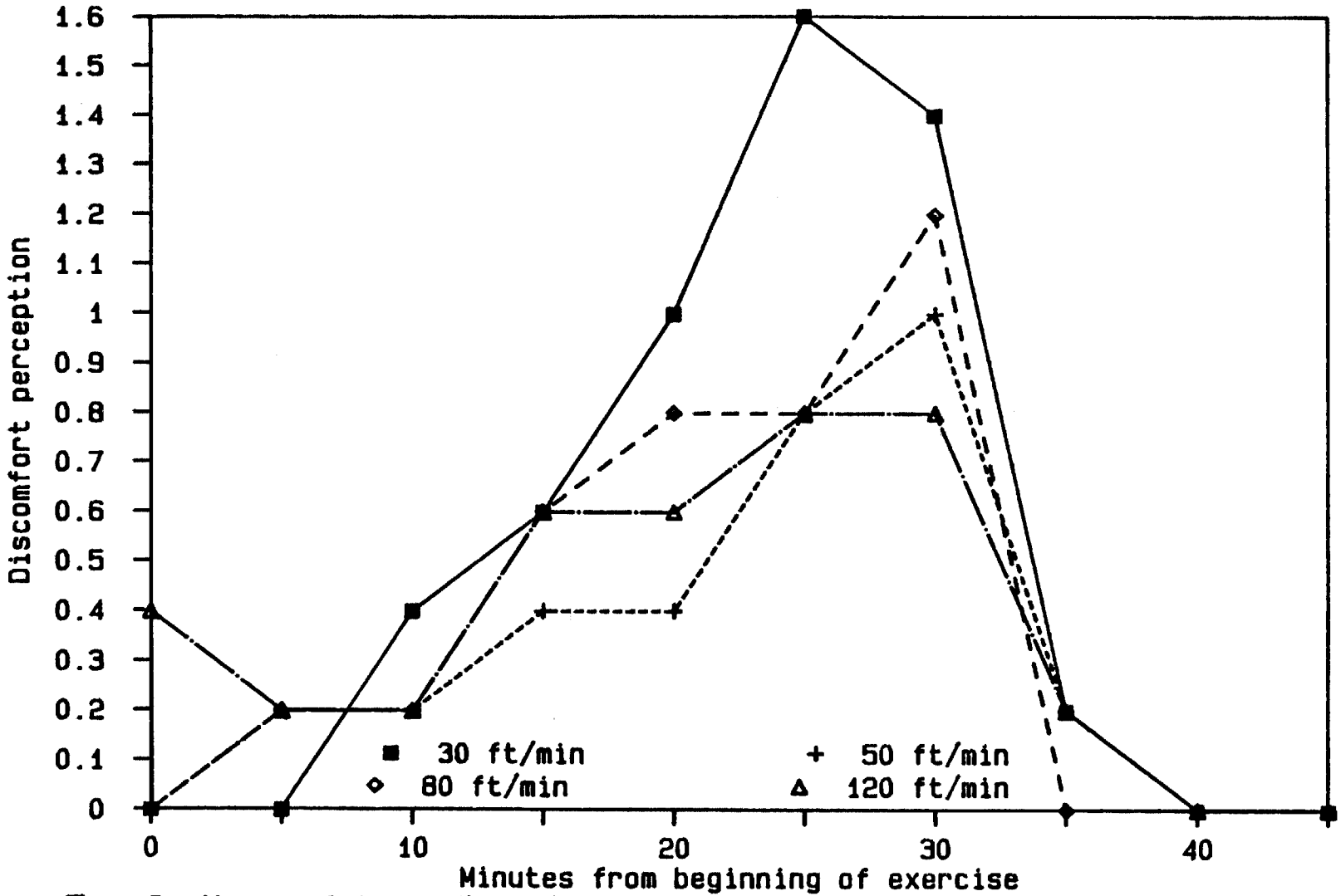

Figure 5.— Mean comfort perception during and after 30 minute exercise at different air velocities.

DISCUSSION

These results suggest little difference in the contribution of the studied air velocities to thermal homeostasis and comfort. No statistically significant effects of air velocity were observed, nor were there consistent trends in the observed parameters.

That mean energy expenditures were less than planned suggests the desirability of further study using exercise levels more closely resembling the space station protocol. Nevertheless, their similarity at the four velocities studied validates comparisons of other measured parameters.

That the smallest body weight loss occurred at 120 ft/min might be due to this highest velocity fostering more efficient evaporative cooling. This suggestion is strengthened by the greatest accumulation of sweat at the lowest velocity. More thorough analysis of these weights relative to factors such as surface area, energy expenditure and insensible evaporation may be useful.

Increases in rectal and body temperatures indicated heat storage at all air velocities. That increase in body temperature in all cases was smaller than rectal increase is explained by smaller increases or declines in skin temperature, probably the effect of evaporative cooling. That the greatest increase in rectal temperature occurred at the lowest air velocity is a reasonable corollary of reduced evaporative cooling, but a further, unfulfilled corollary would be a smaller decline in skin temperature and larger increase in body temperature than at the intermediate velocities.

Greater evaporative cooling similarly would explain the smallest rise in body temperature and greatest drop in skin temperature occurring at 120 ft/min. This conclusion is weakened by the second greatest drop in skin temperature occurring at the lowest air velocity and by only small changes at intermediate velocities.

During the post-exercise period, rectal temperatures declined more consistently than body temperatures and skin temperatures were erratic. This may reflect rectal temperature being affected more by activity and skin temperature by environment. The primary purpose of this period was to assure recovery of homeostasis; no effort was made to control the posture or location of subjects in relation to air flow. Environmental variability during this period might have contributed to variable skin

temperatures. Temperature changes might have been more informative if this variability had been reduced.

Subjective sensation of being cooler before and after exercise at the higher velocities than at the lower velocities can be explained by greater convective cooling and post-exercise evaporative cooling. Lower comfort at the highest velocity than at lower velocities at the beginning of exercise probably was associated with this perception of coolness.

During the later part of the exercise period, greater discomfort was perceived at 30 ft/min than at higher velocities. A possible explanation of lesser convective and evaporative cooling is not supported by changes in measured temperatures. Greater skin wettedness as a possible explanation is corroborated by the greatest accumulation of sweat at this velocity. Decreased sensation of air movement is another possible cause.

Increased perception of warmth and slightly decreased comfort with increasing activity at all air velocities corresponds with increases in body and rectal temperatures. It is notable that at all these velocities the mean thermal sensation never exceeded warm, mean discomfort at worst was categorized between uncomfortable and slightly so, and that post-exposure perception rapidly returned to near thermal neutrality and comfort.

Although this study has revealed little difference in the effectiveness of different low air velocities under the conditions of the study, these data should be analyzed more rigorously. Perhaps also the study should be repeated under more precisely controlled conditions and using more powerful measures to either validate its results or otherwise elucidate the effects of different air velocities. In addition to suggestions made above, air flow should be more uniformly controlled or at least more completely characterized. Temperature data might be more informative if skin temperatures were measured at a larger number of sites, especially on the dorsal surface most directly affected by air flow in this study. The use of larger numbers of subjects might also help to overcome the effects of large individual differences in response to the test protocol.

REFERENCES

Berenson, P.J.; and Robertson, W.G.: Temperature. In Parker, J.F., Jr.; and West, V.R. (Eds.): Bioastronautics Data Book, second edition, NASA SP-3006, 1973, pp 65-148.

Gagge, A.P.; Stolwijk, J.A.J.; and Hardy, J.D.: Comfort and thermal sensations and associated physiological responses at various ambient temperatures. Environ. Res., vol. 1(1), 1967, pp 1-20.

Givoni, B.; and Goldman, R.F.: Predicting metabolic energy cost. J. Appl. Physiol., vol. 30(3), 1971, pp 429-433.

NONINVASIVE ESTIMATION OF FLUID SHIFTS BETWEEN BODY COMPARTMENTS BY MEASUREMENT OF BIOELECTRIC CHARACTERISTICS

Final Report

NASA/ASEE Summer Faculty Fellowship Program--1989

Johnson Space Center

Prepared by:	Phillip A. Bishop, Ed.D.
Academic Rank:	Assistant Professor
University Department: Performance	Area of Health and Human University of Alabama Tuscaloosa, AL 35487

NASA/JSC

Directorate:	Space and Life Sciences
Division:	Medical Sciences
Branch:	Cardiovascular Laboratories
JSC Colleague:	Suzanne Fortney, Ph.D.
Date Submitted:	August 17, 1989
Contract Number:	NGT44001800

ABSTRACT

Previous research has established that bioelectrical characteristics of the human body reflect fluid status to some extent. It has been previously assumed that changes in electrical resistance (R) and reactance (X) are associated with changes in total body water (TBW). The purpose of the present pilot investigation was to assess the correspondence between body R and X and changes in estimated TBW and plasma volume during a period of bedrest (simulated weightlessness). R and X were measured pre-, during, and post- a 13 day bedrest interspersed with treatments designed to alter body fluid status. Although a clear relationship was not elucidated, evidence was found suggesting that R and X reflect plasma volume rather than TBW. Indirect evidence provided by previous studies which investigated other aspects of the electrical/fluid relationship, also suggests the independence of TBW and electrical properties. With further research, a bioelectrical technique for noninvasively tracking fluid changes consequent to space flight may be developed.

INTRODUCTION

That body fluid volumes are altered as a consequence of simulated or actual space flight is well established (7). It is generally believed that the loss of intravascular fluid (blood plasma) contributes significantly to the observed decline in orthostatic tolerance subsequent to microgravity exposure. Body fluid compartments have been studied in simulated weightlessness studies (bedrest, and water immersion) by invasive means, but the time requirements and the necessity of blood withdrawal and isotope injection required by these measurements, have generally precluded their use during space flight. The development of an accurate noninvasive technique for estimating the shift in body fluids throughout the course of an extended duration space flight would provide considerable information useful in understanding and protecting against the adverse effects of prolonged microgravity exposure.

The work of Nyboer (18) and others has shown that bioelectrical characteristics respond to changes in body fluids. This technique involves introduction of 0.8-4 milliamps of high frequency (50-100 kHz) current into the body via surface electrodes. These current levels at these frequencies are safe and painless. Tetrapolar electrodes are employed with two electrodes used for current injection and two used for voltage pickup, which obviates skin-electrode impedance complications (14,18). Knowledge of the injected current and frequency and the voltage drop and phase shift across a body part can be used to calculate resistance and reactance which can be combined to yield impedance. Basic electrical theory can be used to derive an equation for volume:

$$\text{volume}=\text{resistivity}*\text{length}^2/\text{resistance}. \qquad \text{(Eq.1)}$$

Since within a given subject, under certain conditions, short term resistivity and length (distance between electrodes) remain constant, resistance and volume are inversely related.

Previous cross-sectional research (4,5,10,13,14,23,24,27) has demonstrated strong relationships between impedance and TBW or fat free mass (which is correlated to TBW). Numerous investigators have observed high test-retest reliability and also good correspondence between separate laboratories (12).

Studies by Nyboer, (18), Spence et al. (25) and Patterson (19) have demonstrated strong correlations between impedance and acute weight changes (i.e. fluid volume changes) in hemodialysis patients, and studies by Carlson et al. (2), and Mayfield and Uauy (15), have demonstrated strong

correlations between impedance and hydration status of burn victims, and infantile diarrhea patients, respectively. It has been demonstrated that bioelectrical properties can be used to estimate cardiac output (9), total body water (23), and limb blood flow (11).

Recently, Patterson (19) has argued that measures of impedance of individual limbs and the trunk (segmental measures) should be better predictors of TBW or fat free mass than the right side whole body measurements. Right side whole body measurement is the most common technique used currently. He bases his argument on the observation that the small bony cross-sections of the wrist and ankle contribute to produce limb impedances which are much higher than trunk impedance. Consequently, when these impedances are summed, the trunk, where most of the resting blood volume is located, has a disproportionately small contribution to the overall measured impedance value. Conversely, the wrist and ankle, which are not much influenced by fluid shifts, strongly influence the total impedance. Patterson presented data from duplicate measurements on patients before and after hemodialysis and found that combined segmental measures yielded a higher correlation coefficient, (r=.87) than whole body measures (r=.64), in predicting weight changes subsequent to dialysis. However, Patterson's report did not include a rigorous statistical analysis of all the data.

All the bioelectrical/hydration relationship studies, have been cross-sectional or acute treatments without consideration of fluid shifts or of specific resistivity changes. A comprehensive longitudinal (i.e. pre-post systematic fluid manipulation) study of the relationship between hydration status and segmental and whole body resistance and reactance in healthy humans has not been reported. The purpose of the present pilot investigation was to determine the correspondence between changes in segmental limb R and X and estimated changes in body fluid compartments.

Because fluid shifts and losses have been implicated in orthostatic intolerance, decreased cardiovascular function, and space adaptation syndrome, the ability to continuously monitor fluid levels would contribute greatly to our understanding of the physiological responses to acute and chronic exposures to microgravity. The use of reactance measurements as well as resistance measurements may permit discrimination between extra- and intra- cellular water compartments (15,16,17).

METHODS

Subjects

Subjects were two volunteers for a previously approved 13 day bedrest study at Johnson Space Center. Subjects had given prior informed consent for measurement of bioelectrical properties. Subjects were fully advised of the nature of this specific aspect of the bedrest study, and gave permission prior to each measurement.

Conditions

These measurements were made during the course of a 13 day six degree head down tilt bedrest (-6HDT) which was intended to determine the effectiveness of lower body negative pressure (LBNP) and fluid loading in ameliorating loss of orthostatic tolerance consequent to fluid shifts associated with -6HDT and similar to those observed in microgravity. After a two day ambulatory hospitalization, subjects underwent a 13 day bedrest interrupted by LBNP response tests and LBNP and fluid treatments. Subjects were kept on a 2476 Kcal diet with 2500 ml of additional daily fluid intake. This food and fluid level replicates the average intake of the astronauts during Shuttle flights. Body weights were determined with a portable bed scale (Techtronix) just after the noon meal each day. Blood samples were collected prior to breakfast each day. Blood volumes were determined from red blood cells labeled with ^{51}Cr. Plasma volumes were determined from blood volumes corrected for blood removal and hematocrits.

Bioelectrical Measurements

Resistance and reactance were measured at three sites with a RJL analyzer at 50 Khz with 0.8 mA induced current. Prejelled double electrodes (BOMED) were located at the antecubital fossa, just anterior and centered on the acromium process, just distal to the inguinal fold on the anterior surface, and on the anterior surface superior to the patella. In each case, except the inguinal, the electrode was located with the distal border located at the landmark. Injection and current pick-up electrodes were 5cm apart. Inter-electrode distances and limb circumferences at the midpoint between electrodes were measured with a cloth tape. This electrode arrangement permitted determination of three separate electrical measurements designated arm, trunk, and leg. Segmental measurements were used rather than whole-body measurements in keeping with Patterson's (19) observations regarding joint-induced alterations in electrical resistivity. For simplicity, segmental R's were summed to represent an estimator of total body R and designated "combined R". For ease of comparison, resistances and reactances values were also converted to their inverse, conductance.

RESULTS

Figures 1a and 1b, and 2a and 2b, are illustrations of alterations in segmental resistance and reactance throughout the time course of bed rest for subjects A and B, respectively. Subject B underwent two LBNP treatments with saline ingestion and a presyncopal LBNP (labeled PSL) which are shown in the figures.

Figures 3a and 3b portray combined conductance (inverse resistance) and body weight changes (which approximate TBW changes) by day for each subject. Figures 4a and 4b portray combined conductance and plasma volume for each test day of the experiment. Figures 5a and 5b portray combined reactive conductance and plasma volume by day for each subject.

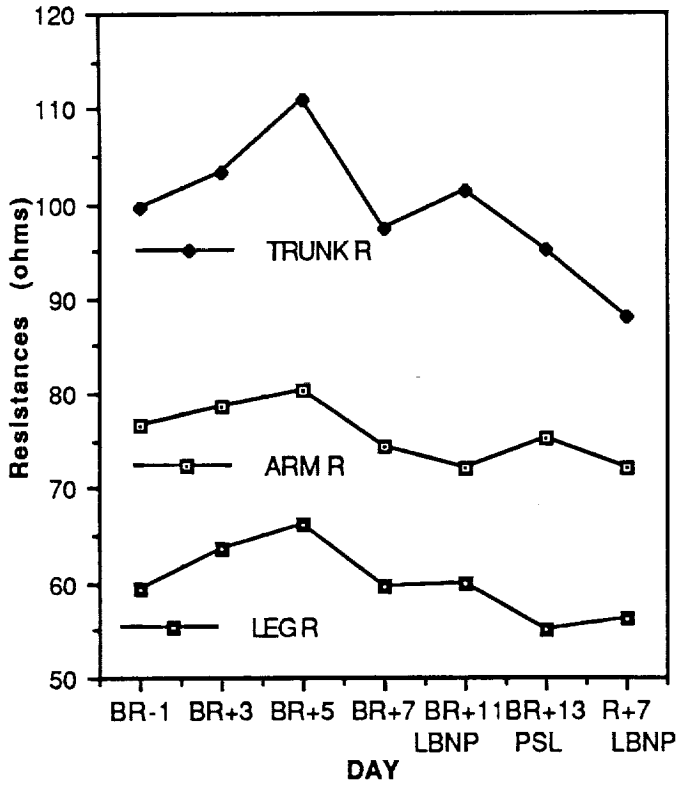

FIG.1a. Segmental resistances by day. Subj A.

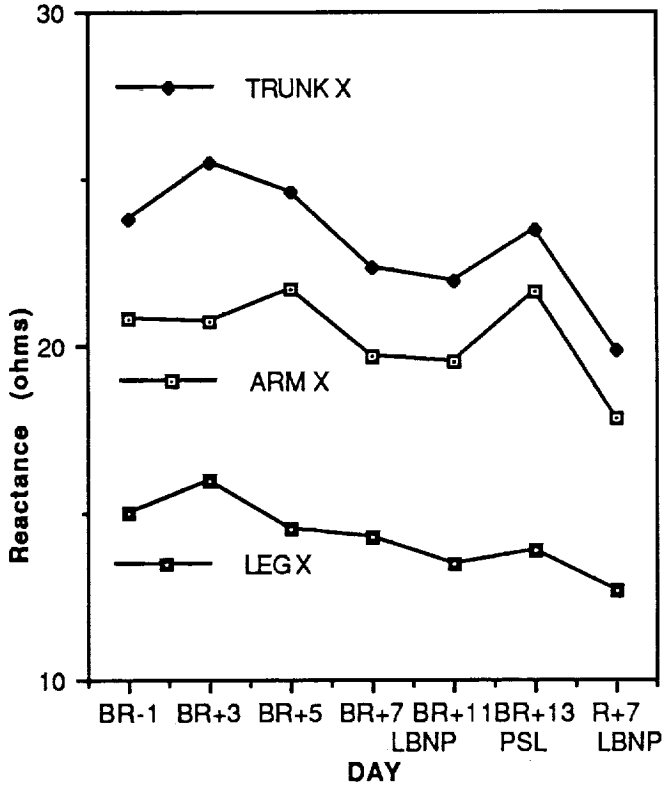

Fig 1b. Segmental Reactances by day. Subj. A.

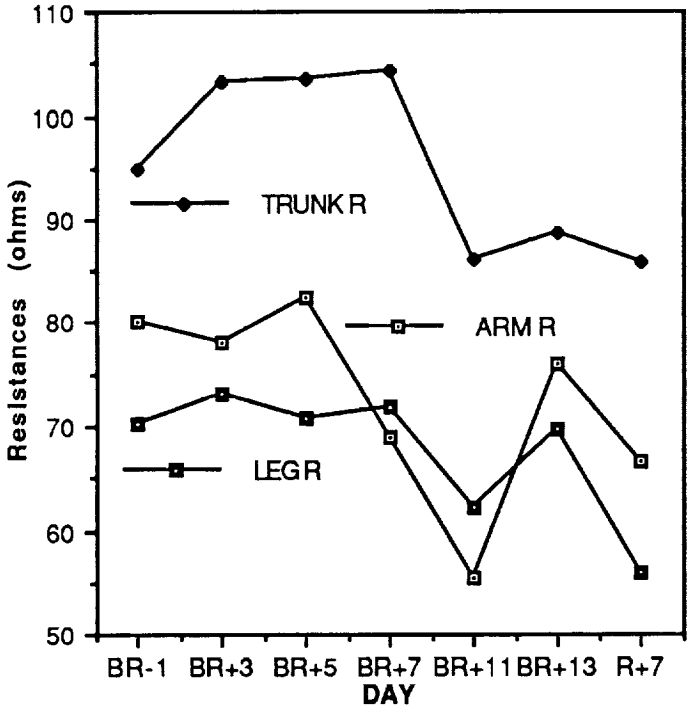

Fig 2a. Segmental resistances by day. Subj. B.

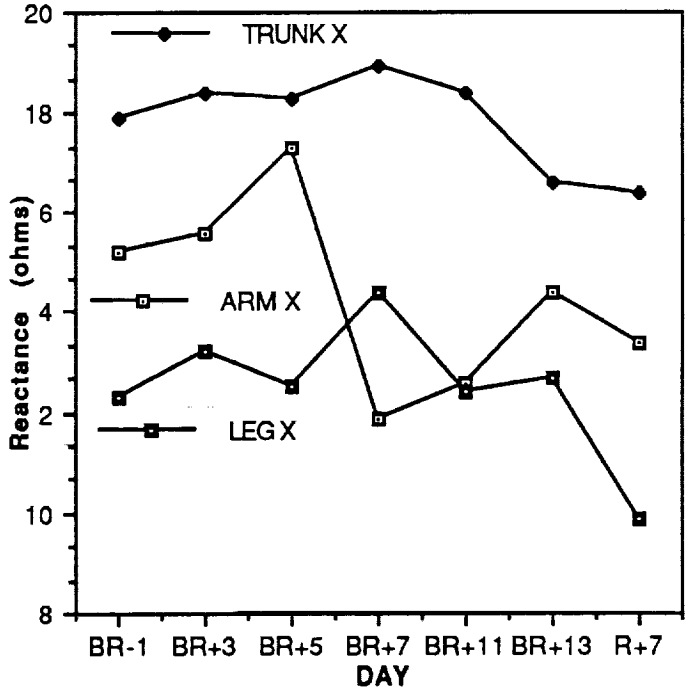

Fig. 2b. Segmental reactances by day. Subj B.

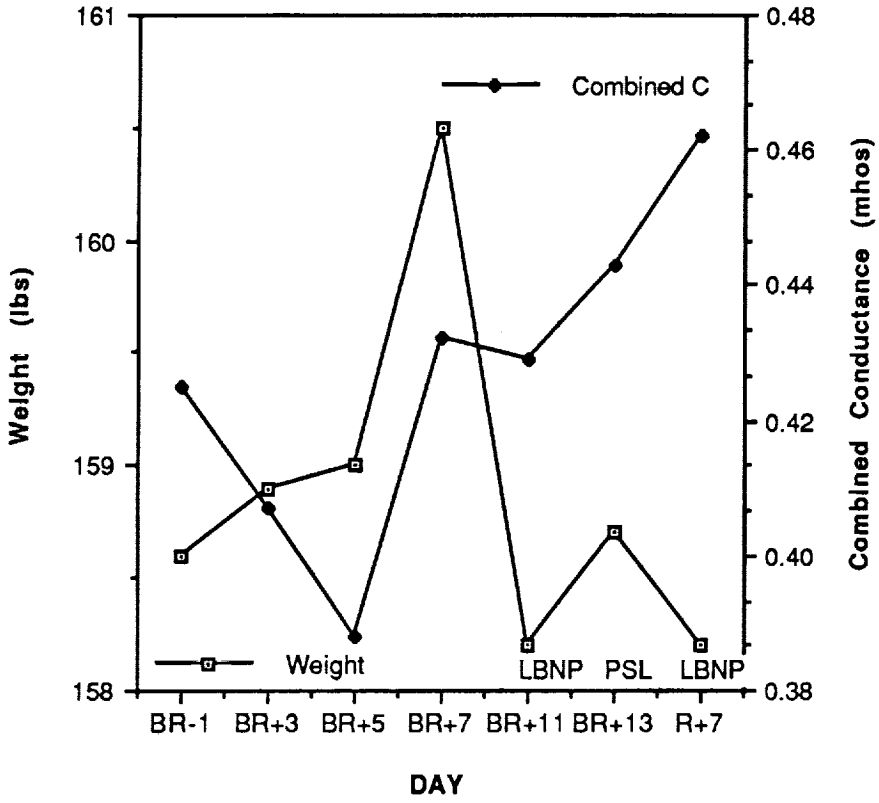

Fig 3a. Combined conductance and body weight by day. Subj A.

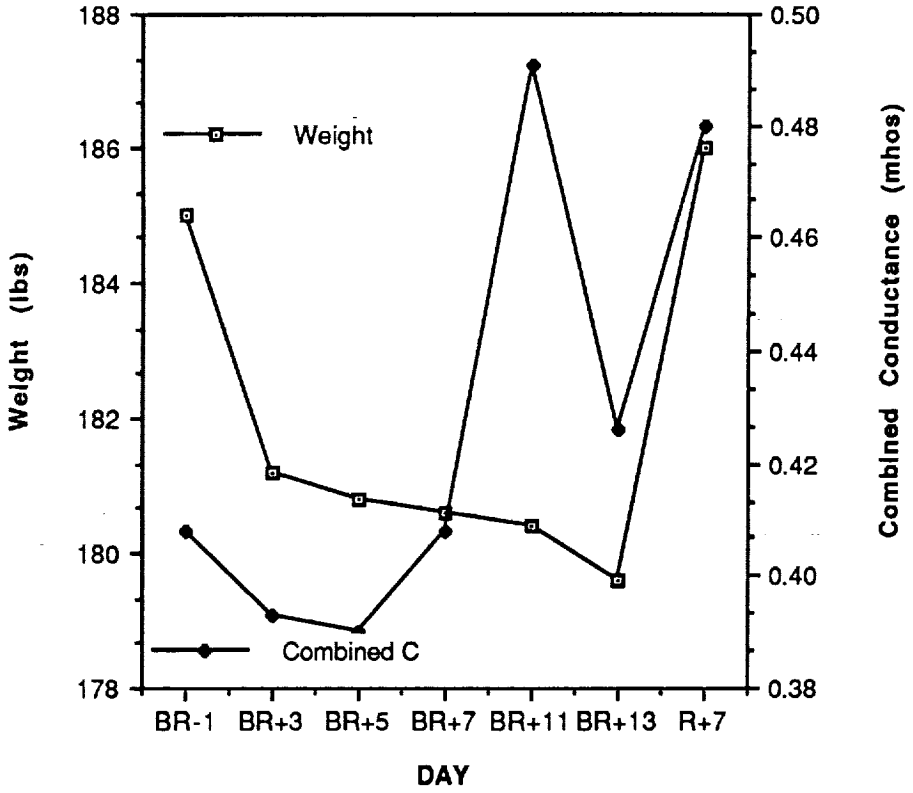

Fig 3b. Combined conductance and body weight by day. Subj B.

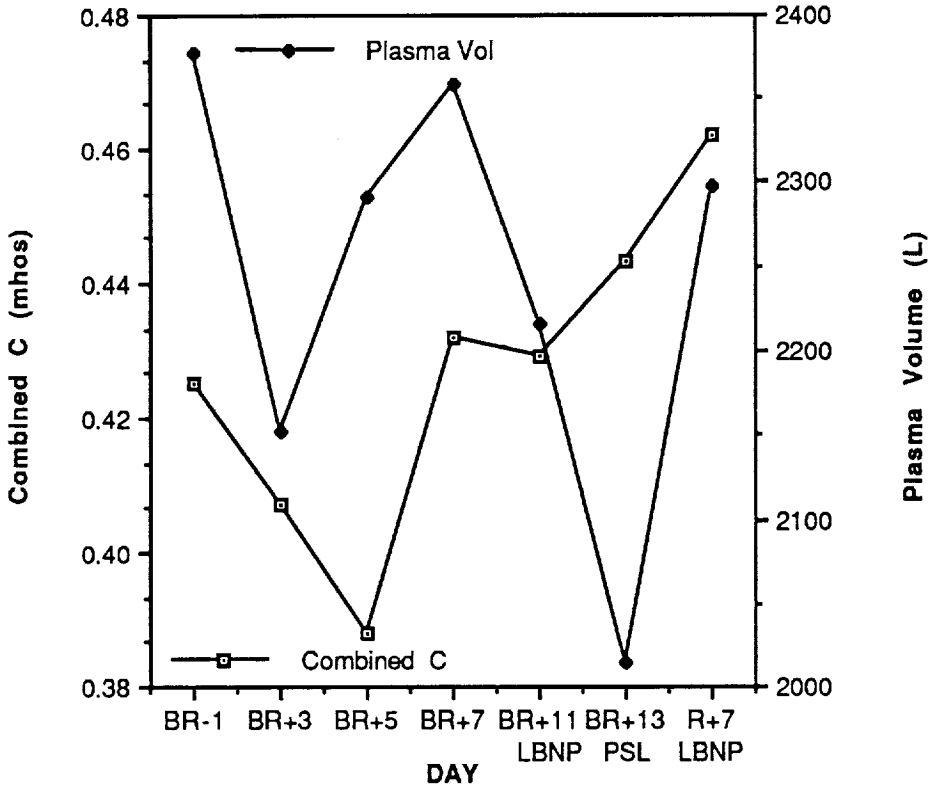

Fig 4a. Combined Conductance and plasma volume by day. Subj. A.

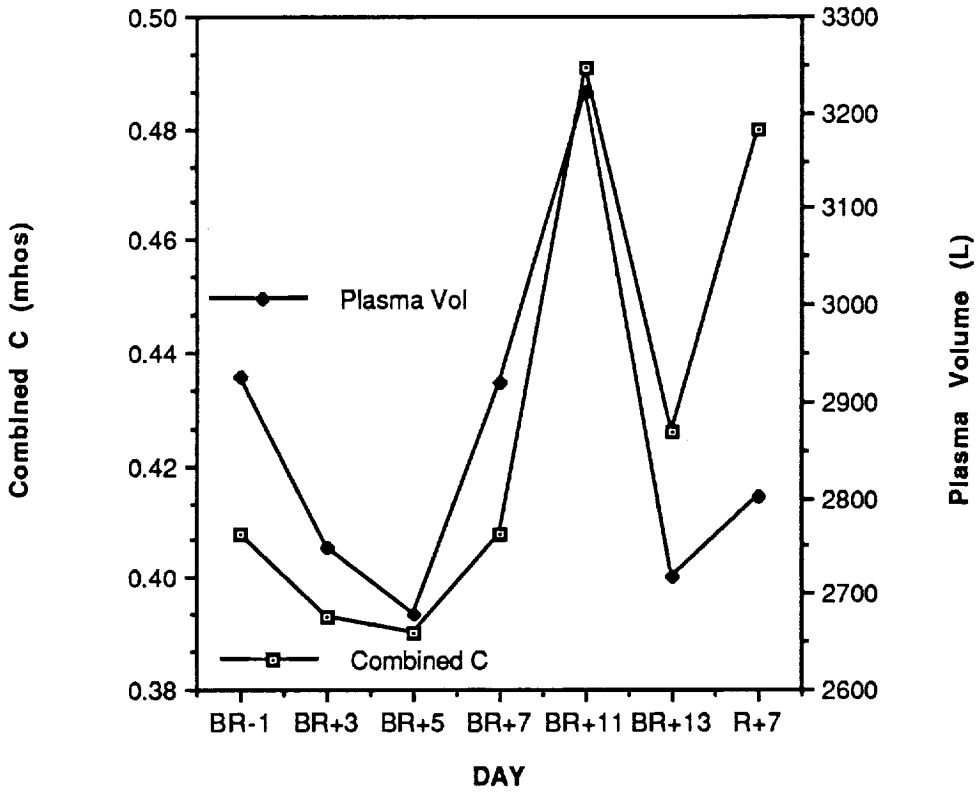

Fig. 4b. Combined conductance and plasma volume by day. Subj. B.

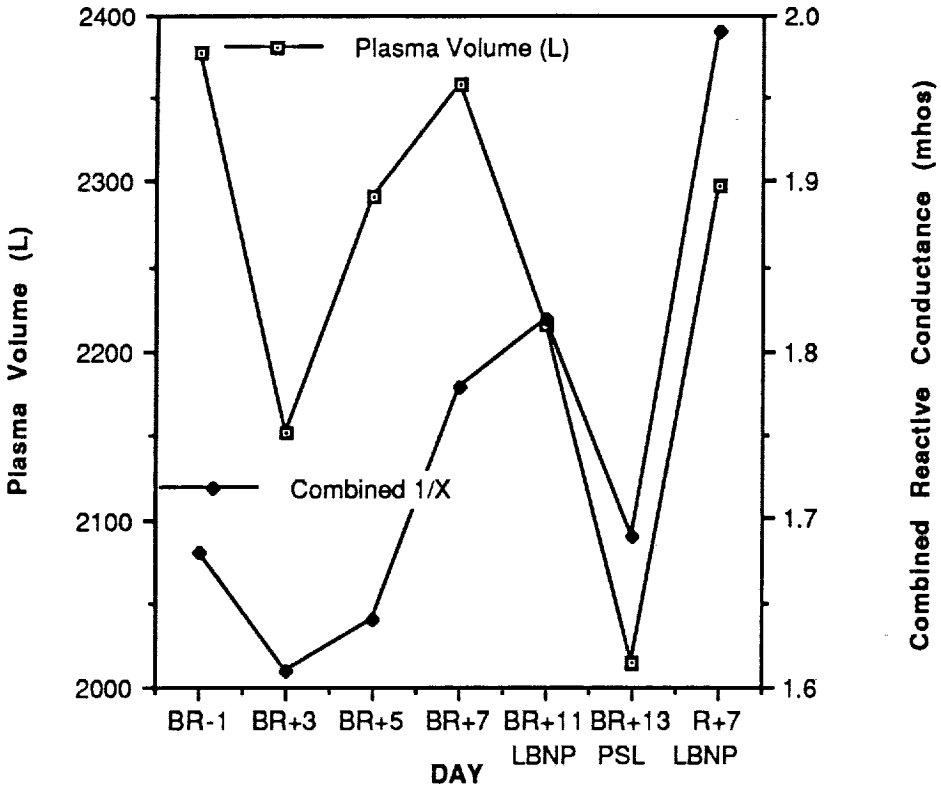

Fig. 5a. Combined reactive conductance and plasma volume by day. Subj. A.

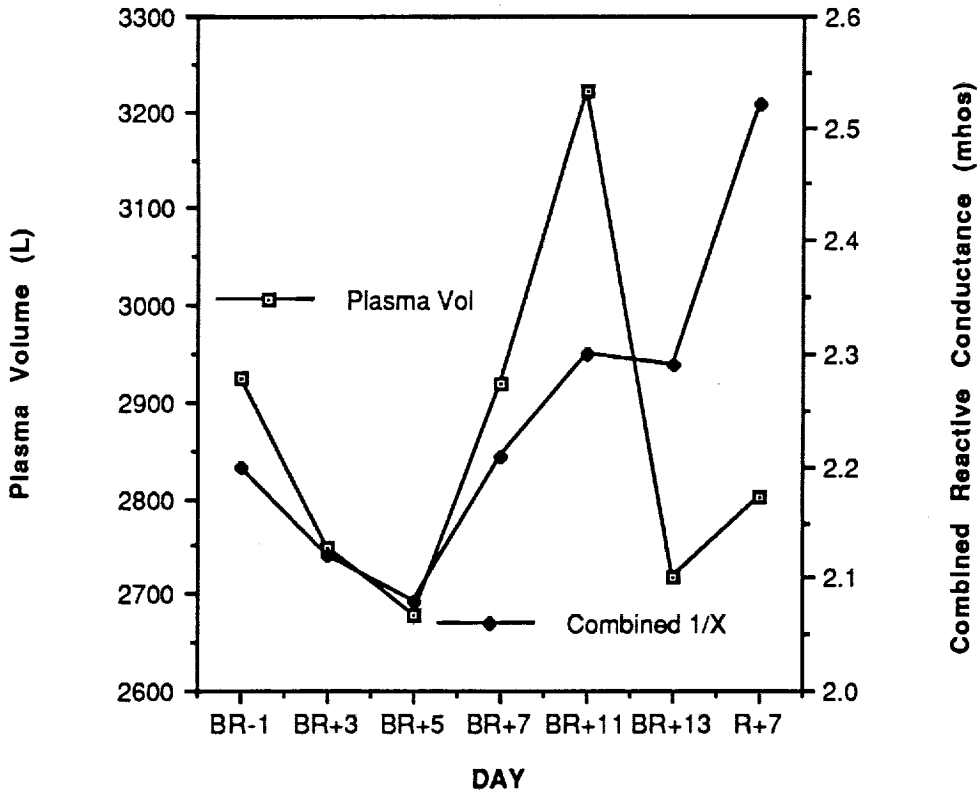

FIG. 5b. Combined reactive conductance and plasma volume by day. Subj. B.

DISCUSSION

Previously cited works suggest that total body water is strongly related to electrical resistance. The findings in the present investigation suggests that human bioelectrical properties may be related to fluid levels in various compartments rather than total body water. For both subjects, individual segmental R's and X's roughly paralleled each other, except arm R and X in Subject B showed an exaggerated drop on bedrest day 5 (BR+5). The segmental approach resulted in arm, trunk, and leg R's which were similar in magnitude. This approach appeared to alleviate previously discussed joint interference problems. In both subjects, body weight loss, which should reflect TBW, appears to be disassociated from conductance (inverse resistance). If TBW and resistance were inversely related, as has been generally believed, good correspondence should have been observed. Since TBW is not altered during LBNP, if R and TBW were related, this relationship should remain robust. In Subject B, rapid weight loss, which should reflect TBW loss, was not closely paralleled by any bioelectrical measurement (Fig.3b). In subject A, combined R roughly tracked plasma volume, but LBNP apparently changed somewhat the relationship between plasma volume and resistance. But, for subject B, combined resistance was closely linked to plasma volume changes (Fig.4b). Combined X appeared to track changes in plasma volume better than R in subject A, but less well than R in subject B (Figs. 5a and 5b).

Interpretation of these data is complicated by the observation that changes in resistance measurements do not consistently relate to changes in fluid levels in a simple way. In the case of dehydration by heating, Hutcheson et al. (6) report a decrease in body weight accompanied by a decrease in impedance (which would be interpreted as an increase in TBW by equation 1). Likewise, Caton et al.'s (3) observations that resistance decreases as skin temperature increases, suggests that the distribution of blood (i.e. into the skin in the case of heating) influences electrical properties. The authors speculate that the shift of fluid between plasma and interstitium may also be involved. This is further substantiated by the observation that impedance changes with changes in posture (20). Obviously, temperature changes and postural changes reflect fluid redistribution rather than changes in total body fluid volume. Changes in specific resistivity are too small and in some cases in the wrong direction to account for these observations.

Many previous investigators have assumed that specific resistivity was unchanged throughout the course of their measurements of bioelectrical properties. Bonnardeaux (1) and Salansky and Utrata (21) reported data from animal studies

which suggest that blood osmolality and impedance are inversely related. Likewise Kobayashi et al. (8) reports on a paper written in Japanese by Tanaka et al. (26) which observed that specific resistivity of blood in humans was related to hematocrit. Kobayashi et al. (8) found that adjustment of specific resistivity for hematocrit resulted in much improved impedance cardiography. Postural changes, changes resulting from dehydration due to unreplaced sweat loss, and metabolic activity can all influence the electrical characteristics of blood which would likely result in alterations of electrical properties independent of changes in fluid volumes. In the present study, plasma osmolality was frequently measured and changed only slightly during the measurement period. For Subject A, however, a lower body negative pressure treatment preceded three of the bioelectrical measurements and caused among other things, hemoconcentration. Despite the lack of fluid loss consequent to LBNP, the resistance measurements were influenced (Fig 4a.).

In view of this somewhat cloudy picture, a number of questions remain unanswered. Among these are:

1) How does specific resistivity vary among individuals?

2) Within individuals, how does specific resistivity vary as intravascular, interstitial, and intracellular fluid levels change?

3) Why do segmental resistances and reactances vary in response to the same general body fluid alteration? (i.e. Why did the resistance and reactance values for the segments fail to unanimously track each other in a parallel fashion?)

4) Which fluid compartment(s) exert the greatest influence on electrical resistance and reactance?

CONCLUSIONS

A large body of literature exists which suggests that alterations in body electrical properties are related to alterations in fluid levels. Among these are studies which demonstrate good correspondence between impedance and cardiac output (8,9), impedance and limb volume (11), and impedance and weight changes consequent to dialysis (19). The present data, although limited to two subjects, suggests that electrical changes may be more closely linked to blood volume rather than TBW. This does not directly contradict previous studies, in that TBW and blood volume are probably closely related. Undoubtedly some of the relationships between electrical characteristics and fluid volumes and distributions are causal. The exact nature of these relationships awaits further research.

REFERENCES

1. Bonnardeaux, J.L. The behavior of blood plasma during asphyxia and water deprivation. Arch. Int. Physiol. Biochem. 80:749-760, 1972.

2. Carlson R., E. Fegelman, R.K. Finley, S.F. Miller, L.M. Jones, R. Richards, and S. Alkire. Assessment of fluid retention in burn patients by using bioelectrical impedance analysis. (Abstract) Am. Burn Assn, Spring, 1986.

3. Caton, J.R., P.A. Mole, W.C. Adams, and D.S. Heustis. Body composition analysis by bioelectrical impedance: effect of skin temperature. Med. Sci. Sports Exerc. 20(5), 489-491, 1988.

4. Hoffer E.C., C.K. Meador, D.C. Simpson. Correlation of whole-body impedance with total body water volume. J. Appl. Physiol. 27(4):531-534, 1969.

5. Hoffer E.C., C.K. Meador, and D.C. Simpson. A relationship between whole body impedance and total body water volume. Annals NY Acad. Sci. 197:452-469, 1970.

6. Hutcheson, L., R.W. Latin, and K.E. Berg. Body impedance analysis and body water loss. Res. Q. Exerc. Sport 59 (4):359-362, 1988.

7. Johnson, P.C. Fluid volume changes induced by spaceflight. Acta Astro. 6:1335-1341, 1977.

8. Kobayashi, Y., T. Andoh, T. Fujinami, K. Nakayama, K. Takada, T. Takeuchi, and M. Okamoto. Impedance cardiography for estimating cardiac output during submaximal and maximal work. J. Appl. Physiol.:Respirat. Environ. Exercise Physiol. 45(3):459-462, 1978.

9. Kubichek, W.G., R.P. Patterson, and D.A. Witsoe. Impedance cardiography as a noninvasive method of monitoring cardiac function and other parameters of the cardiovascular system. Ann. NY Acad. Sci. 170:724-732, 1970.

10. Kushner R.F., and D.A.Schoeller. Estimation of total body water by bioelectrical impedance analysis. Am J. Clin. Nutri. 44:417-424, 1986.

11. Levithan, B.M., L.D. Montgomery, P.K.Bagat, and J.F. Zieglschmid. A comparison of limb plethysmograph systems proposed for use on the space shuttle. Aviat. Space Eviron. Med. 54(1):6-10, 1983.

12. Lohman T.G., S.B. Going, L. Golding, J.H. Wilmore, W. Sinning, R.A. Boileau, and M. Van Loan. Interlaboratory bioelectrical resistance comparisons. (Abstract) Med. Sci. Sports Exerc. 19(2): Suppl., S40, 1987.

13. Lukaski H.C., P.E. Johnson, W.W. Bolonchuk, and G.I. Lykken. Assessment of fat-free mass using bioelectrical impedance measurements of the human body. Am. J. Clin Nutri. 41:810-817, 1985.

14. Lukaski H.C., W.W. Bolonchuk, C.B. Hall, and W. A. Siders. Validation of tetrapolar bioelectrical impedance method to assess human body composition. J. Appl. Physiol. 60(4):1327-1332, 1986.

15. Mayfield S.R., and R. Uauy. Measurement of extracellular water (ECW) in low birth weight (LBW) infants using bioelectrical reactance. Am. Ped. Soc., 1987.

16. McDougall D., and H.M. Shizgal. Body composition measurements from whole body resistance and reactance. Surg. Forum 37:42-44, 1986.

17. Molina S., T. Arango, O. Pineda, and N.W. Solomons. Response of bioelectrical impedance analysis (BIA) indices to rehydration therapy in severe infantile diarrhea. (Abstract) Am. J. Clin Nutri. 45(4):837, 1987.

18. Nyboer J. Workable volume and flow concepts of bio-segments by electrical impedance plethysmography. T.-I.-T. J. Life Sci. 2:1-13, 1972.

19. Patterson R. Body fluid determinations using multiple impedance measurements. IEEE Eng. Med. Biol. March, 16-18, 1989.

20. Quigley, M., S. Siconolfi, J. Agnew, and T. Rehbein. Fluid volume shifts during supine rest: effect on estimated total body water, lean body mass adn percent body fat from total body electrical impedance. Med. Sci Sports Exerc. 21(2):S99, 1989.

21. Salansky, I., And F. Utrata. Electrical tissue impedance of the organism and its relation to body fluids. Physiol Bohem. 21:295-304, 1972.

22. Schloerb P.R., J.H. Gurian, L.M. Lord, E.A. Winiarski, and C.M. Casey. Bioimpendance as a measure of total body water and body cell mass in surgical nutrition. (Abstract) Eur. Surg. Rsch. 18(sl):3, 1986.

23. Schoeller D.A., and R.F. Kushner. Determination of body fluids by the impedance technique. IEEE Eng. Med. Biol. March, 19-21, 1989.

24. Segal K.R., J.G. Kral, J. Wang, R.N. Pierson, T.B. van Itallie. Estimation of body water distribution by bioelectrical impedance. (Abstract) Fed. Proc. 46(4), 1987.

25. Spence J.A., R. Baliga, J. Nyboer, J. Seftick, and L. Fleischman. Changes during hemodialysis in total body water, cardiac output and chest fluid as detected by bioelectrical impedance analysis. Trans. Am. Soc. Artif. Intern. Organs 25:51-55, 1979.

26. Tanaka, K., H. Kanai, K. Nakayama, and N. Ono. The impedance of blood: the effects of red cell orientation and its application. Japan. J. Med. Eng.8:436-443, 1970.(In Japanese).

27. Zabetakis P.M., G.W. Gleim, K.E. Vitting, M.H. Gadensworty, M. Agrawal, M.F. Micheklis, and J.A. Nicholas. Volume changes effect electrical impedance measurement of body composition. (Abstract) Med. Sci. Sports Exerc. 19(2): Suppl., S40, 1987.

N90-24977

IDENTIFYING ATMOSPHERIC MONITORING NEEDS FOR SPACE STATION FREEDOM

Final Report

NASA/ASEE Summer Faculty Fellowship Program--1989

Johnson Space Center

Prepared By:	Dennis M. Casserly, Ph.D.,CIH
Academic Rank:	Assistant Professor
University & Department:	University of Houston - Clear Lake School of Natural and Applied Sciences Division of Life Sciences Houston, Texas 77058

NASA/JSC	
Directorate:	Space and Life Sciences
Division:	Medical Sciences
Branch:	Biomedical Laboratories
JSC Colleague:	Dane M. Russo, Ph.D.
Date Submitted:	August 11, 1989
Contract Number:	NGT 44-001-800

ABSTRACT

The atmospheric monitoring needs for Space Station Freedom were identified by examining from an industrial hygiene perspective: the experiences of past missions; ground based tests of proposed life support systems; the unique experimental and manufacturing facilities; the contaminant load model; metabolic production; and a fire. A target list of compounds to be monitored is presented and information is provided relative to the frequency of analysis, concentration ranges, and locations for monitoring probes.

INTRODUCTION

The Space Station Freedom is designed to operate for extended periods, up to 180 days, without resupply by utilizing a regenerative, nearly closed loop life support system. Under normal operating procedures, overboard disposal of wastes and venting of gases to space will not be allowed. All waste materials will be treated and recycled. Concentrated wastes will be stabilized and stored for ground disposal. The thirty year life of the station and the diversity of materials brought aboard for experimental or manufacturing purposes increases the likelihood of cabin contamination. Sources of contamination include: biological waste production, material off-gassing, process leakage, accidental containment breach, and accumulation due to poor removal efficiencies of the purification units.

An industrial hygiene approach was used to identify monitoring needs for Freedom. Included was a preliminary review of monitoring requirements for analogous ground based situations when breathing air is supplied, in confined spaces and on nuclear submarines. It was clear that continuous monitoring should be provided for components critical for life support, and that intermittent analysis be provided for all agents that may exceed the Space Maximum Allowable Concentration (SMAC). The minimum monitoring effort should include continuous monitoring for: nitrogen (N_2), oxygen (O_2), carbon dioxide (CO_2), carbon monoxide (CO), water (H_2O), hydrogen (H_2), methane (CH_4), hydrocarbons, refrigerants, and halons.[1]

In this paper the monitoring needs are identified by examining: the experiences of past missions; ground based tests; the station configuration; the life support system; the metabolic load from an 8-man crew; the contaminant load model; and a fire scenario.

SPACE STATION

The Space Station Freedom will have four modules: the U.S. Laboratory (USL); the U.S. Habitation module (USHAB); the Japanese Experimental Module (JEM); and the European Space Agency (ESA) module, Columbus. The modules are connected by four resource nodes. An airlock and a logistics module are connected to the resource nodes.

Air Revitalization System

Each module will have an independent Air Revitalization System (ARS) with an Environmental Control Life Support System (ECLSS) and a Trace Contaminant Control System (TCCS). The U.S. modules will have four ARS units, two in each module. Each ARS is designed to support four crew members. One ARS at a time will operate in each module.

The ARS will provide ventilation to each module and node but not to the airlock. Intramodule circulation will approximate near perfect mixing with an intermodule air exchange of 140 cubic feet per minute (CFM).[2] The ventilation design is based: on heat transfer and humidity control to maintain crew comfort; and on O_2 supply and CO_2 removal based on metabolic requirements.[3] The air exchange rate will be 1-2 years, achieved through air loss from leakage and airlock extra vehicular activity (EVA).

The technology base for the TCCS is good and system tests have worked as predicted. The TCCS will consist of fixed bed charcoal filters, high efficiency particulate filters, and a high temperature (680 °C) catalytic oxidizer (palladium/aluminum) with pre and post sorbent beds of lithium hydroxide (LiOH). There will be four units, two in each module. The air flow through each catalytic oxidizer is 2.5 CFM, or 5 CFM for the two U.S. modules.[4] Assuming a station volume of 900 M^3, this is only 0.22 air changes per day of what should be considered as fresh air. This flow rate is low as, the indoor air quality ventilation guideline for fresh air intake is 15 CFM per person.[5] This guideline is intended to keep odors to an acceptable level to 80% of the visitors entering the space and it assumes that one third of the occupants are smoking at the rate of 2.2 cigarettes per hour. The TCCS will receive cabin air from the temperature and humidity control system. It must handle purge gases that will be routed to the TCCS for contaminant removal from the ARS, waste water recovery, urine processing, waste reduction, storage systems, and lab racks.

U.S. Modules

The U.S modules will provide facilities for on-orbit repair, health maintenance, and a number of material processing and biological experiments intended to lead to manufacturing in space.

A maintenance work station will allow on-orbit repair of defective or damaged hardware. Processes likely to be required are drilling, sawing, welding, soldering, and epoxy gluing. A work bench/contaminant control console is envisioned that will collect the particulate and gaseous emissions generated in the repair process near their source.[6] The rack would be equipped with filters and the air recirculated with some venting to the TCCS. The work station would be a source of particulates, metal fumes, and gases not encountered on prior missions.

The health maintenance facility will provide critical care for one individual for 28 days and outpatient care for the crew complement for the mission duration. The equipment and supply list for this facility will be lengthy.[7] It may be an additional source of trace contaminants, mainly sterilants.

The U.S. Laboratory will provide facilities for experiments and manufacturing.[8] The candidate facilities, experimental processes, and materials are being baselined. These processes will generate biologicals, combustion and oxidation products, acid gases, metal and crystal fumes, and assorted lab wastes. Approximately 300 chemicals and mixtures have been identified for use in USL experiments. An evaluation should be made to determine the probability of these agents to approach harmful concentrations. Also, many of these materials are capable of adversely affecting the ECLSS subsystems by poisoning the catalyst or absorption beds, or they could appear in the humidity condensate, the potable water supply. These materials will have to be stored, transported to the point of use, and the waste products handled. The lab racks will be contained with at least a two failure tolerant design. That is, there will be three levels of containment by procedure or seal. Each rack will be equipped with some type of contaminant control equipment and vented to the TCCS. The lab racks should be equipped with monitors, specific for the process they contain to detect internal leaks. The chemical storage area should be monitored, and the cabin atmosphere must be routinely sampled to alert the crew of any leak.

MONITORING NEEDS

Past Experiences

Experiences of past missions and ground based systems tests have identified a number of health concerns that should be addressed in a monitoring plan for Space Station Freedom. Paramount is the flight and post flight health complaints of the crews: headache; irritation of the eyes and upper respiratory tract; and odor complaints, symptomatic of noxious air.[9] Early missions had insufficient monitoring data for evaluation, which indicated a need for a more comprehensive monitoring system. Analyses of activated carbon and LiOH filters of the atmospheric revitalization systems, and the active sampling and analysis for air contaminants of later missions have identified over 250 contaminants in spacecraft air.[10] Most were observed at trace levels, well below the SMAC. Others may have been present in sufficient concentrations to elicit symptoms among crew members, may accumulate to harmful levels during extended missions, or may have potential to poison the spacecraft's life support system.

Nitrogen tetroxide (N_2O_4), hydrazine, and monomethyl hydrazine are the main liquid propellants to be used on Freedom. Because of the quantities involved and the frequency of EVA, some internal contamination will occur. The airlock will likely serve as a decontamination station and will contain a propellant monitor or probe. If elevated propellant concentrations are detected in the airlock, then that atmosphere will be dumped to space to prevent contamination of the cabin atmosphere. The air

revitalization and trace contaminant control systems have not been designed to handle high pollutant loads. N_2O_4 decomposes to NO_2, so elevated NO_2 concentrations can be expected. Some N_2O_4 contamination occurred on Apollo-Soyuz.[9]

Halon 1301 is no longer the primary fire suppressant baselined for Freedom, but it is still used on the Shuttle and baselined for Columbus. Halon was detected on spacelab mission SL-1 and on Shuttle missions STS-3, and STS-4. The trace contaminant control system (TCCS) will only handle modest quantities. Halon degradation products are toxic and will poison the catalytic oxidizer. If a halon release occurs it may be necessary to vent the cabin air to space and repressurize. Monitoring should therefore be required for Halon 1301 as long as it is aboard Columbus and the Shuttle.

Methane (CH_4) is a metabolic product that accumulates as each mission progresses. It will likely be the contaminant of greatest concentration. The Bosch CO_2 reduction system, a candidate for the air revitalization system (ARS), will produce large quantities of methane. A high temperature catalytic oxidizer will be required to keep CH_4 concentrations below 1 ppm.[4,11] Continuous monitoring for methane is recommended.

CO, a product of incomplete combustion, may be released from metabolic processes, smoldering of carbon filters, or fire. The Bosch CO_2 reduction system produces CO and the potential for rapid accumulation exists, if not removed by the trace contaminant control system.[4,11] There are more deaths from CO poisoning than any other chemical agent, therefore, continuous monitoring for CO is recommended.

Ammonia (NH_3) is used in the active thermal control system on the Shuttle and possibly Space Station. It is a metabolic product that will be released from urine processing, and it is also a degradation product of the solid amine resin proposed for the ARS.[12] If not removed NH_3 will exceed SMAC values within days. The condensing heat exchanger is relied upon for NH_3 removal but phosphoric acid impregnated charcoal filters can also remove it. An NH_3 monitor is recommended.

Hydrogen will be produced by electrolysis and used in CO_2 reduction by both the Bosch and the Sabatier processes.[4,11,13] A pressure gradient will be used to minimize the likelihood of explosive mixtures from developing, if a leak occurs. H_2 accumulation is likely and continuous monitoring is recommended.

Toluene was detected on a number of missions. On Shuttle mission STS-2, toluene approached the SMAC value in one sample. Subsequent analyses indicated that for the sample, the additive toxicity hazard index for systemic poisons was exceeded by 1.22 times, with toluene the major constituent.[9] Toluene is also a

contaminant which off-gases from the solid amine resin of the ARS.[12]

Trimethylamine is a principal breakdown product of the solid amine resin of the ARS. The trimethylamine concentration has exceeded safe limits in tests of the ARS.[12] Because of the numerous trace organics off-gassing from solid amine process a post sorbent bed such as phosphoric acid impregnated charcoal will be used.

Glutaraldehyde escaped containment on Spacelab mission SL-D1. Glutaraldehyde is a preservative and disinfectant with irritating properties. It may also be used in electrophoresis experiments on Space Station.

Silicon oil was released on mission 61A, wetting surfaces and making decontamination difficult. Silicon compounds are catalyst poisons and will occur on Space Station.

Freons have been detected on all Shuttle missions.[14] The degradation products are corrosive, irritating, toxic, and catalyst poisons. Freon 12 will be on Freedom and continuous monitoring is recommended.

A computer model developed from Shuttle activated charcoal canister analysis for TCCS contaminant removal studies indicated that five contaminants may exceed SMAC values: propenal (acrolein), an irritant; benzene, a systemic poison and carcinogen; o-diethylphthalate, an irritant; propylfluorosilane, an irritant and catalyst poison; and 2-methylhexane, a central nervous system depressant.[15] Benzene has also temporarily exceeded SMAC values during preflight off-gassing tests.[14]

Ethanal (acetaldehyde), ethanol, dichloromethane, and acetone have a high frequency of occurrence on shuttle missions and are likely to be present on Freedom.[14]

Oxidation products will be produced in the catalytic oxidizer. Post sorbent beds are necessary to prevent the release of oxidants and free radicals to the cabin air from the TCCS. Also, it has been hypothesized that secondary pollutants are important in cabin atmospheres. Trial simulations have indicated that spacecraft cabins may develop elevated NO_2 concentrations and O_3 concentrations exceeding SMAC values.[16] Oxidation products, NO_2, O_3, and formaldehyde, were among the contaminants suspected of causing irritation on Shuttle flights, although particulates from biological sources were an undisputed cause of crew discomfort.[17] Intermittent monitoring is recommended for these contaminants.

Contaminant Load Model

The Space Station trace contaminant load model is being used to design the ECLSS such that no substance will exceed the SMAC.[18] In the model the generation rates in mg/day for 214 contaminants were estimated for the Space Station, consisting of two habitation modules, two laboratory modules and a logistics module. That configuration is slightly larger than the configuration presently baselined. The generation rates, the corresponding SMACs, and the Space Station volume (900 M^3) were used to estimate the time required to reach ½ SMAC, provided no removal mechanisms were operating. Those agents without a SMAC were assigned a conservative value of 0.1 mg/M^3. The time in days is given by:

$$T_{½SMAC} = \frac{\text{SMAC (mg/M}^3\text{) [SS Volume (900 M}^3\text{)] (0.5)}}{\text{Generation rate (mg/day)}}$$

Contaminants not reaching ½ SMAC within 365 days would be controlled by leakage alone, provided all contaminant sources were considered by the model. In such a case, monitoring would not be necessary. Any contaminant which would not reach ½ SMAC within 90 days could be excluded from monitoring requirements (provided all contaminant sources were considered by the model), since the SMAC would not be reached for 180 days. Presumably, samples will be returned for exhaustive ground based analysis at least every 180 days, thus providing adequate time for identifying any etiological agent and remedial action.

From the trace contaminant load model analysis, 34 contaminants were identified and listed below as candidates for onboard monitoring:

methanol
isopropyl alcohol
isobutyl alcohol
n-butyl alcohol
cyclohexanol
n-butylaldehyde
hexanal
heptanal
m-xylene
indene
propylbenzene
p-cymene
ethyl cellosolve
butylacetate
furan
sylvan
ethylacetoxyacetate
vinyl chloride
allyl chloride
chlorobenzene
isobutylene chloride
trichloroethylene
tetrachloroethylene
methyl ethyl ketone
methyl isobutyl ketone
cyclopentanone
methylheptanone
isobutyl ketone
acetonitrile
nitromethane
mercury
trimethylsilanol
p-dioxane
tetramethyl-1,2-epoxyethane

Although Freon 113 was identified as a major contaminant in the model, it is not baselined for use in Freedom and can be excluded from consideration in monitoring. This list can be further refined by determining SMACs for those compounds with conservative values of 0.1 mg/M^3 assigned and by considering the ECLSS removal efficiency for each agent.

The contaminant load model did not consider: contaminants from new systems and technologies; chemicals used for experimental and manufacturing purposes; cleansers; disinfectants; maintenance and repair activities; nor a full metabolic load from an 8-man crew.

The load model also only considers the independent action of each contaminant. An evaluation should consider additive toxicological effects, as more than one contaminant will likely be present. Remember, it is standard practice to assume additive effects, unless independent action is known. Since the ECLSS design is based on a contaminant load model using 7-day SMACs and considers only independent action, an evaluation by toxicological effects category is necessary.

Metabolic Load

The trace contaminant load model considered metabolic contaminants from the breath, sweat, and flatus of only one crew member. Off-gassing from urine and feces were not considered since the waste management system was assumed to contain and eliminate these metabolites as a source of atmospheric contamination. However, the analysis of Skylab 4 atmosphere shows 40 % of the volatiles to be of physiological orgin. The major constituents were acetone, 2-butanone, 2-propanol, 4-methyl-2-pentanone, and 2-octanone.[19] The Space Station cabin atmosphere will be subject to the metabolic wastes of 8 crew members, and the waste management system will be vented to the TCCS which must handle the load. Major metabolic products which must be removed by the ARS and the TCCS are CO, CO_2, NH_3, H_2S, CH_4, organic acids, ketones, alcohols, and mercaptans.[20]

Production rates of human metabolites[21] from an 8-man crew were used to determine the time required for these contaminants to reach ½ SMAC. The metabolic products and values are shown below. Acetone, CO, and NH_3 values include loadings from other sources previously discussed.

METABOLIC PRODUCTS (8-MAN CREW)

Contaminant	TIME to ½ SMAC (Days)
CO	6.9
NH_3	2.1
Acetone	76
Ethanol	8.1
Methyl Mercaptan	14
Ethyl Mercaptan	14
Propyl Mercaptan	14
Pyruvic Acid	1.0
Indole	0.7
Skatole	1.2

Fire

An unusual odor and crew headaches occurred on Shuttle flight STS-6. Burnt wire insulation from an electrical short was the suspected causal agent.[9] Electrical fire can produce a number of noxious agents including halogenated organics, benzene derivatives, nitriles, and cyanates.[22] Space Station design must be able to handle such contingencies either through the TCCS or a smoke removal unit,[23] without having to rely on venting the cabin air to space and repressurizing. The trace gas monitoring system should be able to detect and quantify contaminants representative of those generated by an electrical short or fire.

To ascertain monitoring needs following a combustion incident, the hypothesized concentrations of pyrolysis products after a fire and their corresponding SMACs were used to estimate a factor proportional to monitoring importance.

Contaminant	Concentration[23] (PPM)	SMAC (PPM)	Concentration/SMAC
CO2	10,000-100,000	5,000	2-20
CO	3,000-30,000	25	120-1200
HCN	5-100	1	5-100
HCl	5-100	1	5-100
NO2	1-100	0.5	2-200
H2S	1	2	0.5
SO2	100	1	100

Although the concentration of pyrolysis products vary widely from fire to fire, smoke detectors provide adequate warning of toxic products, since smoke is generally produced in copious amounts. Analysis of fire reports involving death or serious injury where smoke detectors have been installed show that the detector was inoperative or evacuation was not possible.

Investigation of fire fatalities have shown CO to be the primary toxicant with HCN often present in toxic quantities. However, documented cases of HCN being the primary toxicant are rare.[24]

Of the toxic gaseous products presented above, CO is expected to exist in highest concentration relative to its SMAC, therefore, if CO is below its SMAC value then the other toxic products would likely be also. Because of the uncertainty of predicting the concentration of pyrolysis products after a fire, monitoring should be considered for other toxic products as well: HCN, NO_2, HCl, and SO_2. Although no specific data could be found on the production of $COCl_2$, HF, COF_2, and short chain aldehydes, contingency monitoring should be considered because of their toxic and corrosive action.

For fire safety concerns, CO_2 will be used for fire suppression, followed by venting cabin air to space and repressurizing. Smoke detectors are an integral part of the fire detection and suppression system. To protect from toxic combustion products, infrared monitors have been previously recommended for CO, hydrogen fluoride (HF), and hydrogen cyanide (HCN).[25]

Volatiles will be released to the atmosphere from electrolysis and from phase change urine processing. Carboxylic acids and phenols will be major contaminants.[26,27] Iodination products from the water disinfection process may cross the air/water interface and permeate the life support environment. The identity of these products, their expected concentrations, and their medical effects are largely unknown.[28] However, the byproduct concentrations and effects of iodination are probably less than those resulting from chlorination.

CONCLUSIONS

The monitoring system for Space Station Freedom must be adaptable to accommodate new parameters and concentration ranges. All agents should be monitored that have a reasonable probability of occurrence at or above some action level, such as ½ SMAC. This would include the capability to monitor for toxics after a fire or spill so a pressurized element could be declared safe for entry or for removing protective gear donned during an incident. The analytical method relied upon must be able to quantify at action level concentrations. The basis for monitoring should be the contaminants: toxicity, quantities or production rates, removal efficiencies of the ECLSS system, and capacity to poison the ECLSS system. The importance for monitoring is increased by the relatively low air flow rate through the TCCS and high reliance on the TCCS for contaminant removal.

Continuous monitoring of cabin return air is required for major components and those critical for life support. The minimum

monitoring effort should include continuous monitoring for: N_2, O_2, CO_2, CO, H_2O, H_2, CH_4, non-methane hydrocarbons, aromatics, and halocarbons. There should be a sample line to each module routine comparison of atmospheres from remote sections of the spacecraft.

A monitor or probe will be needed in the EVA airlock for analysis of propellants: N_2O_4, hydrazine, and monomethyl hydrazine.

Other chemicals targeted for routine monitoring include: Freon 12, HCl, HCN, NH_3, O_3, NO_2, H_2S, HF, formaldehyde, Halon 1301, toluene, acetaldehyde, ethanol, acetone, dichloromethane, glutaraldehyde, trimethylamine, benzene, o-diethylphthalate, propylfluorosilane, 2-methylhexane, acrolein, methanol, vinyl chloride, isopropyl alcohol, allyl chloride, isobutyl alcohol, chlorobenzene, n-butyl alcohol, isobutylene chloride, cyclohexanol, trichloroethylene, n-butylaldehyde, tetrachloroethylene, hexanal, methyl ethyl ketone, heptanal, methyl isobutyl ketone, m-xylene, cyclopentanone, indene, methylheptanone, propylbenzene, isobutyl ketone, p-cymene, acetonitrile, ethyl cellosolve, nitromethane, butylacetate, mercury, furan, trimethylsilanol, sylvan, p-dioxane, ethylacetoxyacetate, tetramethyl-1,2-epoxyethane, methyl mercaptan, ethyl mercaptan, propyl mercaptan, pyruvic acid, indole, and skatole.

The chemical list can be refined by considering the removal efficiencies of the ECLSS and by assigning SMAC values to those compounds for which a value of 0.1 mg/M^3 was assumed. Also, an evaluation by toxicological effects category should be done to address additive effects. The above list was determined by considering independent action only, and more than one contaminant will be present.

Each experiment and manufacturing process must be evaluated in great detail for possible sources of cabin contamination. Lab facilities will be sources of biologicals, combustion and oxidation products, acid gases, metal and crystal fumes, and assorted lab wastes. The lab racks should be equipped with monitoring devices specific to the process being contained. The chemical storage area should also be equipped with a monitoring probe.

Finally, sample collection and preservation will have to be continued for ground based analyses, to confirm the accuracy and reliability of the onboard monitoring system.

REFERENCES

1. **Casserly, D. M. and D. M. Russo:** "A Rationale for Atmospheric Monitoring on Space Station Freedom." Proceedings of the 19th Intersociety Conference on Environmental Systems, San Diego, CA, July 1989. Paper No. 89154.

2. **Davis, R. G. and J. L. Reuter:** "Intermodule Ventilation Studies for the Space Station." Proceedings of the 17th Intersociety Conference on Environmental Systems, Seattle, WA, July 1987. Paper No. 871428.

3. **Reuter, J. L., L. D. Turner, and W. R. Humphries:** "Preliminary Design of the Space Station Environmental Control and Life Support System." Proceedings of the 18th Intersociety Conference on Environmental Systems, San Francisco, CA, July 1988. Paper No. 881031.

4. **Ray, C. D., K. Y. Ogle, R. W. Tipps, R. L. Carrasquillo and P. Wieland:** "The Space Station Air Revitalization Subsystem Design Concept." Proceedings of the 17th Intersociety Conference on Environmental Systems, Seattle, WA, July 1987. Paper No. 871448.

5. **Janssen, J. E. and D. T. Grimsrud:** "Ventilation Standard Draft Out for Review." ASHRAE Journal. pp. 43-45. November 1986.

6. **Junge, J.:** "A Maintenance Work Station for Space Station." Proceedings of the 16th Intersociety Conference on Environmental Systems, San Diego, CA, July 1986. Paper No. 860933.

7. **Harvey, W. T., S. M. Farrell, J. A. Howard Jr., and F. Pearlman:** "Space Station Health Maintenance Facility." Proceedings of the 16th Intersociety Conference on Environmental Systems, San Diego, CA, July 1986. Paper No. 860922.

8. **Perry, J. P. and W. R. Humphries:** "Process Material Management in the Space Station Environment." Proceedings of the 18th Intersociety Conference on Environmental Systems, San Francisco, CA, July 1988. Paper No. 880996.

9. **Rockoff, L. A.:** "Internal Contamination Issues." Proceedings of the Seminar on Space Station Human Productivity, NASA, Ames Research Center, Moffett Field, CA, March 1985. Paper N85-29543.

10. **Buoni, C., R. Coutant, R. Barnes, and L. Slivon:** "Space Station Atmospheric Monitoring Systems." Proceedings of the 37th International Astronautical Congress, Innsbruck, Austria, October 1986. Paper A87-15845.

11. **Wagner, R. C., R. Carrasquillo, J. Edwards, and R. Holmes:** "Maturity of the Bosch CO_2 Reduction Technology for Space Station Application." Proceedings of the 18th Intersociety Conference on Environmental Systems, San Francisco, CA, July 1988. Paper No. 880995.

12. **Wood, P. C. and T. Wydeven:** "Stability of IRA-45 Solid Amine Resin as a Function of Carbon Dioxide Absorption and Steam Desorption Cycling." Proceedings of the 17th Intersociety Conference on Environmental Systems, Seattle, WA, July 1987. Paper No. 871452.

13. **Boehm, A. M., C. K. Boynton, and R. K. Mason:** "Regenerative Life Support Program Equipment Testing." Proceedings of the 18th Intersociety Conference on Environmental Systems, San Francisco, CA, July 1988. Paper No. 881126.

14. **Coleman, M. E.:** "Summary Report of Post Flight Atmospheric Analysis for STS-1 to STS 41C." NASA-JSC Memorandum SD4-84-351, January 1985.

15. **Schwartz, M. R. and S. I. Oldmark:** "Analysis and Composition of a Model Trace Gaseous Mixture for a Spacecraft." Proceedings of the 16th Intersociety Conference on Environmental Systems, San Diego, CA, July 1986. Paper No. 860917.

16. **Brewer, D. A. and J. B. Hall Jr.:** "A Simulation Model for the Analysis of Space Station Gas-Phase Trace Contaminants." Acta Astronautica. Vol. 15, No. 8, pp. 527-543, 1987.

17. **Brewer, D. A. and J. B. Hall Jr.:** "Effects of Varying Environmental Parameters on Trace Contaminant Concentrations in the NASA Space Station Reference Configuration." Proceedings of the 16th Intersociety Conference on Environmental Systems, San Diego, CA, July 1986. Paper No. 860916.

18. **Leban, M. I. and P. A. Wagner:** "Space Station Freedom Gaseous Trace Contaminant Load Model Development." Proceedings of the 19th Intersociety Conference on Environmental Systems, San Diego, CA, 1989. Paper No. 891513.

19. **Liebich, H. M., W. Bertch, A. Zlatkis, and H. J. Schneider:** "Volatile Organic Components in the Skylab 4 Spacecraft Atmosphere." Aviation, Space, and Environmental Medicine. Vol. 46, No 8, 1975.

20. **Poythress, C.:** "Internal Contamination in the Space Station." Proceedings of the Seminar on Space Station Human Productivity, NASA, Ames Research Center, Moffett Field, CA, March 1985. Paper N85-29549.

21. **Coleman, M. E., D. L. Pierson and N. M. Cintron:** "Toxicological Requirements and Support Plan for the Space Station." JSC 32016, NASA-JSC, Houston, TX, June 1988.

22. **Nulton, C. P. and H. S. Silvus:** "Ambient Air Contamination-Characterization and Detection Techniques." Proceedings of the Seminar on Space Station Human Productivity. NASA, Ames Research Center, Moffett Field, CA, March 1985. Paper No. N85-29546.

23. **Birbara, P. J. and J. T. Leonard:** "A Smoke Removal Unit." Proceedings of the 17th Intersociety Conference on Environmental Systems, Seattle, WA, July 1987. Paper No. 871449.

24. **National Fire Protection Association:** "Fire Protection Handbook." 15th Ed. Quincy, MA, NFPA, 1981.

25. **Cole, M. B.:** "Space Station Internal Environmental and Safety Concerns." In Spacecraft Fire Safety. NTIS HC A07/MF A01. NASA, 1987.

26. **Dehner, G. F. and D. F. Price:** "Thermoelectric Integrated Membrane Evaporation Subsystem Testing." Proceedings of the 17th Intersociety Conference on Environmental Systems, Seattle, WA, July 1987. Paper No. 871446.

27. **Fortunato, F. A. and K. A. Burke:** "Static Feed Electrolyzer Technology Advancement for Space Application." Proceedings of the 17th Intersociety Conference on Environmental Systems, Seattle, WA, July 1987. Paper No. 871450.

28. **Sauer, R. L., D. S. Janik, and Y. R. Thorstenson:** "Medical Effects of Iodine Disinfection Products in Spacecraft Water." Proceedings of the 17th Intersociety Conference on Environmental Systems, Seattle, WA, July 1987. Paper No. 871490.

EFFECT OF FLUID COUNTERMEASURES OF VARYING OSMOLARITY ON CARDIOVASCULAR RESPONSES TO ORTHOSTATIC STRESS

Final Report

NASA/ASEE Summer Faculty Fellowship Program--1989

Johnson Space Center

Prepared By:	John E. Davis
Academic Rank:	Assistant Professor
University & Department:	Alma College Department of Exercise and Health Science Alma, Michigan 48801
NASA/JSC	
Directorate:	Space and Life Sciences
Division:	Medical Sciences
Branch:	Space Biomedical Research Institute
JSC Colleague:	John B. Charles
Date Submitted	August 11, 1989
Contract Number:	NGT 44-001-800

ABSTRACT

Current operational procedures for shuttle crewmembers includes the ingestion of a fluid countermeasure approximately 2 hours before reentry into the earth's gravitational field. The ingestion of the fluid countermeasure is thought to restore plasma volume and improve orthostatic responses upon reentry. The present countermeasure consists of ingesting salt tablets and water to achieve an isotonic solution. It has yet to be determined whether this is the optimal drink to restore orthostatic tolerance. It is also not known whether the drink solution is effective in increasing plasma volume. The purpose of this study was evaluate the effectiveness of drink solutions of different osmolarity on restoring plasma volume and orthostatic responses. Six men (age = 31 $\pm$ 3.5 yrs, weight = 80.2 $\pm$ 4.7 kg, height = 179.8 $\pm$ 2.6 cm) were tested after giving informed consent and a medical screening. Each subject participated in four conditions. In all four conditions lower body negative pressure (LBNP) was used to test orthostatic responses. In the first condition, orthostatic responses were tested after no change in hydration state of the subject (euhydrated). In the second condition, the subject was dehydrated with lasix administration (20 mg IV). This was done to simulate the loss of plasma volume during spaceflight. In a third condition, orthostatic responses were tested following dehydration and rehydration with an isotonic countermeasure (1 liter of .9% saline). In the final condition, a hyperosmotic drink solution (1 liter of 1.07% saline) was given after lasix dehydration. Plasma volume, leg circumference, plasma osmolarity, forearm blood flow, heart rate, stroke volume, blood pressure, thoracic fluid index, and cardiac dimensions (echocardiography) were measured during rest, LBNP exposure, and recovery. Subjects lost approximately 12% of the initial plasma volume (420 ml) as a result of dehydration with lasix. Rehydration with the isotonic solution partially restored plasma volume, whereas the hypertonic drink solution fully restored plasma volume back to the euhydrated level. Thoracic fluid index (TFI) increased during LBNP in all conditions. However, the starting level of TFI were different, reflecting the differences in plasma volume. This suggests that there was a greater central blood volume during the euhydrated and hypertonic conditions than in the dehydrated and isotonic conditions. Even though there were differences in plasma volume and TFI, there were few differences in any other responses measured. Heart rate was slightly elevated during the dehydrated condition relative to the other three conditions. Stroke volume, systolic and diastolic blood pressure, forearm blood flow, and leg circumference were not different between conditions. The 12% reduction in plasma volume observed in this study was not sufficient to produce profound differences in the cardiovascular responses to orthostatic stress. This suggests that other mechanisms might be operational in producing the orthostatic intolerance following short duration space flight.

INTRODUCTION

Orthostatic hypotension has been commonly reported after space flight by crewmembers both during reentry and upon egress from a spacecraft. The decrease in blood pressure could have severe ramifications on the ability of the crew to control the spacecraft during reentry and any emergency egress that might occur. Orthostatic intolerance after short duration space flight (5-14 days) is thought to be a result of a reduction in plasma volume.

Plasma volume decreases during spaceflight as a result of a negative water balance. The decrease in plasma volume has been reported to be between 8 and 15% (8). In microgravity, there is a redistribution of fluids from the lower body to the head and upper body. Originally this was thought to result in a suppression of antidiuretic hormone and a potentiated diuresis (7). Recent studies have suggested that atrial natriuretic factor (ANF) is involved in the control of plasma volume during volume expansion (9,10). It is possible that ANF is involved in plasma volume regulation during space flight.

Crew members are well suited to a microgravity environment. However, upon return to a gravitational environment they are hypovolemic relative to preflight and thus more prone to orthostatic intolerance. A study by Bungo and Charles(1) has indicated that fluid ingestion prior to reentry minimizes the impairment of orthostatic responses following spaceflight. They attribute the improvement in orthostatic responses in those crewmembers that ingested a fluid countermeasure to a restoration of plasma volume as a direct result of the ingestion of the solution. No controlled measurements of plasma volume with and without the countermeasure have ever been made.

The present countermeasure consists of ingesting salt tablets and eight ounces of water approximately 2 hours before reentry. This is thought to result in an isotonic solution (.9% saline). A recent study by Bungo et al. (2) has looked at the ingestion of drinks of varying osmolarity and composition on plasma volume. They found that a hypertonic drink solution was more effective in increasing and maintaining plasma volume (4 hours).

To date, no studies have looked at the relationship between plasma volume and LBNP tolerance in a controlled study. The purpose of this study was to evaluate the effectiveness of drink solutions of varying osmolarity on restoring plasma volume and orthostatic responses.

HISTORICAL BACKGROUND

For a detailed historical background, please see 1988 Summer Faculty Fellowship Report (4).

METHODS

Six volunteers were recruited for the study by Krug International. All subjects were medically screened and given a detailed explanation of the study. Informed consent was obtained from all subjects before participating in the study. The study was approved by the JSC IRB. Each subject participated in four conditions: 1) LBNP control - euhydrated (EUH), 2) LBNP following lasix dehydration (DEH), 3) LBNP following lasix dehydration (20 mg IV) and rehydration (ISO) with an isotonic drink solution (1 liter of a .9% saline solution), and 4) LBNP following dehydration with lasix and rehydration (HYPER) with a hypertonic drink (1 liter of a 1.07% saline solution). Control LBNP tests were administered to each subject until a consistent pattern of responses was produced. Lasix was used to simulate the decrease in plasma volume observed during spaceflight. This dosage of lasix produced approximately a 12% reduction in plasma volume from the euhydrated level as has been reported previously (4). We randomized the order of treatments to eliminate any effects of one LBNP test on a subsequent test. All experiments began at the same time of day for each individual subject to eliminate any circadian effects on our findings. Testing began 2 hours after the ingestion of a small meal. Lower body negative pressure was performed approximately 3 hours and 30 minutes after ingestion of fluids. At least 72 hours was allowed between testing sessions.

Lower body negative pressure was applied using a chamber sealed at the waist with a rubber gasket. A vacuum pump was then used to withdraw air out of the chamber. The LBNP protocol is displayed in Table 1. The test was terminated if the subject's systolic blood pressure dropped suddenly (greater than 25 mmHg in 1 minute), systolic pressure reached 80 mmHg, bradycardia occurred (drop in HR greater than 15 BPM), subject distress, or subject request. Before, during, and immediately after LBNP a series of physiological measures described below were determined every minute. Only the results from the last 3 minutes from each stage were analyzed as the first 2 minutes at each stage represent transition responses.

Table 1. LBNP protocol

Time at Stage (min)	Pressure (mmHg)
20	0
5	-5
5	-10
5	-20
5	-30
5	-40
5	-50
5	0

Blood samples were taken from an antecubital vein before lasix injection (baseline) after lasix injection, after drink ingestion, 2 and 1/2 hours after drink ingestion, 90 minutes before, and immediately after LBNP. Changes in plasma volume were calculated from hematocrit (microhematocrit technique) and hemoglobin (Coulter Counter) ratios using the formula of Dill and Costill (5). A direct measurement of plasma volume was performed once (human serum labeled 125-I) in each subject before the first experimental testing. This value was used as the absolute plasma volume and changes were expressed relative to that value. Plasma osmolality was determined using freezing point depression on all blood samples. A 5 ml sample was required to do all of the hematological analysis. Plasma levels of antidiuretic hormone, atrial natriuretic factor, aldosterone, and catecholamines (epinephrine, norepinephrine) were measured for certain blood samples.

Leg circumference measurements were made every minute with a mercury-in-silastic strain gauge. The changes in leg circumference during LBNP exposure were used to approximate the amount of venous pooling in the legs.

Venous occlusion plethysmography with a mercury-in-silastic strain gauge was used to measure forearm blood flow. The forearm vasoconstrictor response as indicated by this technique was measured at each step of LBNP. Heart rate was determined using a three lead EKG. Blood pressure was measured once a minute using a standard auscultatory technique. 2-D and M-Mode echocardiography (ATL 4000 S/LC ultrasound system, ATL, Botheli, WA.) was performed at each stage of LBNP in order to assess relative changes in left ventricular dimensions with LBNP. Thoracic fluid index and stroke volume were measured with bioelectrical impedance (BOMED). Thoracic fluid index represents the impedance to current flow and thus is inversely related to the amount of fluid in the chest.

EMG was used to assess abdominal and leg muscle tension in order to monitor for muscle tensing. The subject was asked to maintain a resting EMG level throughout all LBNP tests.

RESULTS

Plasma Volume and Plasma Osmolarity.

Plasma volume decreased by approximately 12% as a result of lasix injection (Figure 1). Drink ingestion with the isotonic drink solution partially restored plasma volume to euhydrated levels. Ingestion of the hypertonic drink solution (HYPER) fully restored plasma volume to euhydrated levels. Plasma osmolarity did not change through any of the dehydration or rehydration procedures (Figure 2). This indicates the fluid losses and gains were isotonic relative to the plasma. There was a slight increase in plasma volume in all four conditions from the post drink to the pre

LBNP sample. This was probably a result of a change in posture (sitting to supine). During LBNP there was a decrease in plasma volume in all four conditions. This hemoconcentration has been commonly observed in the literature.

Thoracic Fluid Index.

Thoracic fluid index (TFI) increased in all four conditions with increasing levels of LBNP (Figure 3). This represents an increase in blood pooling in the legs and less in the thorax. The starting TFI was also different between condition, reflecting the different plasma volumes at the start of LBNP.

Heart Rate and Stroke Volume.

Heart rate increased in all conditions with increasing levels of LBNP (Figure 4). Heart rates tended to be higher at the higher levels of LBNP in the dehydrated condition than in the euhydrated, isotonic, or hypertonic conditions. Stroke volume decreased with increasing LBNP (Figure 5). Even though plasma volume and TFI were different between the conditions, stroke volumes were similar in the four conditions.

Blood Pressure.

Systolic blood pressure decreased with increasing levels of LBNP (Figure 6). However, there were no differences in systolic blood pressure between conditions. Diastolic pressure tended to increase at the higher levels of LBNP in the dehydrated, isotonic, and hyperhydrated conditions (Figure 7). There were no differences in mean arterial blood pressure with increasing LBNP stage or between conditions.

Forearm Blood Flow and Leg Circumference.

Forearm blood flow decreased in all conditions with increasing levels of LBNP (Figure 8). This was a reflex response to maintain blood pressure in the face of falling venous return. There were no differences between conditions. Leg circumference increased with increasing levels of LBNP (Figure 9). As LBNP level increases, venous pooling in the legs increase. There were no differences in leg circumference with differing hydration states.

DISCUSSION

Lasix reduced plasma volume by 12% in the present study. This was similar to the reduction observed in our previous study (4). Rehydration with an isotonic solution (present operational countermeasure) partially restored plasma volume to the euhydrated level. When subjects ingested the hypertonic solution, plasma volume was fully restored to the euhydrated level. These data support a recent study (2) which demonstrated that plasma volume increased following ingestion of both an isotonic and hypertonic drink solution, but the plasma volume was maintained longer with the hypertonic solution.

Bungo and Charles (1) found that ingestion of a drink solution improved orthostatic tolerance after spaceflight. They attributed the decrease in orthostatic tolerance (higher heart rates, lower blood pressures) to the decrease in plasma volume that has been observed after space flight (8). We expected to see improved orthostatic responses after rehydration with both the isotonic and hypertonic drink solutions in comparison to the dehydrated condition, our model for space flight. However, there were only minor differences between conditions in heart rate, stroke volume,blood pressure (systolic and diastolic), forearm blood flow, and leg circumference.

It is possible that the differences in plasma volume produced in this study were not great enough to produce marked differences in cardiovascular responses. Other studies using exercise as a stressor have shown that plasma volume differences of the magnitude observed in this study produce significant differences in cardiovascular responses (6).

It is also possible that the reduction in plasma volume produced by lasix administration does not truly model spaceflight. Lasix did produce a 12% reduction in plasma volume which is consistent with space flight reductions in plasma volume. Our model might not have produce some of the other physiological alterations that have been observed with space flight. However, most of the alterations that would influence orthostatic responses are thought to occur in response to longer duration space flight (greater than 14 days). Although a recent study by Convertino et al. (3) has demonstrated changes in venous compliance with 4 days of 6° head down bed rest. This reduction in venous compliance was inversely related to the loss of the size of the leg muscle compartment. This might be a contributing factor to the orthostatic intolerance that occurs after short duration spaceflight and might be more important than plasma volume alterations.

Another explanation could be the difference in the composition of the countermeasure. The present countermeasure consists of ingesting 2 salt tablets and 8 ounces of water every 30 minutes for 2 hours prior to reentry. In the present study, subjects ingested a solution of .9% saline. Perhaps there are differences in the physiological effects of ingesting a solution verses salt tablets and water.

CONCLUSIONS

A hypertonic drink solution was more effective in restoring plasma volume after dehydration than an isotonic solution. However, there were no differences in their effects on an orthostatic challenge. These data suggest that the plasma volume differences produced in this study were not sufficient to produce differences in the cardiovascular responses to an orthostatic challenge, or there are other changes that occur during space flight that are more important in determining orthostatic intolerance.

REFERENCES

1. Bungo, M. W., J.B. Charles, and P.C. Johnson. Cardiovascular deconditioning during space flight and the use of saline as a countermeasure to orthostatic tolerance. Aerospace Med. 56: 985-990, 1985.

2. Bungo, M.W., M.A.B. Frey, J.M. Riddle, and J.B. Charles. Effect of hyperosmotic saline ingestion on plasma volume and urine flow. Aerospace Med. 60: 499, 1989.

3. Convertino, V.A., D.F. Doerr, K.L. Mathes, S.S. Stein, and P.B. Buchanan. Changes in volume, muscle compartment, and compliance of the lower extremities in man following 30 days of exposure to simulated microgravity. Aerospace Med. 60: 653-658, 1989.

4. Davis, J.E. A model for plasma volume changes during short duration space flight. In Summer Faculty Fellowship Report, eds. R. Bannerot and S. Goldstein, NASA Report # NGT 44-005-803, 1988.

5. Dill, D.B., and D.L. Costill. Calculation of percentage changes in volumes of blood, plasma, and red cells in dehydration. J. Appl. Physiol. 37:247-248, 1974.

6. Fortney, S.M., C.B. Wenger, J.R. Bove, and E.R. Nadel. Effect of blood volume on forearm venous and cardiac stroke volume during exercise. J. Appl. Physiol. 55: 884-890, 1983.

7. Gauer, O.H., and J.P. Henry. Neurohumoral control of plasma volume. Int. Rev. Physiol. 9:145 -190, 1976.

8. Johnson, P.C. Fluid volume changes induced by spaceflight. Acta Astro. 6:1335-1341, 1977.

9. Lang, R.E., H. Tholken, D. Ganten, F.C. Luft, H. Rushoka, and T.H. Urger. Atrial natriuretic factor: a circulating hormone stimulated by volume loading. Nature 314: 264-266, 1985.

10. Sakamoto, H., and F. Marumo. Atrial natriuretic peptide secretion in response to volume expansion and contraction in normal man. Acta End. 118:260-268, 1988.

Figure 1. Plasma volume plotted as a function of sample number. Mean + SE

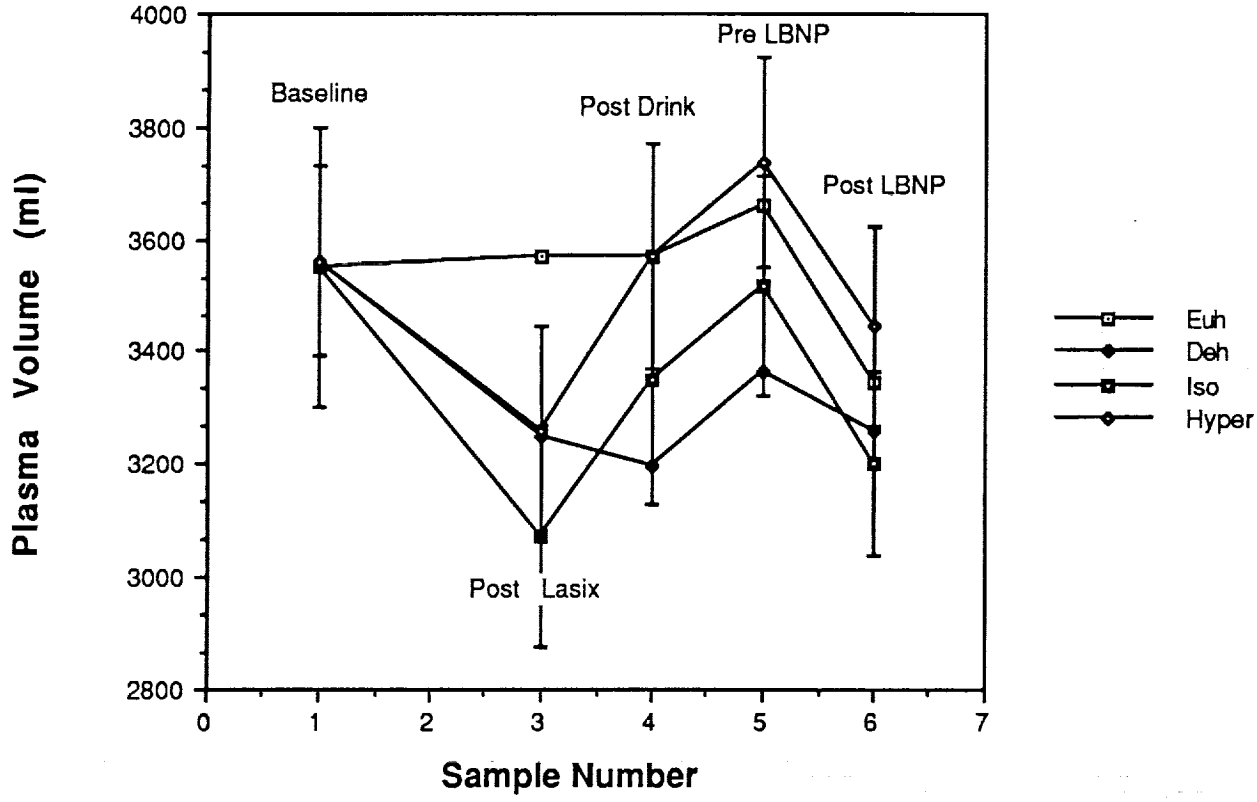

Figure 2. Plasma Osmolarity plotted as a function of sample number. Mean + SE

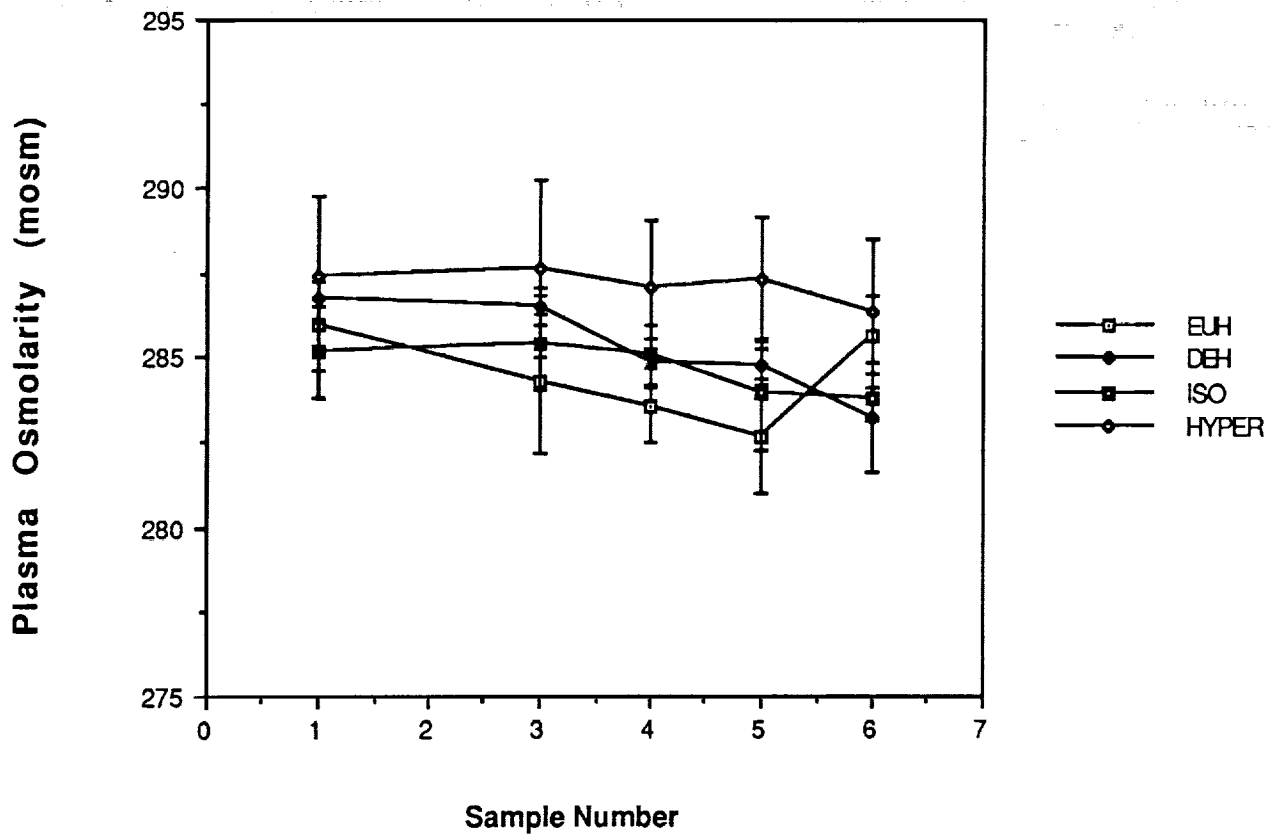

Figure 3. Thoracic fluid index plotted as a function of LBNP stage. Mean + SE.

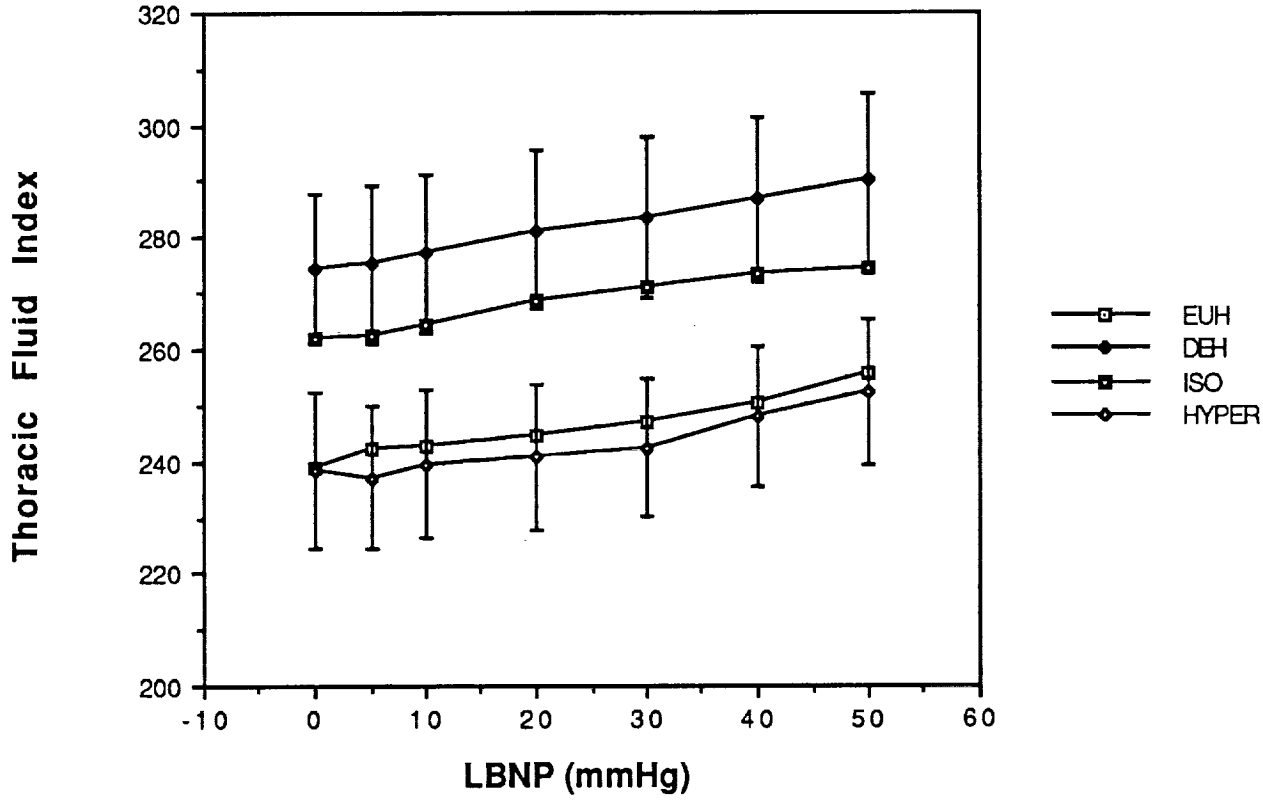

Figure 4. Heart rate plotted as a function of LBNP stage. Mean + SE.

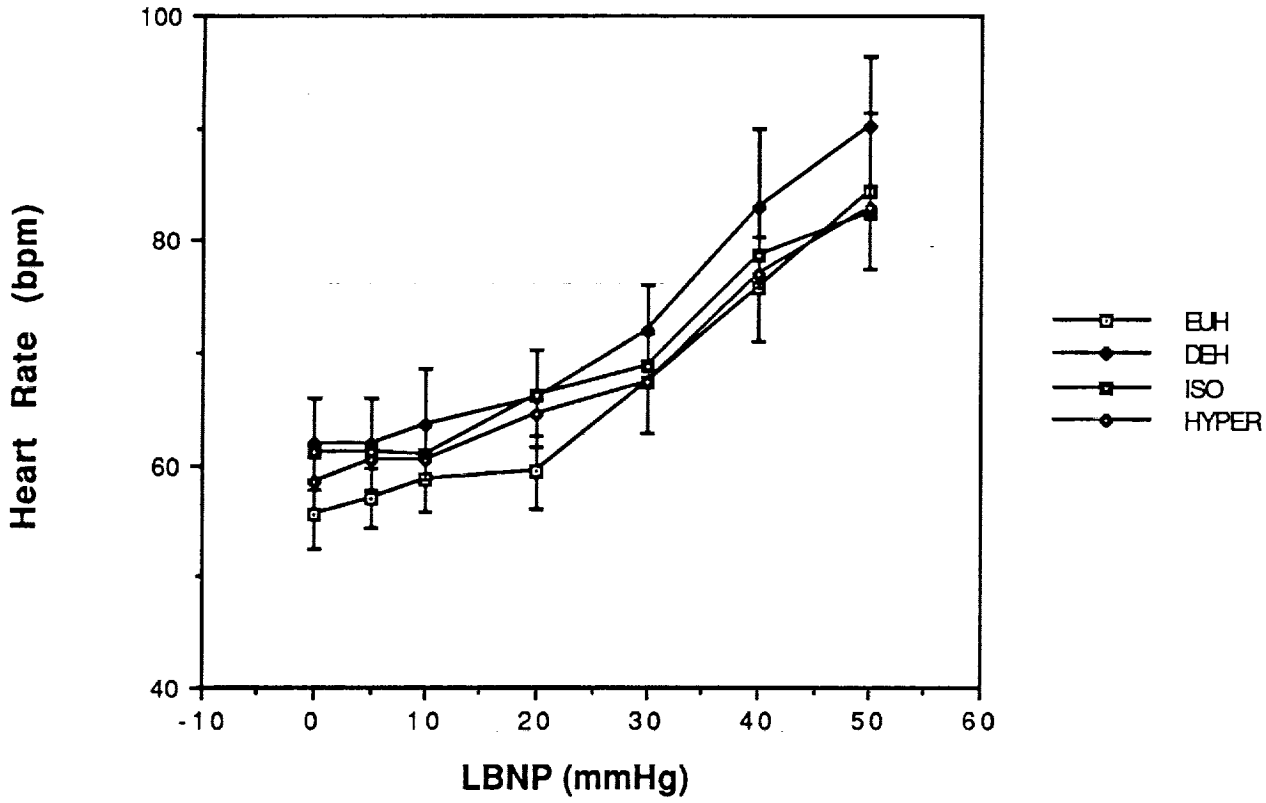

Figure 5. Stroke volume plotted as a function of LBNP stage. Mean + SE.

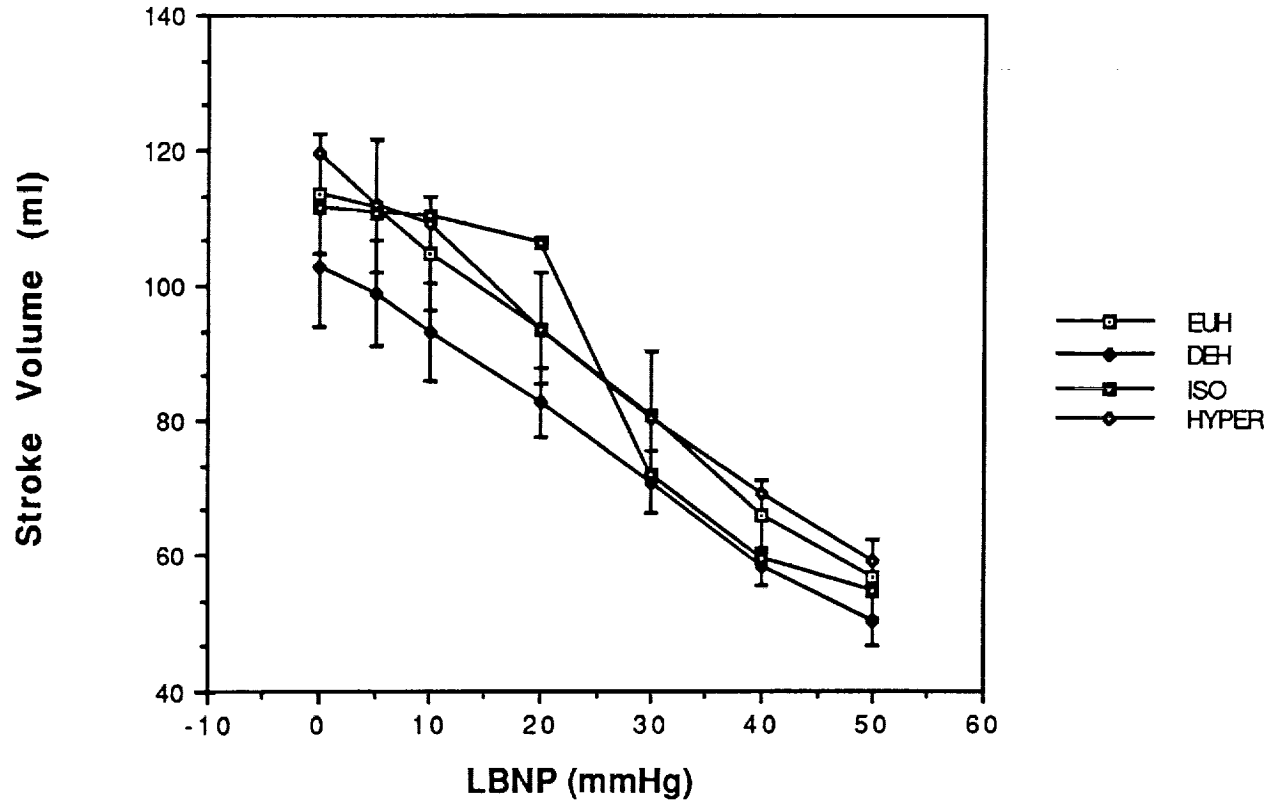

Figure 6. Systolic Blood Pressure plotted as a function of LBNP stage. Mean + SE.

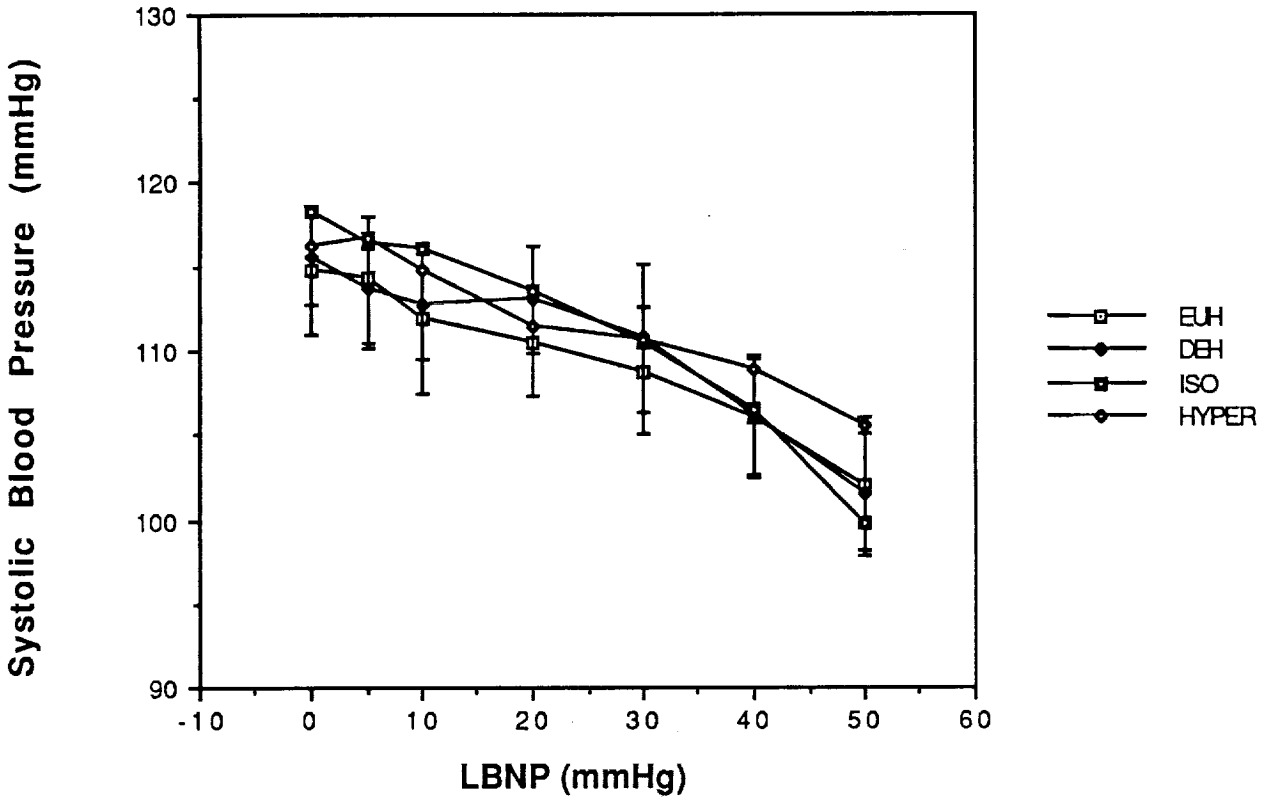

Figure 7. Diastolic blood presure plotted as a function of LBNP stage. Mean +SE.

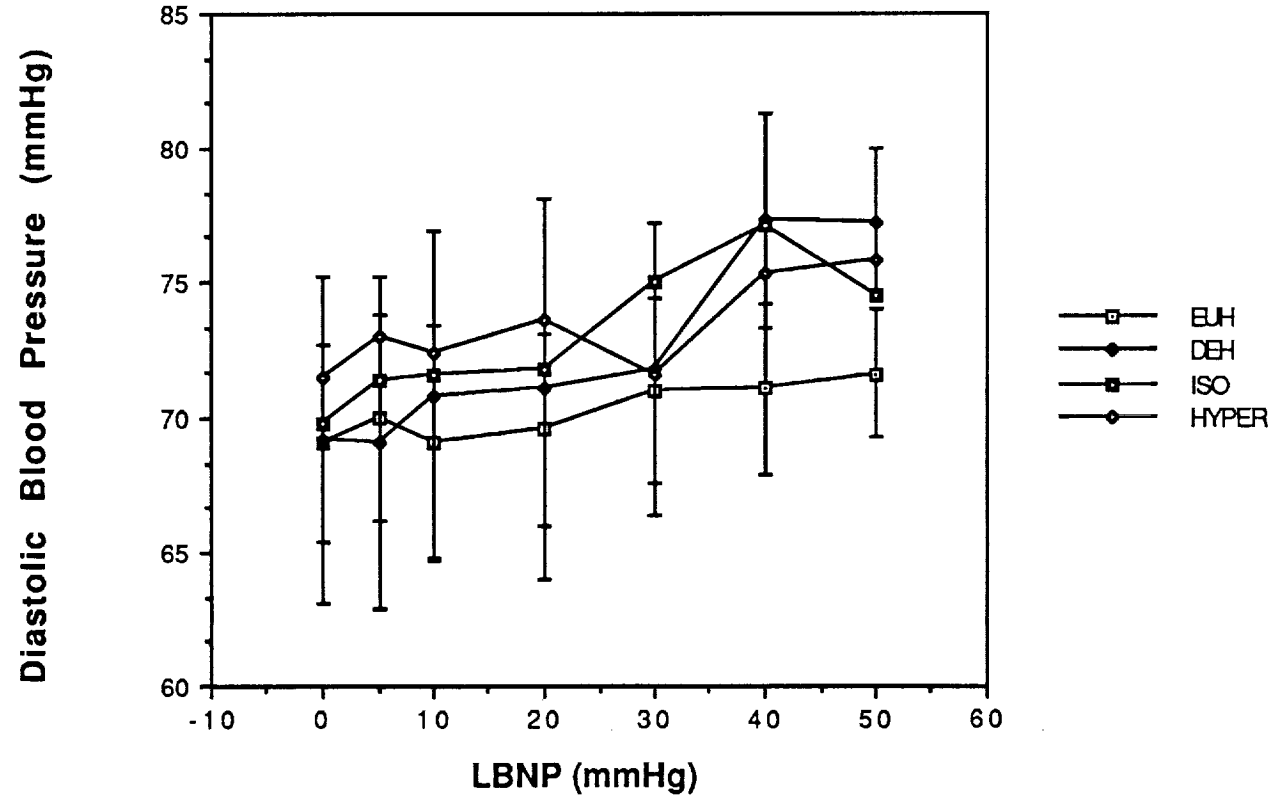

C-2

Figure 8. Forearm blood flow plotted as a function of LBNP stage. Mean + SE.

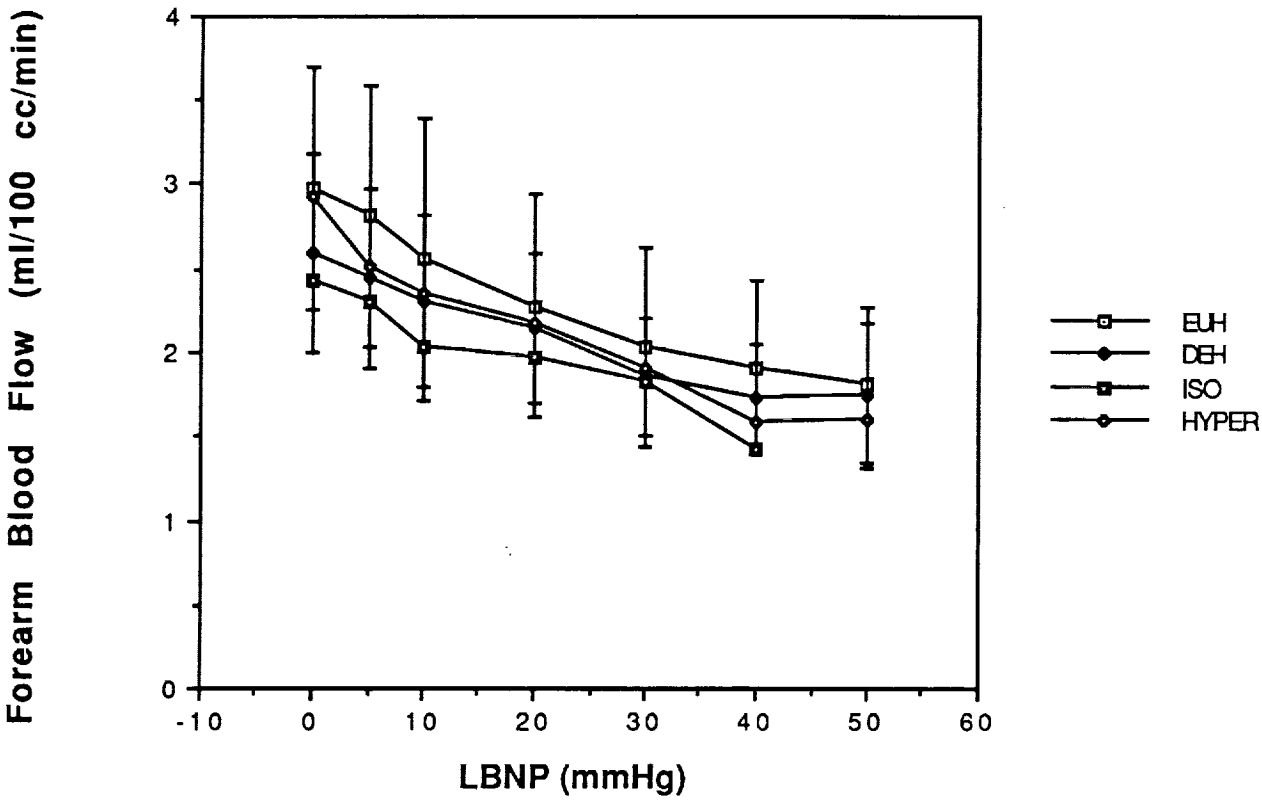

Figure 9. Change in leg circumference plotted as a function of LBNP stage. Mean + SE.

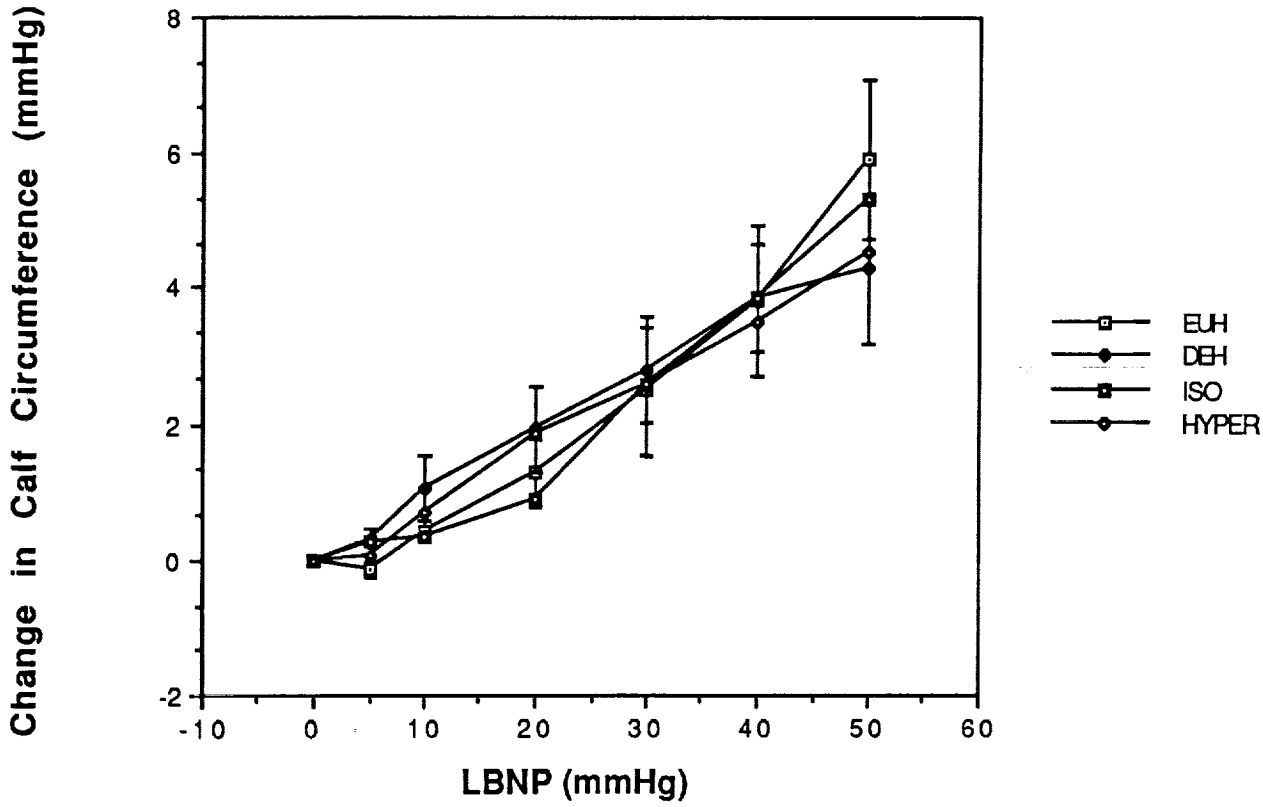

SOLVING PROBLEMS BY INTERROGATING SETS OF KNOWLEDGE SYSTEMS: TOWARD A THEORY OF MULTIPLE KNOWLEDGE SYSTEMS

FINAL REPORT

NASA/ASEE Summer Faculty Fellowship Program -- 1989

Johnson Space Center

Prepared By:	Andre de Korvin, Ph.D.
Academic Rank:	Professor
University & Department:	University of Houston - Downtown
	Applied Mathematical Sciences
	Houston, Tx. 77002
NASA / JSC	
Directorate:	Mission Support
Division:	Mission Planning and Analysis
Branch:	Technology Development and Applications
JSC Colleague:	Robert Lea, Ph.D.
Date Submitted:	August 11, 1989
Contract Number:	NGT 44-001-800

ABSTRACT

The main purpose of the present work is to develop a theory for multiple knowledge systems. A knowledge system could be a sensor or an expert system, but it must specialize in one feature. The problem is that we have an exhaustive list of possible answers to some query (such as "What object is it?"). By collecting different feature values, we should, in principle, be able to give an answer to the query, or at least narrow down the list.

Since a sensor, or for that matter an expert system, do not in most cases yield a precise value for the feature, uncertainty must be built into the model. Also, we must have a formal mechanism to be able to put the information together. We chose to use the Dempster - Shafer approach to handle the problems mentioned above.

We introduce the concept of a state of recognition and point out that there is a relation between receiving updates and defining a set valued Markov Chain. Also, deciding what the value of the next set valued variable is can be phrased in terms of classical decision making theory such as minimizing the maximum regret. Other related problems are looked at.

INTRODUCTION

The purpose of the present work is to show how taking independent and very diverse evidence, we can piece things together to arrive at an answer to the question: "What object is it?". We will take the Dempster - Shafer approach to put the evidence together. Such an approach has recently been taken in expert systems, see [2], [3], and [4]. However, to the best of this writer's knowledge, the results shown here are original. We start out with a simple example.

Consider the following data which assigns masses to subsets of {Bird, Plane, & Superman} according to the velocity observed:

VELOCITY	B	P	S	{BP}	{BS}	{PS}	{BPS}
0 - 100	.5	.1	.1	.2	.04	.04	.02
101 - 200	0	.4	.1	0	0	.5	0
201 - 500	0	.5	.1	0	0	.4	0
> 500	0	.1	.7	0	0	.2	0

NOTE:

- Birds don't fly with velocity > 100.
- Superman likes to fly at over 500 but he can fly at any speed he wants to.

It should be noted that the sum across each row is 1. The interpretation of the results says, for example, that at velocities exceeding 500 mph, the expert believes that the object is Superman. That expert doesn't totally rule out the possibility of plane as he assigns a mass of .1 to that event, and also that expert is somewhat unsure if the object is Plane or Superman and therefore, he assigns a mass of .2 to that aggregate. Note that we do not have Probability of {PS} be the sum of the Probability of P and of S. Masses assigned to sets that are not singletons denote the uncertainty of the expert. For example, .02 assigned to {BPS} reflects the degree of total ignorance that the expert has regarding what the object is when the object travels at less than 100 mph. Such a mass assigned is typical of the Dempster - Shafer approach to handle uncertainty in expert systems. See [10].

We now write down the data relative to observed color:

COLOR	B	P	S	{BP}	{BS}	{PS}	{BPS}
SILVER	.05	.6	.05	.1	0	.15	.05
WHITE	.1	.1	.05	.5	.05	.15	.05
RED	.1	.1	.1	.2	.2	.2	.1
BLUE	.1	.1	.1	.2	.2	.2	.1
RED-BLUE	.04	.04	.8	0	.05	.05	.02
OTHER	.6	.1	0	.3	0	0	0

NOTE:

- Red and blue generate the same (conditional) mass
- A gray bird may appear silver
- Superman wears red and blue but from some angles he may appear all red or all blue
- When flying at certain speeds, Superman may appear as a white or silver streak
- Color other than red, blue, white, silver rules out Superman

These two tables sum up the information collected from the experts. What we would like to do, of course, is to put these two pieces of evidence together.

CONCEPTS AND NOTATIONS

We now will formally define the concept of a mass function. A mass function is a function from subsets of the frame of discernment Θ into [0, 1] satisfying the following conditions:

(i) $m(\varnothing) = 0$

(ii) $\sum m(A) = 1$ where the sum is over all subsets of Θ

If m_1 & m_2 are two mass functions, we define

$$(m_1 \oplus m_2)(C) = \sum_{A \wedge B = C} m_1(A)\, m_2(B) \Big| (1 - k)$$

Where k is the conflict

$$k = \sum_{A \wedge B = \varnothing} m_1(A)\, m_2(B)$$

The operation defined above defines how to put information together. If two knowledge systems generate m_1 & m_2, $m_1 \oplus m_2$ is the mass generated by combining the two knowledge systems, see [10]. For a very readable interpretation of the combination rule in the setting of databases, see [12].

The belief generated by m is defined by

$Bel(A) = \sum m(B)$ over all *sets* B *such that* $B \subset A$. Also we define the plausability by

$$Pls(A) = \sum m(B) \quad \text{over all sets } B \text{ such that } B \wedge A \neq \varnothing$$

Now if the l^{th} sighting takes place at time t_l, set $dt_l = t_l - t_{l-1}$

Obviously, dt_l denotes the elapsed time between sightings. Assume that we have a weight function $\lambda(\bullet)$ satisfying

$$(i)\ 0 \leq \lambda(dt_l) \leq 1, \quad dt_l > 0$$

$$(ii)\ \lambda(dt_l) \text{ non decreasing as a function of } dt_l$$

We use weight to adjust masses. There are two ways to adjust

$$m_1(\bullet) = m_1(\bullet)$$

a) $$m_l(\bullet) = \lambda(dt_l)\, m_l(\bullet) + (1 - \lambda(dt_l))\, m_{l-1}(\bullet)$$

b) $$m_l(\bullet) = \lambda(dt_l)\, m_l(\bullet) + (1 - \lambda(dt_l))\, m_{l-1}(\bullet)$$

If λ is high i.e., dt_l high, go with the current observation

If λ is low i.e., dt_l low, go with the accumulated data.

Note that the first update is Markov - like as it only uses the mass collected on the previous sighting.

For our example, we could define the weight function by:

$$\lambda\ (dt_l) = \begin{cases} dt_l\ /\ 300 & if\ dt_l \le 300 \\ 1 & \text{otherwise} \end{cases}$$

That is, after 5 minutes, forget the previous observations and assume that a new object is being observed. The rationale for this is that the data has become too old to be reliable.

Going back to our example of bird, plane, and Superman, assume we have three sightings:

SIGHTING	TIME	dt_l	VELOCITY	COLOR
1	1:00 p.m.	0	101 - 200	WHITE
2	1:01 p.m.	60	201 - 500	WHITE
3	1:29 p.m.	1740	0 - 100	OTHER

The combined masses, not time adjusted are given below:

SIGHTING	B	P	S	{BP}	{BS}	{PS}	{BPS}
1 $m_1(\cdot)$	0	.7750	.1	0	0	.125	0
2 $m_2(\cdot)$	0	.8101	.0886	0	0	.1013	0
3 $m_3(\cdot)$	.811	.1024	0	.0866	0	0	0

The combined masses, time adjusted are given below:

SIGHTING	B	P	S	{BP}	{BS}	{PS}	{BPS}
1 $m_1(\cdot)$	0	.775	.1	0	0	.125	0
2 $m_2(\cdot)$	0	.78202	.09772	0	0	.12026	0
3 $m_3(\cdot)$	.811	.1024	0	.0866	0	0	0

NOTE: m_3 is not really time adjusted as sightings are more than 5 minutes apart.

Computing the belief, at each sighting, with respect to the time adjusted mass we have:

SIGHTING	OBJECT	Bel (•)	Bel (¬ •)	Bel (•) - Bel (¬ •)	CLASSIFICATION
1	B	0	1	-1	P
	P	.775	.1	.675	
	S	.1	.775	-.675	
2	B	0	1	-1	P
	P	.78202	.09772	.6843	
	S	.09772	.78202	-.6843	
3	B	.811	.1024	.7086	B
	P	.1024	.811	-.7086	
	S	0	1	-1	

The rationale for the table above is that Bel (•) - Bel (¬ •) measures how much a specific object exceeds, belief - wise, its competition. This criterion was already used in [8]. Thus the conclusion is that a plane was observed on the first and second sighting and a bird was observed on the last sighting. This example shows that there will be a payoff in studying a multi-knowledge systems setting. We also remark that a similar, but somewhat more complex approach could be used to obtain classification sequences.

MESHING THE INFORMATION COLLECTED FROM MULTIPLE KNOWLEDGE SYSTEMS

In this section, we consider the composition rule to be defined by the numerator only of $(m_1 \Theta m_2)$ (C). (Thus the empty set may pick up mass).

We now shift somewhat our perspective. Consider Knowledge Systems $KS_1, KS_2, \ldots KS_n$

KS_j reads the J^{th} feature and interprets its value to be f_j^i with a probability α_{ji}

It is important to keep in mind that in this setting, each knowledge system specializes in recognizing a specific feature.

Thus, KS_i defines the mass m_j on Θ by

$$m_j(A_{ji}) = \alpha_{ji} \text{ where}$$

$$A_{ji} \text{ denotes all objects of } \Theta \text{ whose } j^{th} \text{ feature has value } f_j^i$$

After we have interrogated $KS_1, KS_2, \ldots, KS_q$ possible answers are in sets $A_1t_1 \wedge A_2t_2 \wedge \ldots \wedge A_qt_q$. Let X_q be set-valued variables whose values are $A_1t_1 \wedge \ldots \wedge A_qt_q$ ($t_1, \ldots, t_q$ range over all possible values of the corresponding features). X_q indicates the current state of recognition. X_q may be viewed as a random set [9].

We have shown that X_q forms a (non-stationary) Markov chain. In fact, the transition probabilities are given by

$$Pr\left(X_{q+1} = A_{1t_1} \wedge \ldots \wedge A_{qt_q} \wedge A_{q+1\,t_{q+1}} \;\middle|\; X_q = A_{1t_1} \wedge \ldots \wedge A_{qt_q}\right) = \sum m_{q+1}\left(B_{q+1,i}\right)$$

Where the sum is over sets $B_{q+1,i}$ such that

$$A_{1t_1} \wedge \ldots \wedge A_{qt_q} \wedge B_{q+1,i} = A_{1t_1} \wedge \ldots \wedge A_{qt_q} \wedge A_{q+1t_{q+1}}$$

If

$$Pr\left(X_q = A_{1t_1} \wedge \ldots \wedge A_{qt_q}\right) = \mu_q\left(A_{1t_1} \wedge \ldots \wedge A_{qt_q}\right) \quad \text{then}$$

$$\mu_{q+1}\left(A\right) = \sum_B Pr\left(X_{q+1} = A \;\middle|\; X_q = B\right)\mu_q\left(B\right) \quad \text{where}$$

A is of the form $A_{1t_1} \wedge \ldots \wedge A_{qt_q} \wedge A_{q+1t_{q+1}}$ and B is of the form $A_{1u_1} \wedge \ldots \wedge A_{qu_q}$ with $B \wedge A_{q+1t_{q+1}} = A$

Since X_q forms a Markov Chain, a study of absorbing sets as well as entry and exit times could be made. We choose not to deal with these rather general questions but rather to pause some specific problems such as: what is the probability of realizing for the first time, as we interrogate KS_{q+1}, that the answer is not in the frame of discernment. What is the probability of getting no information from KS_{q+1}? (Of course we assume that $KS_1, KS_2, \ldots, KS_q$ were already interrogated). The answer to such questions has been derived and is given below.

Pr (Realizing for the 1^{st} time at time $q+1$ that answer not in frame of discernment)

$$= \sum m_{q+1}\left(B_{q+1,i}\right)\mu_q\left(A_{1t_1} \wedge \ldots \wedge A_{qt_q}\right)$$

where the sum is over all local elements $B_{q+1,i}$ of m_{q+1} such that

$$A_{1t_1} \wedge \ldots \wedge A_{qt_q} B_{q+1,i} = \varnothing \text{ yet } A_{1t_1} \wedge \ldots \wedge A_{qt_q} \neq \varnothing$$

That is, the averaged Bel_{q+1} of being outside the range of X_q when KS_{q+1} is interrogated.

$$Pr \text{ (No Info. from } KS_{q+1}) \qquad = \sum m_{q+1}\left(B_{q+1,i}\right)\mu_q\left(A\right)$$

where the sum is over $B_{q+1,i}$ superset of A, and A is of the form $A_{1t_1} \wedge \ldots \wedge A_{qt_q}$

Using the transition probabilities we have

$$Pr\left(X_{q+1} = A_{q+1t_{q+1}} \wedge \ldots \wedge A_{1t_1} \ldots X_1 = A_{1t_1}\right)$$

$$= Pr\left(X_1 = A_{1t_1}\right)\ldots\left(\sum m_2\left(B\right)\right)\ldots\left(\sum m_{q+1}\left(B\right)\right)$$

where the first sum is over all $B \wedge A_{1t_1} = A_{2t_2} \wedge A_{1t_1}$, and the last sum is over all B such that $B \wedge A_{qt_q} \wedge \ldots \wedge A_{1t_1} = A_{q+1t_{q+1}} \wedge \ldots \wedge A_{1t_1}$

All of this points out that it is very important to carefully evaluate X_q

TRUNCATING THE INFORMATION

Let $\{A_1, A_2, \ldots\}$ be distinct focal elements of $m_1, m_2, \ldots$ We can view KS_t as confirming A_i to the degree α_{ti} Let α_{ti^*} be the largest α_{ti} for t fixed (i^* depends on t).

Now view KS_t as confirming A_{i^*} to the degree α_{ti^*} and ignore the rest of the information yielded by KS_t (i.e., take only the highest confirmation of KS_t). If $s_1, s_2, \ldots s_k$ supported A_{i^*}, A_{i^*} is supported to the degree $1-(1-s_1)(1-s_2)\ldots(1-s_k)$

If the resulting mass on A_i is

$$Evi_i(A_i) = p_i, \text{ we set } Evi_i\{A_1, \ldots A_n\} = r_i, \text{ where } p_i + r_i = 1$$

The rationale for doing this is to trust our estimate of the mass on each A_i, which came from the highest degrees of confirmation, and to ignore the rest, i.e., spread the rest of the mass on all the possibilities.

It can be shown, see [1] that

$$Bel(A_j) = Kp_j \prod_{i \neq j} r_i \quad \text{Where}$$

$$K = 1 \Big| \left[\prod_j r_j \left(1 + \sum_i p_i \Big| r_i \right) \right]$$

At stage $q+1$, we then pick A_j maximizing Bel coming from $m_1, m_2, \ldots m_{q+1}$. In this way, prior information given by $m_1, \ldots m_q$, as well as the current information yielded by m_{q+1}, is taken into account.

We can extend this to keeping the two highest confirmations KS_t, as mentioned ealier, assigns α_{ti^*} to A_{i^*} and if the second highest α_{ti}, call it β_{tj^*}, is assigned to

$$\{A_i \,/\, i \neq i^*\} \text{ (spread around the 2nd highest)}$$

The rest $1 - \alpha_{ti^*} - \beta_{tj^*}$ is assigned to $\{A_1, \ldots A_n\}$

It can be shown , see [1], that

$$Bel(A_j) = K\left[p_j \prod_{j \neq i} d_i + r_j \prod_{j \neq i} c_i \right]$$

$$K = \prod_j d_j \left[1 + \sum_i p_i \Big| r_i \right] - \prod_j c_j$$

Where $p_i + c_i + d_i = 1$.

APPLYING CLASSICAL DECISION THEORY TO SELECT VALUES FOR X_{q+1}

If $KS_1, \ldots KS_q$ yield enough information so that

$$Pr\left(X_q = A_{1t_1} \wedge \ldots \wedge A_{qt_q}\right) = \mu_q\left(A_{1t_1} \wedge \ldots \wedge A_{qt_q}\right)$$

can be trusted then, maximize over $B_{q+1,i}$ the following expression:

$$\sum Belief_{q+1}\left(A_{1t_1} \wedge \ldots \wedge A_{qt_q} \wedge B_{q+1,i}\right)\mu_q\left(A_{1t_1} \wedge \ldots \wedge A_{qt_q}\right)$$

$Belief_{q+1}$ is generated by $m_1 \oplus \ldots \oplus m_{q+1}$

We view this as making a decision in the environment $A_{1t_1} \wedge \ldots \wedge A_{qt_q}$ assuming the probabilities are known. Picking the alternative $B_{q+1,i}$ yields a payoff of $Belief_{q+1}(A_{1t_1} \wedge \ldots \wedge A_{qt_q} \wedge B_{q+1,i})$ and we maximize the averaged payoff. What if $KS_1, \ldots KS_q$ are not too reliable? We know the patterns but we are not sure about their probabilities. Pick the alternative $B_{q+1,i}$ so as to maximize the minimum of

$$Bel_{q+1}\left(A_{1t_1} \wedge \ldots \wedge A_{qt_q} \wedge B_{q+1,i}\right) - Bel_{q+1}\left(A_{1t_1} \wedge \ldots \wedge A_{qt_q} \wedge \bigvee_{j \neq i} B_{q+1,i}\right)$$

Here the minimum is taken over all environments $A_{1t_1} \wedge \ldots \wedge A_{qt_q}$. Bel_{q+1} is generated by m_{q+1}. The motivation is that picking the minimum represents the worst environment for payoff of alternative $B_{q+1,i}$ over competing alternatives. Picking the maximum represents then the maximum gain. This approach is pessimistic in nature (going to the worst environment and then making the best of a bad situation). At the other end of the spectrum, the maximum of the maximum represents the optimistic attitude.

Picking a convex combination of the two represents a compromise.

Another approach yet is to minimize the largest regret. Let

$$T\left(A_{1t_1} \wedge \ldots \wedge A_{qt_q}\right) = D_i\left(A_{1t_1} \wedge \ldots \wedge A_{qt_q}\right) - \max_i D_i\left(A_{1t_1} \wedge \ldots \wedge A_{qt_q}\right)$$

Where D_i denotes the above difference of beliefs. T measures the regret of picking the alternative $B_{q+1,i}$ over the best alternative $(T \leq 0)$ Picking the minimum over the environment, produces the largest regret. Picking then the maximum, minimizes that largest regret.

DECISION MAKING AND TRUNCATING THE INFORMATION

Here, we believe that some patterns are a definite possibility. We also want to ignore the rest of the patterns, also we do not trust any probabilities functions associated with $KS_1, \ldots KS_q$. Going back to the previous section, we see that the four previous algorithms are well defined if we restrict the environments $A_{1t_1} \wedge \ldots \wedge A_{qt_q}$ to a fixed set P. We now refine this by allowing P to be a fuzzy set. Thus

$$P = \sum a_{q(t_1 \ldots t_k)} \Big| A_{1t_1} \wedge \ldots \wedge A_{qt_q}$$

Here $a_{q(t_1 - t_k)}$ denotes the degree of membership of

$A_{1t_1} \wedge \ldots \wedge A_{qt_q}$ in P.

We now must define an appropriate fuzzy set of payoffs. In the case of an optimistic or pesimistic or a somewhere in between attitude, we consider

$$C_i\left(P\right) = \sum a_{q(t_1 \ldots t_k)} \Big| \left[Bel_{q+1}\left(A_{1t_1} \wedge \ldots \wedge A_{qt_q} \wedge B_{q+1,i}\right) - Bel_{q+1}\left(A_{1t_1} \wedge \ldots \wedge A_{qt_q} \wedge \bigvee_{j \neq i} B_{q+1,j}\right)\right]$$

We need to be able to take the minimum or maximum element of a fuzzy set.

If $A = \sum a_i \Big| a_i$ Set

$$\psi(\lambda) = Min\left\{a_i \Big| a_i \geq \lambda\right\}$$

The minimum of A is defined as

$$\int_0^1 \psi(\lambda)\, d\lambda$$

This coincides with minimum in the crisp case and is defined in [11] Again the 4 algorithms defined earlier now make sense.

THE GENERAL CASE

We interrogate $KS_1, \ldots KS_q$ and split the corresponding patterns into disjoint blocks P_k. The blocks could correspond to classifications such as highly likely, likely, somewhat likely patterns, etc. ... We also assume P_k are fuzzy sets (is $A_{1t_1} \wedge \ldots \wedge A_{qt_q}$ highly likely?). We set

$$P_j = \sum a_{q(t_1 \ldots t_k),j} \Big| A_{1t_1} \wedge \ldots \wedge A_{qt_q}$$

Also we assign masses to each block, reflecting the weight put on the blocks (this reflects the trust put on the corresponding patterns in the class). Let

$$m\left(P_j\right) = a_j$$

The first criteria, for example, would maximize over the alternatives $B_{q+1,i}$

$\sum_k l_i\left(P_k\right) m\left(P_k\right)$ where $l_i\left(P_k\right)$ is the minimum of the fuzzy set

$$\sum a_{q(t_1 \ldots t_k),k} \left| \left[\mathrm{Bel}_{q+1}\left(A_{1t_1} \wedge \ldots \wedge A_{qt_q} \wedge B_{q+1,i}\right) - \mathrm{Bel}_{q+1}\left(A_{1t_1} \wedge \ldots \wedge A_{qt_q} \wedge \overset{\vee}{i \neq j} B_{q+1,j}\right)\right]\right.$$

It is clear that the other three algorithms generalize to this situation. The sets are replaced by "averages" and the minimum and maximum need to be taken over fuzzy sets, as explained earlier. For other methods available in the setting of decision making, the reader is referred to [5], [6], and [7].

TOWARD A GENERAL THEORY OF MULTIPLE KNOWLEDGE SYSTEMS

The previous discussion points out the importance of building a formal theory for the multiple knowledge systems setting. Our present work generalizes the situation described in [8] and constitutes the first steps toward such a theory. Our basic assumptions are:

(i) Our knowledge systems are independent

(ii) Each knowledge system specializes in one feature

(iii) Each feature may have several knowledge systems assigned to it.

We may not want to access all KS's and therefore, we have to solve the following problem:

The access problem: Which sets of KS's does one access? (some KS may run in parallel)
In what order does one access these sets?

We have performance parameters such as reliability, expense, response time, etc... Information regarding these parameters are contained in special KS's called CKS's (Control Knowledge Systems).

Each CKS specializes in one performance parameter

One performance parameter may correspond to several CKS's.

Each KS has two components:

a) The observational component which reports on the value of a specific feature. It may return a value or a probability distribution over the set of possible feature values (e.g., red or .8/red + .2/blue).

b) The judgemental component which reports on how likely it is that the true answer lies in some set of possible answers given that a specific value of a feature has been observed.

We define a control strategy to be a sequence of performance parameters specifications. This generates an access to a set of $KS's$. After these $KS's$ have been used, the belief structure of the frame of discernment is updated. Then stopping rules are looked at. If stopping criterias are not met, we go to the next control strategy.

If all control strategies have been exhausted, a decision is made as to what the probable answer is.

Access Policy

Each control strategy is a list of performance objectives. On the l^{th} control strategy, let Θ_l denote all <u>available</u> $KS's$ $\Theta_1 \supset \Theta_2 \supset \ldots \supset \Theta_l \ldots$ as we don't want to reuse the same $KS's$ (we want to have independent sources of information). The decision as to what $KS's$ to use is made on information contained in the $CKS's$.

Each CKS has two components:

a) Component - A which decides on what are the best subsets of Θ_l to consider when the value of performance objective P_j p_j^k

i.e., If $CKS_j^1, \ldots CKS_j^{r_j}$ specialize on performance j

Component A computes all

$$u_{jt}^{(k)} : 2^{\Theta_l} \rightarrow \left[0, 1 \right] \quad \text{which}$$

represent

$$u_{jt}\left(\bullet \,\middle|\, p_j^k \right) \qquad 1 \le t \le r_j$$

We define $u_{jt}^{(k)}\left(B\right) = 0$ if B contains any pair of $KS's$ which can't run in parallel

Thus $u_{jt}^{(k)}$ is non-zero only on sets of $KS's$ that run in parallel

b) Component - B which makes a probabilistic judgement of what is the best value of performance P_j. i.e., for CKS_t,

$$\beta_{jk}^{(t)} = Pr\left[P_j = p_j^k \,\middle|\, CKS_j^t \right]$$

Let $B \subset \Theta_l$ (set of available $KS's$) Define

$$n_j\left(B \,\middle|\, CKS_j^t \right) = \sum_k \beta_{jk}^{(t)} u_{jt}^{(k)}\left(B\right)$$

Here $u_{jt}^{(k)}\left(B\right)$ is given by component A of CKS_j^t for each value p_j^k and $\beta_{jk}^{(t)}$ is given by component $-$ B of CKS_j^t for each value p_j^k. In other words, the above expression represents how good, on the average, the set B is as determined by CKS_j^t

We now want to mesh all the CKS for a fixed performance.

$$n_j\left(B \,\middle|\, CKS_j^1, \ldots CKS_j^{r_j} \right) = \overset{r_j}{\underset{t=1}{\oplus}} n_j\left(B \,\middle|\, CKS_j^t \right)$$

Now to mesh all the performance parameters

$$n\left(B \,\middle|\, \text{all the CKS involved}\right) = \overset{s}{\underset{t=1}{\oplus}}\, n_{j_t}\left(B \,\middle|\, CKS^{1}_{j_t}, \ldots CKS^{r_{j_t}}_{j_t}\right)$$

Now look at all $B \subset \Theta_l$ made up of KS's that can be accessed in parallel For such B's maximize

$$Bel(B) - Bel(\neg B)$$

At this point, we have picked a set of KS's to run in parallel.

We now have to interrogate the KS's that are in B and update our belief structure on the frame of discernment (and go from Θ_l to Θ_{l-1})

Now we have KS^{t}_{i} Recall it has an observational and a judgemental component

The judgemental component is represented by

$$v^{(k)}_{it} : 2^{\Theta_Q} \rightarrow \left[\, 0, 1 \,\right]$$

This represents

$$v^{k}_{it}\left(A \,\middle|\, f^{k}_{i}\right)$$

the degree of belief that A is the smallest set containing the right answer, given feature value f^{k}_{i}

The observational component returns either a single value but in more complex case, a probability distribution. The notation:

$$KS^{1}_{l}\left(i_1\right), \ldots KS^{s_l}_{l}\left(i_{s_l}\right)$$

means that KS's on the l^{th} strategy that are in the selected set B report on features $i_1, i_2, \ldots i_{s_l}$

The observational components report

$$a^{k}_{l}\left(i_t, t\right) = Pr\left[f^{k}_{i_t} \,\middle|\, KS^{t}_{l}\left(i_t\right)\right]$$

(the l index refers to the l^{th} control strategy)

Thus, we define masses (over fixed features)

$$m_{lt}\left(A \,\middle|\, KS^{t}_{l}\left(i_t\right)\right) = \sum_{k} a^{k}\left(i_t, t\right) v^{k}_{i_t t}\left(A\right)$$

(the averaged mass assigned by the judgemental component)

We now mesh over all features (determined by B, the selected set)

$$m_l\left(A \,\middle|\, KS^{1}_{l}, \ldots KS^{sl}_{l}\right) = \overset{sl}{\underset{t=1}{\oplus}}\, m_{lt}\left(A \,\middle|\, KS^{t}_{l}\left(i_t\right)\right)$$

At the end of the L control strategy, our total information is summed by

$$m_L\left(\bullet \,\middle|\, \text{all KS's involved}\right) = \overset{l}{\underset{l=1}{\oplus}}\, m_l\left(\bullet \,\middle|\, KS^{1}_{l}, \ldots KS^{sl}_{l}\right)$$

We now must deal with the decision rule of what object must be selected as a plausible answer.

Step 1:

Let a in Θ_Q be the element maximizing

$$Bel_L(a) - Bel_L(\neg a)$$

If L denotes last control strategy, pick 'a'

else go to Step 2

Step 2:

a) If $\delta_1 > 0$ denotes some fixed threshold

Pick 'a' if $Bel(a) > \delta_1$

b) If $\delta_2 > 0$ denotes some fixed number

Pick 'a' if $Pls_L(a) - Bel(a) < \delta_2$

c) Combined 'a' and 'b'

If a doesn't satisfy the criterion, go to the next control strategy. The rationale for the stopping rule is 'c' is that we would like the belief in 'a' to exceed some threshold and have uncertainty relative to a drop below some predefined level.

It is clear that much research remains to be done. For example, degradation of the information contained in the $KS's$ has not been considered in the last part of this report. This and additional problems will be addressed in future work. Finally, for applications of the Dempster-Shafer approach to artificial intelligence, the reader is referred to [3] and [4].

REFERENCES

1. J. A. Barnett (1981), "Computational methods for a Mathematical Theory of Evidence" Proceedings IJCAI-81 Vancouver, B.C. pp 868-875.

2. Davis, L.S., Rosenfeld, A. "Computer Vision Systems". Hanson, A.R., and Riseman, E.M. eds,.101, Academic Press, New York (1978).

3. Garvey, T.D., (1976) "Perceptual Strategies For Purposive Vision" SRI International Tech. Note No. 117, Artificial Intelligence, Ctr, Menlo Park, California.

4. J. Gordon and E. H. Shortliffe (1984), "The Dempster-Shafer Theory of Evidence Rule-based Expert Systems: The MYCIN experiments of the Stanford heuristic programming project" Eds B. G. Buchanan and E. H. Shortliffe. pp 272-292. Addison - Wesley.

5. Kleyle, R.M. and de Korvin, A. (1984), "Switching Mechanisms in a Generalized Information System", Cybernetics and Systems, Vol. 15, pp. 145-167.

6. Kleyle, R.M. and de Korvin, A. (1986), "A Two Phase Approach to Making Decisions Involving Goal Uncertainty", Journal of Information Science, Vol. 12, pp. 161-171.

7. Kleyle, R.M., de Korvin, A. "A Belief Function Approach To Information Utilization In Decision Making". Accepted for publication in the Journal of the American Association for Information Science.

8. A. de Korvin, R. Kleyle and R. Lea, "An Evidential Approach to Problem Solving When a Large Number of Knowledge Systems are Available", submitted.

9. H. T. Nguyen (1978), "On random Sets and Belief Functions", J. of Math Analysis and Appl. 65, pp 531-542.

10. Schafer, G. (1976), A Mathematical Theory of Evidence. Princeton, NJ, Princeton University Press.

11. R. R. Yager (1986), "A General Approach to Decision Making With Evidential Knowledge", Uncertainty in Artificial Intelligence. Eds L. N. Kanac and J. F. Lemmer, North Holland, pp 317-327.

12. Zadeh, L.A. (1986), "A Simple View of the Dempster-Shafer Theory of Evidence and its Implication for the Rule of Combination", The AI Magazine, pp. 85-90.

N90-24980

UTILIZATION OF MOIRÉ PATTERNS AS AN ORBITAL DOCKING AID TO SPACE SHUTTLE/SPACE STATION FREEDOM

Final Report

NASA/ASEE Summer Faculty Fellowship Program--1989

Johnson Space Center

Prepared By:	Edwin L. Dottery
Academic Rank:	Assistant Professor
University and department:	United States Military Academy Department of Physics West Point, NY 10996
NASA/JSC	
Directorate:	Engineering
Division:	Communications & Tracking
Branch:	Tracking Techniques
JSC Colleague:	Richard D. Juday, Ph.D.
Date Submitted:	August 12, 1989
Contract Number:	NGT 44-0010800

ABSTRACT

Moiré patterns are investigated as possible docking aids for use between the National Space Transportations System (Space Shuttle Orbiter) and the Space Station Freedom. A sight reticle placed in optical conjunction with a docking target can generate moiré fringes from which position and alignment can be inferred. Design specifications and a mathematical development to meet those specifications are discussed. A motion based simulator and experimental hardware have been constructed.

INTRODUCTION

Space operations in the mid to late 1990's will require frequent rendezvous and docking missions between the Space Shuttle and numerous on orbit spacecraft, especially construction and servicing of the Space Station Freedom (SSF). At costs on the order of $3,000 a pound for carrying Shuttle payloads to low earth orbit, any hardware or protocol which can be developed to reduce the amount of contingency fuel required to be carried aloft, at the expense of payload, will quickly pay for itself. To ensure a successful docking between Shuttle and SSF, current scenarios and simulations dictate a large, heavy capture mechanism with a large capture cross section. Alternatively, a smaller mechanism with a correspondingly smaller capture cross section requires a greater quantity of reaction control system (RCS) propellant and exacerbates the problem of Shuttle plume impingement on SSF. Either solution reduces the Shuttle payload on every docking mission to SSF.

Improved pilot sighting and sensing systems are an alternative to the "brute force" solutions mentioned above. One of several techniques proposed to alleviate the docking scenario is the utilization of moiré patterns generated between a sight and a docking target. Moiré patterns are the fringes generated between two approximately equally spaced grids[1]. They can be designed to have the property of being quite sensitive to their relative translation and rotation, and their basic properties have been commented on since the 1800's.[2] Contemporary applications are numerous and include

[1]The French word "moiré" and its English translation "water" may both mean a wavy pattern imprinted on fabric, as in "watered silk". The term moiré has now come to represent many families of interference fringes.
[2]Lord Rayleigh (J.W. Strutt), Phil. Mag. 47, 81, 193 (1894).

the evaluation of replica gratings[1], metrology in general[2], measurement of refractive index gradients[3], recording contour lines of an object[4]. They even embrace the field of "Optical Art"[5].

While moiré theory and application is well represented in the literature, its use to infer position in three dimensions is very recent[6]. This work is done as an outgrowth of that effort in direct collaboration with the patent applicant and Principal Investigator, Dr. Richard D. Juday.

Patterns can be designed to be sensitive to those parameters which aid successful docking and to be relatively insensitive to those parameters which do not affect the miss distance. In short, the design will enhance the coupling between what the pilot observes in his docking sight and what occurs at the docking port interface.

MOIRÉ THEORY

The theory of moiré fringe formation under incoherent illumination is well established in the literature from different perspectives. The most common theory involves basic geometry[7], discribed by an indicial representation method[8]. Alternatively, the pattern can be thought of as the low spatial frequency components of the combination of the original patterns. The patterns must be resolved into the spatial frequency components to interpret the moiré pattern by the use of communication theory[9]. The latter is the approach used in the calculations to follow. The theory developed in the past for moiré fringe formation under incoherent illumination is almost exclusively restricted to two dimensions. For space docking application involving two independent gratings, offset by a comparatively large distance and each with nominally six degrees of freedom, a slight extension of theory is required. Appropriate

---

[1]J. Guild, The Interference Systems of Crossed Diffraction Gratings (Oxford University Press, London, 1956).

[2]J. Guild, Diffraction Gratings as Measuring Scales (Oxford University Press, London, 1960).

[3]Y. Nishijima and G. Oster, J. Opt. Soc. Am. 54, 1 (1964).

[4]D.M. Meadows, W.O. Johnson, and J.B. Allen, Applied Optics, Vol. 9, 4 (1970).

[5]G. Oster, Applied Optics, Vol. 4, 11 (1965).

[6]R. Juday, Patent disclosure, Feb. 5, 1989.

[7]M. Stecher, Am. J. of Phys. Vol. 32, 4 (1964).

[8]G. Oster, M. Wasserman and C. Zwerling, J of Opt. Soc. Am, Vol. 54, 2 (1964).

[9]Yokozeki, Optical Communications, Vol. 11, 4 (1974).

simulations will also have to be made before final flight hardware can be designed.

The moiré pattern itself, a periodic spatial function, can be formed optically by addition, subtraction, and multiplication of two (or more) spatially varying structures (gratings or filters). The most common way to combine the two original structures is by their transmittance or reflectance functions. The illuminating light is affected by the product of their transmittances and/or reflectances. We say then that when the same light field has impinged on each of the original structures in turn, a multiplicative pattern has emerged. This can be illustrated by the following two periodic structures and their product

$$A(x) = \frac{1}{2}(1 + \cos 2\pi f_1 x) \tag{1}$$

$$B(x) = \frac{1}{2}(1 + \cos 2\pi f_2 x) \tag{2}$$

$$A(x)\,B(x) = \frac{1}{4}(\cos \pi (f_1 + f_2) x * \cos \pi (f_1 - f_2) x) \tag{3}$$

Being a low pass filter, the eye will pass the low frequency component, which will be manifested by readily resolvable fringes. A multiplicative moiré fringe is used in our design.

An additive type pattern, in contrast, occurs when two separate light fields impinge on the two separate structures, and are then superposed to form

$$A(x) + B(x) = 1 + \cos \pi (f_1 + f_2) x * \cos \pi (f_1 - f_2) x \tag{4}$$

which yields a modulated sinusoid that is far more difficult to resolve. This effect would be important if an attempt were made to modify the existing Crew Optical Alignment Sight (COAS) to accept a moiré reticle. The COAS works on a projected backlit reticle imaged at infinity. Thus, a moiré-generating reticle inserted in the COAS would yield an additive moiré pattern when placed in conjunction with a moiré-generating docking target placed on SSF. For a more

thorough treatment of types of superposed patterns in optics, see Bryngdahl.[1]

DOCKING ENVIRONMENT AND GEOMETRY

The current Shuttle to SSF docking scenario involves a series of primary, secondary, and emergency sensors. These include ground tracking, rendezvous radar, the star tracker, and visual acquisition to bring the Shuttle to the vicinity of SSF. The docking scenario is specified for a totally passive SSF, although it is assumed that SSF Attitude Control System (ACS) is operational. At approximately 50 feet out, the pilot, flying from the aft bay, observing through the overhead window, will attempt to keep the Shuttle within an acceptance cone with a full width vertex angle of 6-10 degrees. From here until docking, the pilot will probably have range and range rate data fed to him via a laser sensor. At from 10-20 feet from docking, the pilot will attempt to hold his lateral misalignment to less than a six inch radius circle. He makes closing velocity (z-direction) and lateral alignment corrections (x-y) by pulsing Reaction Control System (RCS) thrusters. The other three degrees of freedom, roll, pitch and yaw, are held steady within one-degree accuracy by the Shuttle Attitude Control System (ACS). Roll, pitch and yaw are also held steady within one-degree accuracy by the ACS on the SSF. These attitude uncertainties are known as the deadbands of the Shuttle ACS and SSF ACS, respectively. The anticipated closing velocity is on the order of one-tenth of a foot per second.

This final closing range, from 10-20 feet to dock, is where accuracy must be improved to less than approximately six inches. Current contingency docking scenarios for the Shuttle to the docking mast of SSF utilizing the COAS do not provide adequate accuracies (close to twelve inches) for a single docking attempt. Shuttle Closed Circuit Television (CCTV), placed at the docking port, does meet the requisite accuracy (approximately three inches), but is objectionable from a reliability standpoint[2]. Though the COAS is a reasonably precise instrument for the applications it was originally designed for, its difficulty with Space Shuttle/Space Station Freedom docking is the offset distance from the sight to the docking port adapter. Figure 1 shows how this offset acts as a lever arm, converting acceptable roll,

---

[1]O. Bryngdahl, Opt. Soc. of Am., Vol. 66, 2, (1976).

[2]Miss distances were provided based on simulations run by Brian Rochon, as presented in Analytical Docking Contact Conditions, April 13, 1989.

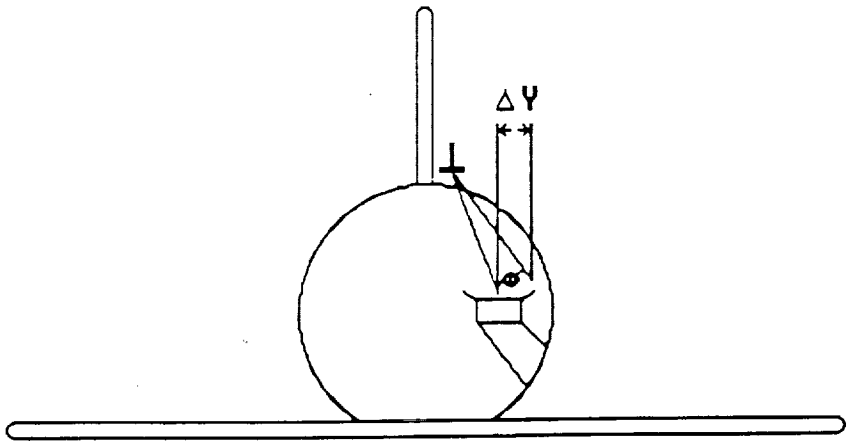

Roll Induced System Error

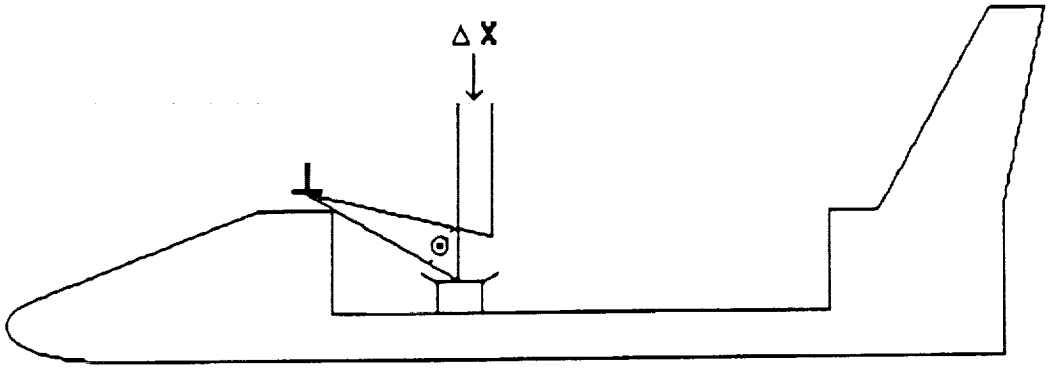

Pitch Induced System Error

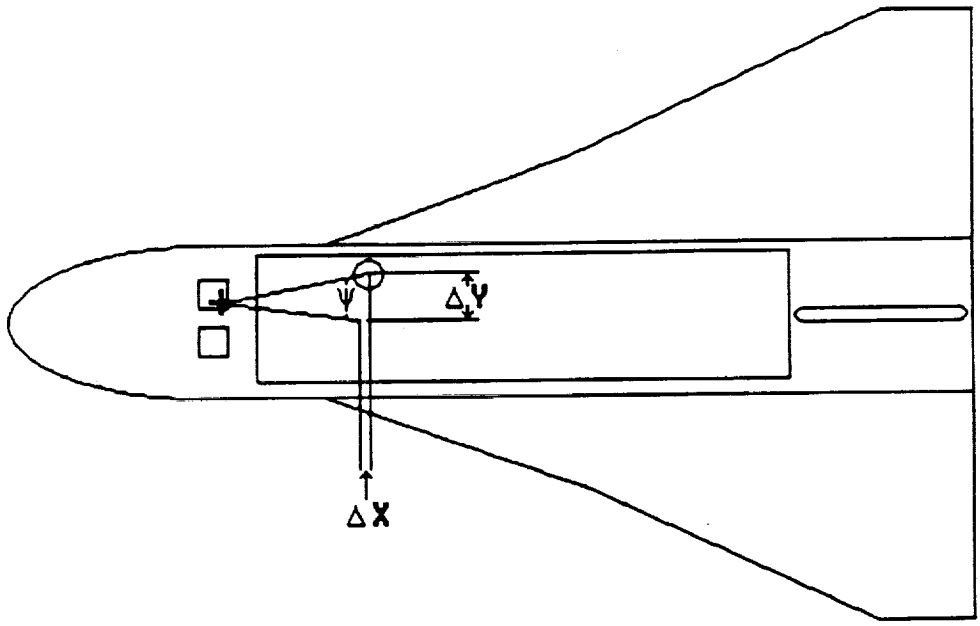

Yaw Induced System Error

figure 1.

pitch and yaw deadband error of the shuttle at the sight-docking target point of reference, into an unacceptable miss distance at the docking port. The same lever arm also affects instrument error and pilot error. Our design, essentially replacing the COAS with a robust, simple, small telescope must negate this effect to achieve miss distances less than six inches.

Referring to figure 2, note where and how our COAS-replacement system will be mounted. It will be mounted in approximately the same location as the COAS in the aft bay overhead window. This figure shows the baseline SSF docking scenario, using a docking mast which will retract to mate airlocks after hard dock is achieved. Figure 3 shows the docking mast retracted. The standoff distance from the COAS or COAS-replacement to the SSF docking target is approximately 18 feet, if a non-retractable target is used.

DESIGN CRITERIA AND THE FIRST GENERATION DESIGN

Our design criteria, which should serve to minimize miss distances, are:

1. Maximal sensitivity to x-y translation as measured at the docking port location.
2. No yaw sensitivity about the docking port.
3. Acceptable sensitivity to roll and pitch.
4. Simple to interpret patterns.

The first criterion underscores that it is how far off you miss the docking port--not how close your sight is to its target's bullseye--that is critical (and is presently a problem with the COAS). Second, some yaw is acceptable about the docking port (<u>not</u> the center of mass). Sensitivity to yaw about the docking port should be removed, so a pilot will not inadvertently correct for a perceived (but not actual) misalignment. Third, some roll and pitch will be present due to the deadbands of the ACS. Our design must be able to accept this. Finally (and on occasion, neglected), the design must give completely unambiguous cues to the pilot during those critical last seconds of docking, both in terms of how far and in which direction from the optimum docking position he is, and in his ability to sense his direction of motion.

Even a casual examination of commercially produced moiré patterns indicates that a variable frequency, ("chirped") pattern can give excellent sensitivity. Yaw insensitivity can be readily included

DOCKING MAST SYSTEM

STRUCTURES & MECHANICS DIVISION

ES63 / G. A. LANGE

INITIAL CONTACT CONFIGURATION

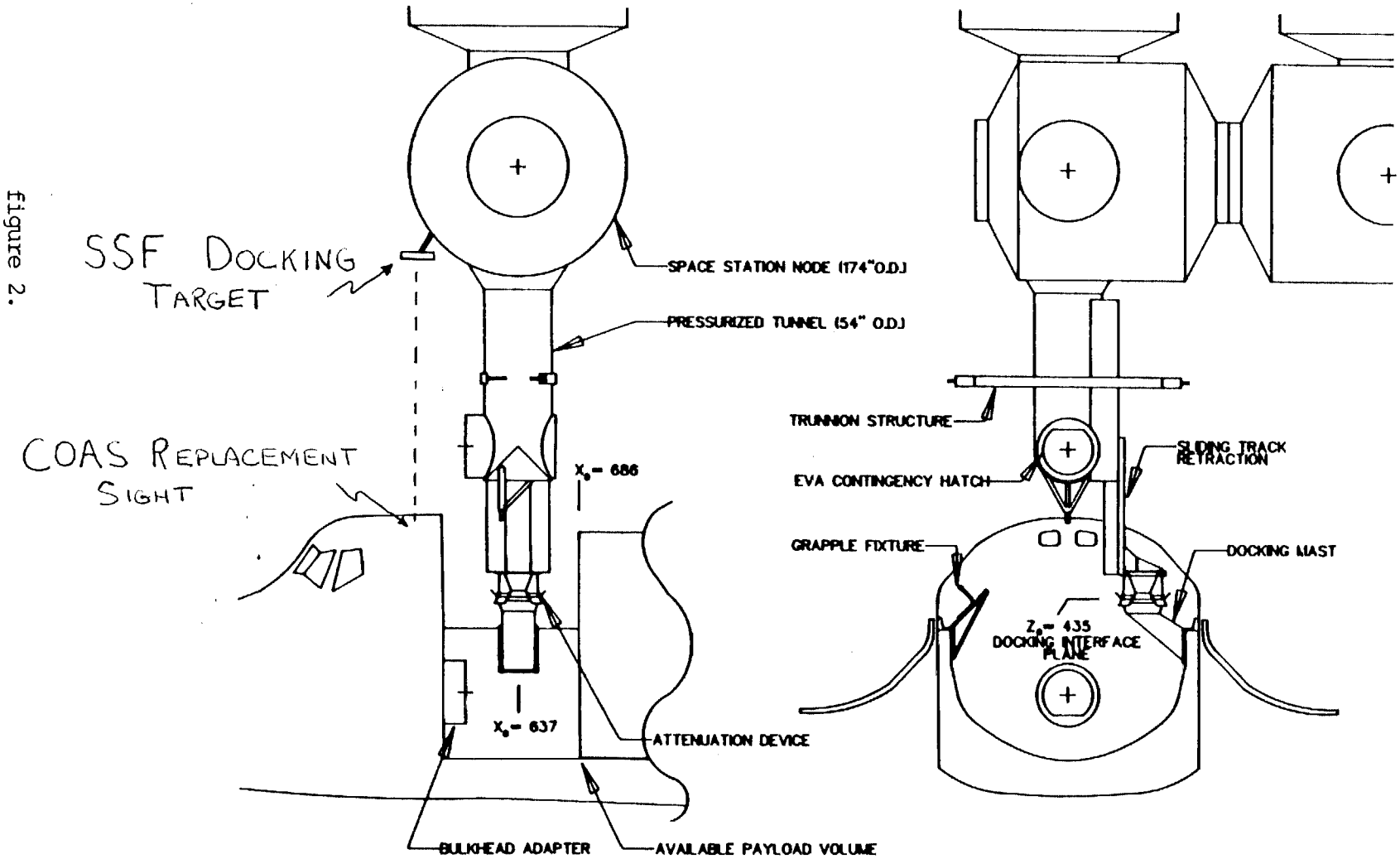

figure 2.

DOCKING MAST SYSTEM

STRUCTURES & MECHANICS DIVISION

ES63 / G. A. LANGE

FULLY DOCKED CONFIGURATION

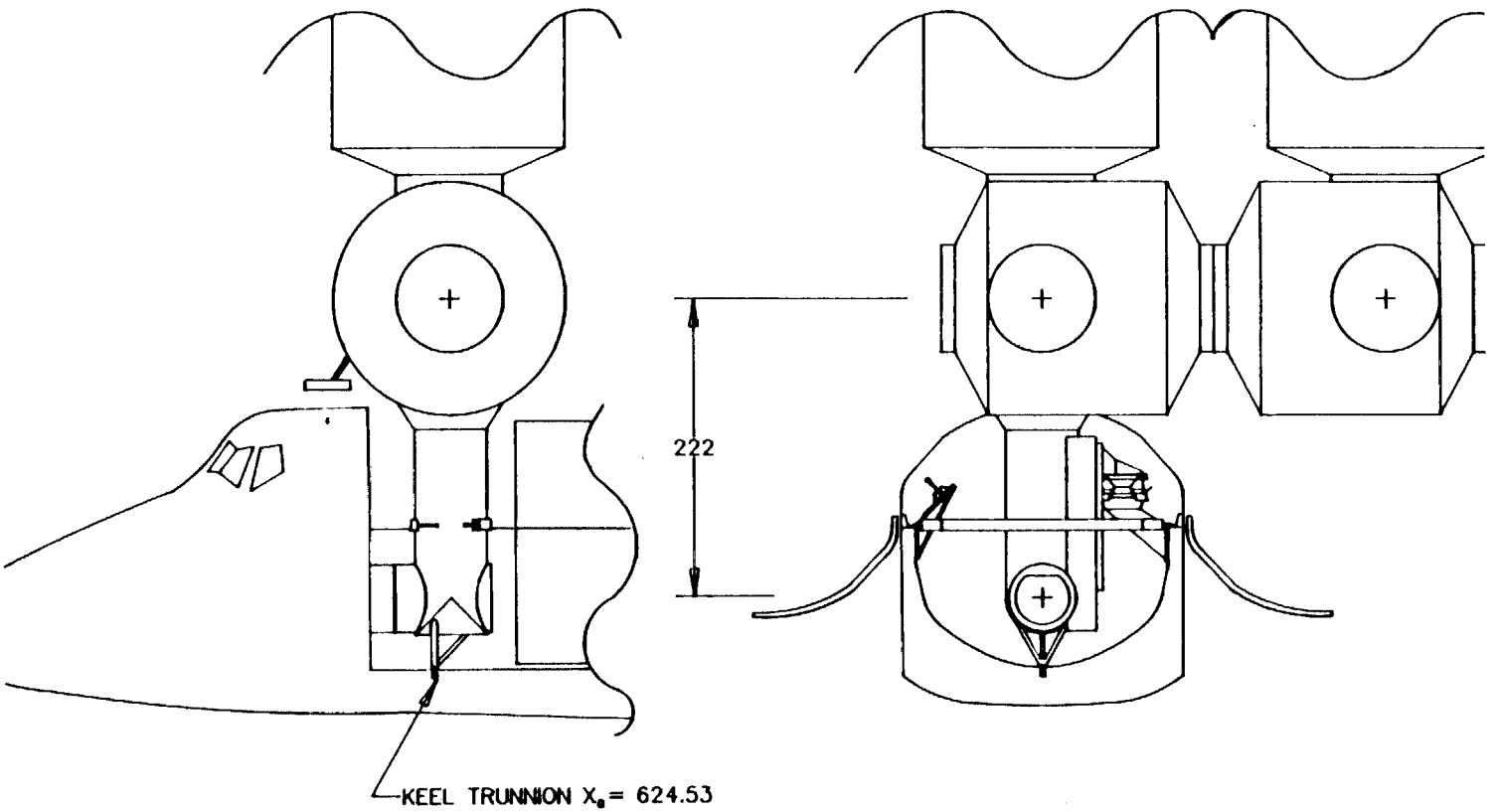

Figure 3.

by making our patterns radially symmetric about the docking adapter axis. Combining these two properties yields an off-axis Fresnel zone plate as an excellent candidate pattern. A zone plate (figure 4) is a series of bright and dark rings about a central circle, and is notable in that each ring and the circle ("zone") has the same area. The equation of the radii that would draw such a figure is

$$r_m = B\sqrt{m} \qquad (5)$$

where r_m is the mth radii, B is some constant to be determined, and m is an integer.

When two identical zone plates are overlapped with an offset less than the radius of the inner circle, a series of bars results perpendicular to the direction of the offset. Figure 5 demonstrates this fringe pattern, while the mathematics of this using the indicial equation method is shown by Oster et al[1].

SIGHT RETICLE AND DOCKING TARGET DESIGN

While an off axis zone plate will generate a series of equally spaced, equal thickness bars, for alignment purposes it is better to vary the frequency function of at least one zone plate to permit centering of the sight. Our first "centering chirp" is of quadratic form.

First, we must select a phase function $\phi(r)$ whose zeros of $\sin\phi(r)$ will correspond to an arc with radius r_m to construct the zone plate. This condition is met by the function

$$\phi(r) = \pi \left(r/B \right)^2 \qquad (6)$$

where B has yet to be specified. We next need to determine the spatial frequency f(r). It relates to phase $\phi(r)$ by

$$f(r) = 1/2\pi \; d\phi(r)/dr = 1/2\pi \; d/dr \left[\pi \left(r / B \right)^2 \right] = r/B^2 \qquad (7)$$

$$f(r) = r/B^2 \qquad (8)$$

[1]G. Oster, M. Wasserman and C. Zwerling, J. Opt. Soc. Am, Vol. 54, 2 (1964).

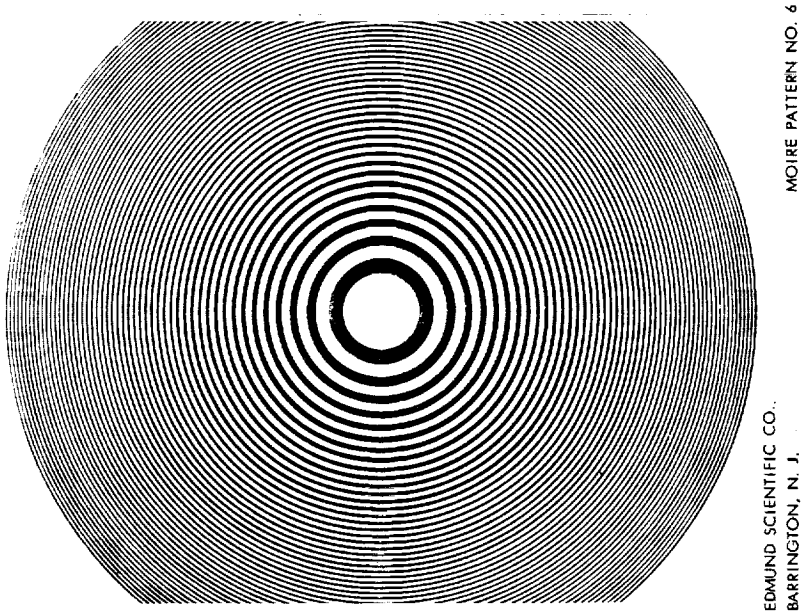

figure 4.

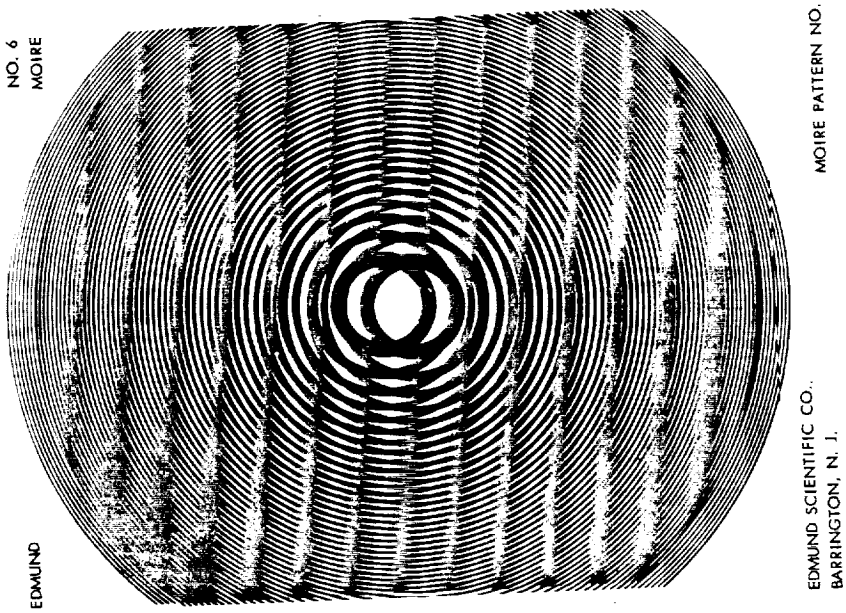

figure 5.

We now subscript T for target and R for reticle, and introduce a quadratic chirp into f_T. This quadratic chirp in f_T is symmetric about the center of the target, which in turn is 114 inches from the docking port (the origin of our pattern). Our target frequency is thus

$$f_T = f_R + D\,(r - 114)^2 + E \qquad (9)$$

which can be interpreted by the following figure

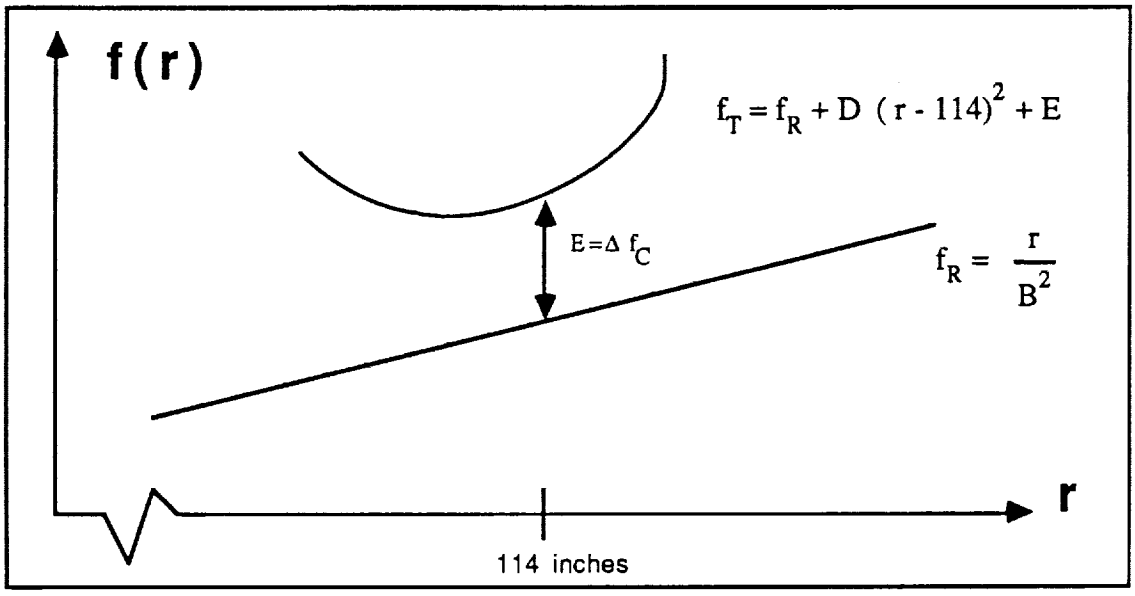

figure 6.

Noting that our target frequency f_T will correspond to the inverse of our chosen arc width, d, constraints may now be imposed to solve for the constants D, E and B. The constraints are:

1. Choose a differential frequency ratio of say, two times, edge to center.
2. Design to give 5 fringes (thus easy to observe) in moiré pattern between r = 102 and r = 126 inches for a 2 foot by two foot target.

From the first constraint, we see that

$$E = 144\,D\,. \qquad (10)$$

Next, the number of fringes must equal the number of arcs in the target less the number of bars in the reticle, edge to edge; thus

$$N \text{ fringes} = (\phi_T - \phi_R)/_{2\pi} . \qquad (11)$$

The phase difference from center to edge has half the fringes, and recalling
N = 5,

$$5\,\pi = \Delta\,\phi_{C\text{-}E} . \qquad (12)$$

This is also equal to the integrated phase from the center to edge

$$2\pi \int_{\xi=0}^{12} (E + D\,\xi^2)\, d\xi \qquad (13)$$

yielding

$$^5/_2 = 12\,E + 576\,D \qquad (14)$$

Rewriting equation (9) at its maximum value at r = 126,

$$[f_T]_{MAX} = \frac{1}{d_{r=126}} = \frac{126}{B^2} + 144\,D + E \qquad (15)$$

and selection of an appropriate cut width d yields suitable solutions for the constants.

To cut the sight reticle recall that a zero occurs (and hence a cut in our pattern) for the sine of the phase function every π radians, so

$$\phi_R\,(r_m) = m\,\pi = \pi\,\frac{r_m^2}{B^2} \qquad (16)$$

which leads immediately to equation (5) to control our cuts.

To find where to make the cuts in the target, its phase function is found as a function of r. This equals the integrated frequency,

$$\phi_T\,(r) = 2\pi \int_0^r f_T\,(\xi)\, d\,\xi \qquad (17)$$

resulting in the following cubic equation for the target phase function,

$$\frac{\phi_T(r)}{2\pi} = \frac{r^2}{2B^2} + rE + \frac{D}{3}\left[(r-114)^3 + 114^3 \right] . \tag{18}$$

As with the phase function of the reticle,

$$\phi_T(r_m) = m\,\pi \tag{19}$$

will lead directly to a cubic equation in terms of m and r_m. An algorithm using Newton's method then solves the cubic and control the cutting of our target pattern.

Finally, our reticle pattern is photo reduced to place it in the focal plane of our telescope.

PHYSICAL IMPLEMENTATION

The objective of the experiment was not only to generate the functions of a suitable moiré-generating telescope reticle and docking target reticle, but also to translate them into laboratory hardware. The patterns were created by cutting a membrane of red plastic layered on a transparent substrate, then peeled to create alternating red and clear arcs. This process is known as "ruby-lithography" or "ruby-lith", and is traditionally used in miniaturized electronic circuit fabrication. Arcs can be cut as close as every 15 mils without undue tearing, but to ease the burden of iterative fabrication, an arc width of about 50-60 mils was selected.

The ruby-lith software had no trouble with either of the equations used to generate the two templates, not even the routine to solve the above mentioned cubic equation using Newton's method, though it was painfully slow and required frequent human-intervention due to memory limitations.

The target pattern eventually used for flight hardware will need to be made of high contrast alternating reflective and absorptive bands, as the shuttle floodlights will be the only lighting we can confidently depend on under our "passive SSF" criteria. For our first generation tests using off-the-shelf ruby lith, a light box or simple lamp will provide high contrast rear illumination.

A target just under two feet square was initially used to ensure the field of view of our test telescope would be filled by the target at the initial test ranges of between 18 and 28 feet.

An inexpensive four power rifle telescopic sight was disassembled to gain access to the focal plane. The eyepiece, photo reduced reticle and telescope were placed in optical mounts, and the photo reduced reticle was placed at the focal plane.

The telescope assembly was mounted on a three degree of freedom motion based, full scale simulator. The "Shuttle" could then translate (z-direction) toward "SSF" at a realistic one-tenth of a foot per second, while simultaneously translating laterally (x & y directions), as illustrated in figure 7. Near term simulator improvements will allow all six degrees of freedom, incorporating roll, pitch and yaw.

Of particular note in the figure is the offset "docking port" marker on the boom of the simulator. This demonstrates in full scale the relation between how close the pilot has in fact docked compared to what he observed in his docking sight.

LABORATORY RESULTS

Laboratory runs are now begining to evaluate the first generation docking targets and reticles. The data will published in a future publication by Juday and Dottery, et. al.

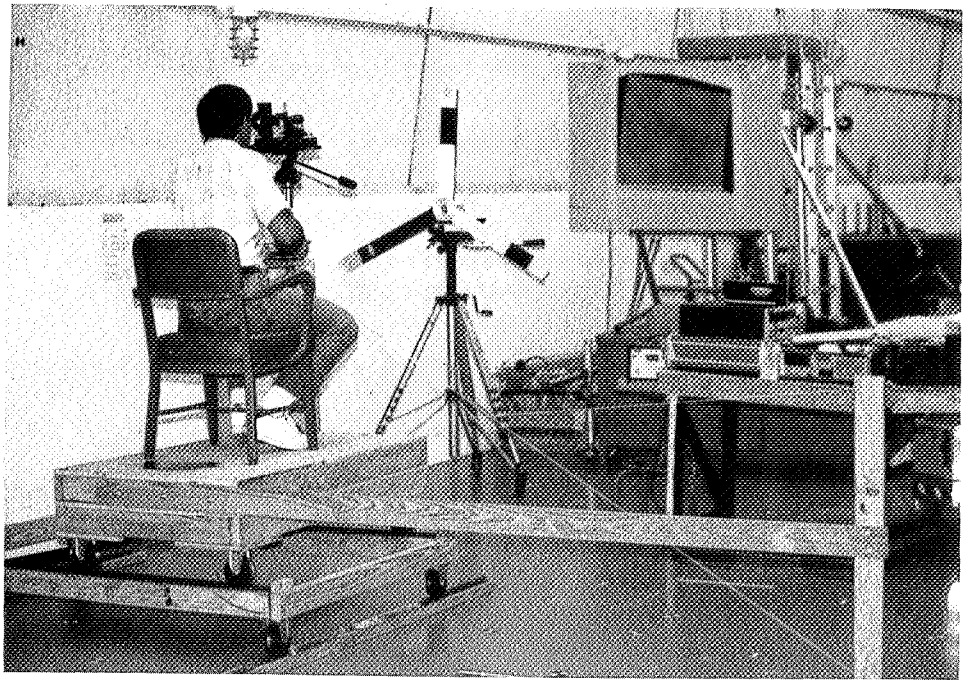

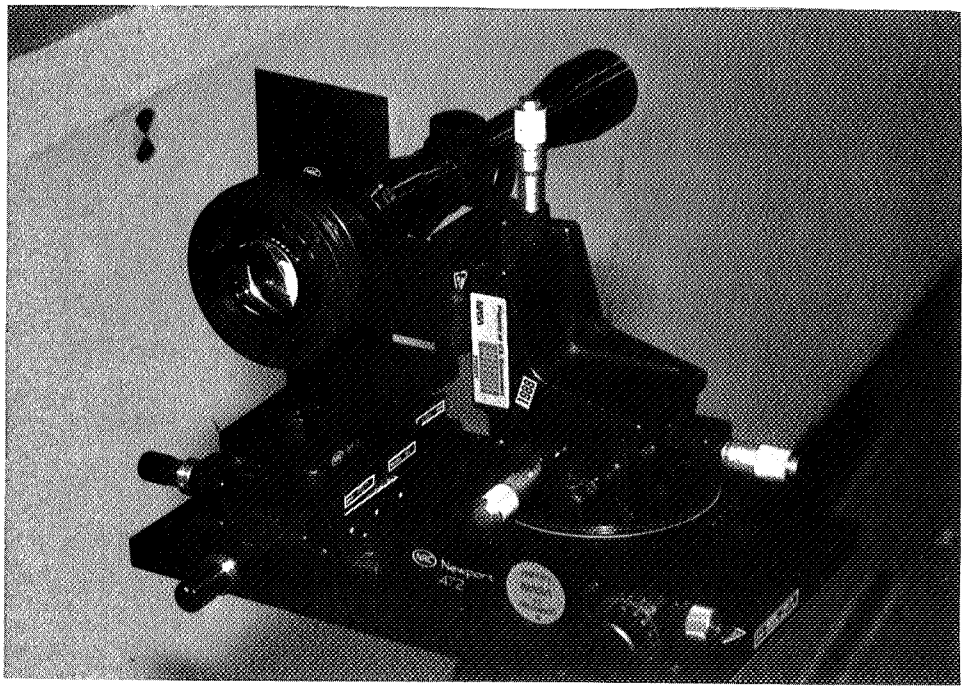

figure 7.

ELECTROCHEMICAL CONTROL OF IODINE DISINFECTANT FOR SPACE TRANSPORTATION SYSTEM AND SPACE STATION POTABLE WATER

Final Report

NASA/ASEE Summer Faculty Fellowship Program--1989

Johnson Space Center

Prepared By:	Richard D. Geer, Ph.D.
Academic Rank:	Associate Professor
University & Department:	Montana State University Department of Chemistry Bozeman, Montana 59717

NASA/JSC

Directorate:	Space and Life Sciences
Division:	Medical Sciences
Branch:	Biomedical Laboratories
JSC Colleague:	Richard L. Sauer, P.E.
Date Submitted:	September 1, 1989
Contract Number:	NGT 44-001-800

ABSTRACT

The National Aeronautics and Space Administration will continue to use iodine as the microbial disinfectant for potable water (PW) on manned space operations. The current method for adding iodine is the "Microbial Check Valve", a passive ion exchange device whose output is temperature dependent and also adds excess iodide to the water. An "active" electrochemical technique, using silver and inert electrodes, is proposed to allow controlled addition and removal of the iodine from the PW by cycling a silver iodide layer. The units can be physically recycled between the two locations for these modes.

The design is based upon the constrains set by the PW system, including conductivity, expected flow rates, and iodine treatment levels. The units require a minimum electrode area of 300 cm^2 and fits into a space of 3x3x5 cm. The efficiency of iodine and iodide removal will depend upon the thickness of silver iodide on the silver electrode, which under nominal conditions could approach 40 μm in 90 days of operation. The time between recycling the units will also depend upon the iodine removal efficiency.

The equilibria for iodine species in the water were evaluated. Graphs for the iodine species, carbonate species and hydrogen ion are presented, based upon levels of iodine added and total inorganic carbon present. The effect of temperature on the residual level of iodine (iodide) and silver in the water is graphically presented. The oxidation and reduction reactions were also examined at the expected concentrations of reactive species in the PW to test the feasibility of the iodine removal and generation processes. The major difficulty encountered was due to the presents of oxygen in the water. While oxygen could possibly help in removing excess iodide, it would cause a problem in the controlled generation of iodine due to its preferential reduction relative to that of silver iodide.

The analytical chemistry required to monitor the performance of the PW system was reviewed. It is clear that potentiometric measurements (like pH) are inaccurate in pure water, but it is possible for conductivity techniques with ion selective electrodes can make accurate measurements. Methods based upon conductivity were used to calculate pH and the concentrations of iodine species in treated water. These methods allowed a check upon the accuracy of the total trace ion analysis of the PW. The report makes a final point that oxygen should be routinely monitored in the PW system.

INTRODUCTION

The National Aeronautics and Space Administration (NASA) plans on using iodine for microbial control in the recycled potable water (PW) system on its Space Station. Iodine is currently used on the Space Transportation System (STS) missions where the water is not recycled but is obtained as a byproduct from the fuel cells. Because of its convenient method of addition and its adequate disinfectant properties, iodine will probably be used in future long duration space ventures like missions to Mars and Lunar base facilities. There is limited experience with the long term use of iodine disinfectant in water and it could present some potential health problems. These include possible formation of toxic compounds from the reaction of iodine with organic material (residual or in the stomach) and increased iodide levels effecting the thyroid function. Iodine levels some what above nominal will give water a noticeable and objectionable taste (however even pure water is noted for its objectionable "flat" taste.) Thus, it would be desireable and perhaps necessary to remove nearly all of the iodine species before the water is consumed. In some situations it may be important to recycle the iodine.

Currently NASA is adding iodine to PW systems by means of a "microbial check valve" (MCV), an effective PASSIVE DEVICE. The MCV consist of a chamber containing a anion exchange resin loaded with iodine (mainly as the triiodide ion, I_3^-) which delivers low levels of iodine (I_2), iodide (I^-) and hydrogen ion (H^+) to the water. The behavior of iodine in this system is characterized by a set of chemical equilibria involving both the ion exchange material and reactions of water. During use the I_2 level slowly drops as the resin iodine load decreases[a]. The equilibrium constants for these processes are temperature dependent and high temperature water can produce iodine levels above the acceptable limits. The MCV also produces H^+ and excess I^-, even when operating at normal temperatures, and the pH of the treated water can fall significantly below the pH 6 limit for the Space Station PW[1]. These problems could be overcome by removing the excess iodine and related ions just before the water is used.

At present NASA has no device for this end-use treatment but they are considering using a high capacity ion exchange unit, working in the reverse mode of the MCV. However the end-use position of the unit requires it to treat hot water where the chemical equilibria are not favorable. Vapor,

---

[a]. Unpublished results from Water and Food Analysis Lab, NASA, Johnson Space Center, Houston TX.

liquid or chemical extraction of I_2 from the water is conceivable, but most methods appear bulky and not suitable for microgravity conditions.

As an alternative to the MCV system, I have studied the possibility of an ACTIVE electrochemical technique for generating, recycling and removing I_2 and its associated ions in PW. In this report the device will be called the EC-MCV (electrochemical microbial check valve), though based upon its construction it is often referred to as the "silver bullet". This report discusses a design based upon the limiting requirements for PW treatment in both the Space Station and STS environments. The advantages of the EC-MCV will be presented along with some possible limiting complications that need to be investigated.

OVERVIEW OF THE EC-MCV

In principle the operation of the EC-MCV is simple and can be followed on the schematic diagram in Figure 1:

- In the Iodine Removal Mode (IRM) the silver electrode reacts spontaneously with any iodine (I_2) or other active iodine species in solution to form a very insoluble coating of silver iodide (AgI). Excess iodide (I^-) can be removed by oxidizing the silver electrode under a controlled potential to form more AgI.

- In the Iodine Generation Mode (IGM) a controlled current is past through the device and the AgI on the silver electrode is reduced to silver and iodide (I^-) is released into the water. Upon reaching the counter electrode the I^- is oxidized to I_2. The iodine level in the water is controlled by the electrode current relative to the water flow rate.

CONSTRAINTS ON THE EC-MCV DESIGN

The nature of the PW system puts severe constraints on practical designs of the EC-MCV and some basic research will be needed to prove this a viable concept.

Conductivity

A major design limitation is the low conductivity of the PW, which is measured in units of Siemens/cm (S/cm) for a one cm^2 area. Its reciprocal (resistivity) is often used and is given in ohm cm. Completely pure water has a value of 0.056 μS/cm or 18.3 MΩ cm. Water samples from the Biofilm Test Bed (BTB), a system designed to simulate aspects of the PW system for the Space Station, have values of 0.2 to 0.5 $\mu S/cm^a$. These low values limit the current densities that the water

can carry with reasonable applied voltages. For an electric field of 1 V/cm the PW will only support current densities of 0.2 to 0.5 $\mu A/cm^2$. Water from the STS fuel cells may be more pure and have lower conductivity. For water with 2 ppm of I_2 added the conductivity increase to about 2 $\mu S/cm$.

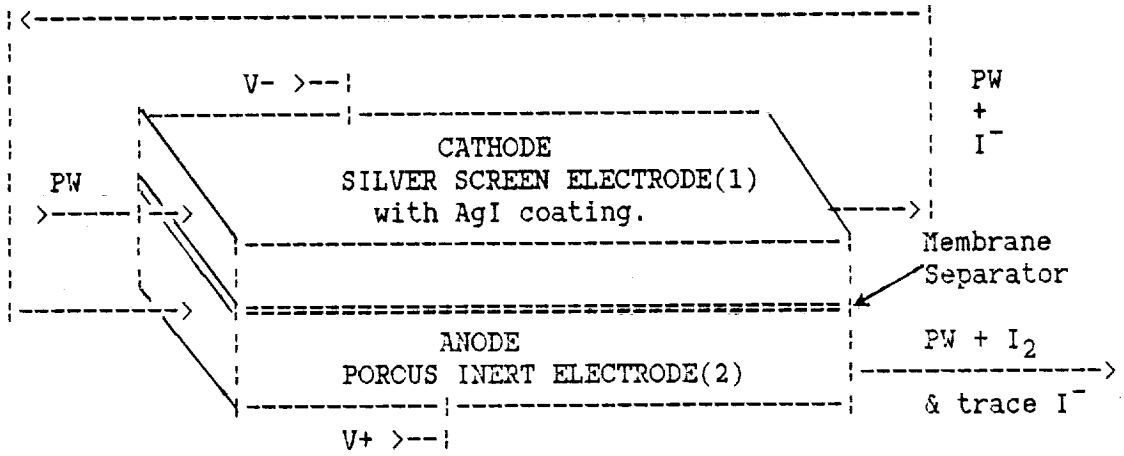

A. Arrangement for adding I_2 to PW at a set rate by controlled current electrolysis.

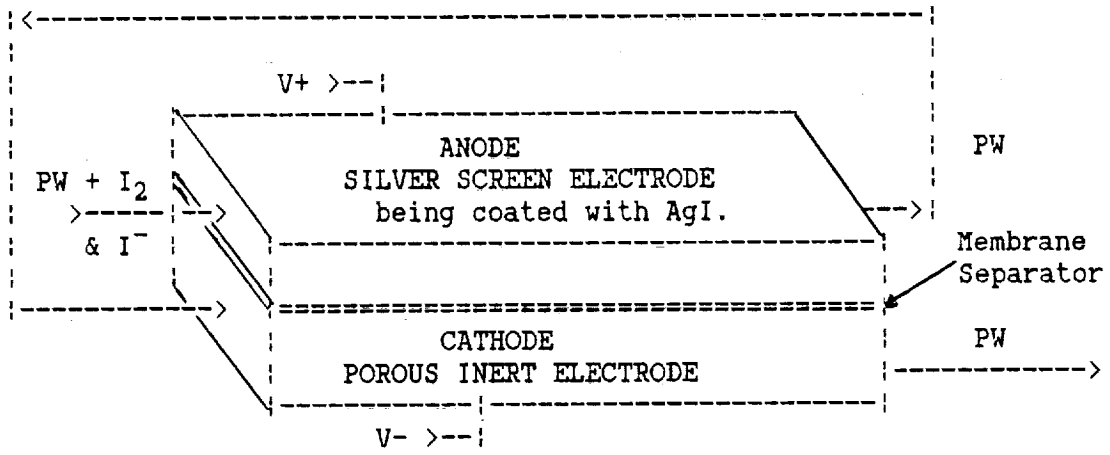

B. Arrangement for removing I_2 and I^- from PW under controlled potential.

Figure 1.- Schematic drawing of the proposed recyclable EC-MCV. (1) The cell consists of a stacked array of alternating thin (<1 mm) electrodes and separators. (2) Possible inert electrode materials are: platinum, titanium, tin, reticulated vitreous carbon, or carbon cloth.

Water Flow Rates

The inflow of PW is one factor determining the rate of iodine addition to the water. The anticipated Space Station flow is 25 l/day (0.3 ml/sec) of humidity condensate from the cabin. The system residence time for the treated water is expected to be about 100 hours, with most of the time in storage tanks. The demand of water at the output will be intermittent, with flows of 10 to 30 ml/sec of either hot or cold water being required[b].

Iodine Treatment Levels

Currently the planned iodine treatment level is 2 to 3 ppm, but a standard MCV using hot water from the STS fuel cells has produced levels above 10 ppm[a]. For the purpose of more complete disinfection even higher levels could be allowed if the total iodine level was reduced before consumption.

Electrode Area

The above requirements set the typical rate of I_2 addition for an EC-MCV at 2 to 3 nanomol/sec, requiring a total current up to 0.6 mA. To handle this current at a current density of 0.2 $\mu A/cm^2$ will require a minimum effective surface area for the electrochemical cell of 300 cm^2. Since the area on each side of the electrode is counted, this is equivalent to a stack of 10 pairs of 3 x 5 cm electrodes. (From here on, this report will deal with a nominal 3 ppm level of added iodine, if higher levels are under consideration the units can be scaled accordingly.)

The iodine removal mode could present some design problems if most of the added iodine ends up in the form of I^- and has to be removed electrochemically. At a projected flow rate of 11 ml/sec this would require a reaction rate of 26 μmol/sec or 25 mA, which translates into a maximum electrode area of 13000 cm^2. This may not be a real constraint, as a EC-MCV unit should produce little or no excess I^-. However, the excess I^- output of a conventional MCV on the BTB is about 0.7 ppm[a] and would require a 3000 cm^2 surface area. The reduction of I_2 in the system is another source of I^-, but these problems may be irrelevant if oxygen is present, see the section on Redox Reactions.

Electrode Construction

A practical design for the electrodes should approach 100

---

[b]. Private communication from Richard L. Sauer, PE, NASA SD4, Johnson Space Center, Houston TX.

% efficiency for the electrode reactions producing I_2 from I^- and forming AgI. To keep the voltage drop low and to maximize the water contact time, the water flow must parallel the electrodes while the charge migration is at right angle through a membrane separator. This requires thin (<1mm) porous electrodes that produce turbulent flow and narrow stagnant diffusion layers at the surface. The typical diffusion distance for an ion is about 40 μm in 1.6 sec and 200 μm in 60 sec[2]. Tending to counter these requirements is the need for the electrodes to have good electrical conductivity, low flow resistance and to be readily fabricated. While one electrode must be made of silver, or silver plated, the choice of material for the counter electrode is only limited by the need for inertness and conductivity. Finely woven metal gauzes have an adequate structure. Titanium, tantalum, or tin might be good choices and are not considered toxic metals. Platinum, palladium and gold are rather expensive and may react with iodide under oxidative potentials[3]. Also to be considered are flexible carbon cloth and reticulated vitreous carbon, which has an excellent pore structure but is brittle.

The calculated EC-MCV performance in Table 1 is based upon a conservative design using 15 pairs of electrodes (each pair being 2 mm thick including membrane separator) with a total area of 450 cm^2 in a 3x3x5 cm space. Research is needed on how the AgI film thickness effects the efficiency of the silver/iodine reaction, as this will determine how often the electrodes need to be recycled. As the silver surface is recycled it should become rough (possibly with dendritic growth) causing the surface to volume ratio to increase substantially, extending the recycle time. Now the questions are how many times can an electrode can be recycled and what limits electrode life.

TABLE 1.- EXPECTED CHANGES IN SILVER ELECTRODE WITH TIME IN THE IODINE REMOVAL MODE AT 3 PPM I_2.

Time	0	7	30	90	days
Ag weight[a]	37.7	37.3	35.8	32.0	g
AgI weight	0	0.97	4.16	12.5	g
AgI thickness[b]	0	3.1	13.	39	μm
Residence time[c]	1.66	1.65	1.61	1.52	sec

[a]. Based upon 15 layers of 3 x 5 cm electrodes of 40 mesh 10 mil smooth Ag wire gauze.
[b]. Calculated for a total Ag surface area of 565 cm^2.
[c]. For a 11 ml/sec flow; the IGM time is about 60 sec.

Other EC-MCV Components

The membrane separators are another critical part of the EC-MCV. They need to be thin and have high conductivity to ions, have limited water passage and be nonreactive to iodine. Nafion by Dupont, a Teflon base cation exchange resin may work well, but bipolar membranes would be preferred. The literature of battery technology may show how this problem was solved some time ago.

The best material for cell body construction is also an open question. Plastic materials like polypropylene, Teflon, epoxy, polycarbonate, and polymethylmethacrylate come to mind. The body design should allow for simple construction and repair. Some potential problems to investigate are: the degree of I_2 adsorption by the body material, is it a reservoir for active iodine, and does it limit bacterial growth on the cell body?

The electronic control for the EC-MCV will not be covered here as the circuits are very simply implemented at these low currents and modest voltages.

CONSTRAINTS ON WATER CHEMISTRY

While source water for the PW system may be fairly pure, its trace constituents and temperature can affect the function of the EC-MCV (as well as the MCV) and the I_2 water chemistry.

Fuel Cell Water

STS fuel cell water entering the MCV is quite warm. The water should be very pure except for the possibility of entrainment of small amounts of potassium hydroxide electrolyte and residual hydrogen gas. However no excessive amounts of K^+ or OH^- have shown up in analyses of PW from this source[a]. It should contain no oxygen or carbon dioxide. Information on its pH and conductivity would be desirable. This water source would be a prime candidate for the EC-MCV because the regular MCV has problems treating hot water.

Humidity Condensate

The Space Station will use humidity condensate from the cabin atmosphere as its source of potable water. This source will have low levels of a number of inorganic ions and a large variety of organic chemicals, mostly in trace amounts[4]. The water should be saturated with O_2, N_2 and CO_2 at their partial cabin pressures. After polishing the water with deionizing resins and activated charcoal filters the water should be at ambient temperature and its composition similar to that observed in the Biofilm Test Bed studies[a].

Chemical Reactions and Equilibria

The addition of I_2 to water sets up several equilibria that are sensitive to the existing pH and the I^- level. These are given in Table 2 along with several other important reactions.

TABLE 2.- CHEMICAL EQUILIBRIA NEEDED TO UNDERSTAND THE CHEMISTRY OF I_2 IN WATER[5,6].

	Reaction	Keq at 25 °C
1	$I_2aq + H_2O \longrightarrow HOI + I^- + H^+$	5.40E-13
2	$I_3^- \longrightarrow I_2aq + I^-$	1.38E-03
3	$I_2aq + H_2O \longrightarrow H_2OI^+ + I^-$	1.20E-11
4	$AgI \longrightarrow Ag^+ + I^-$	8.51E-17
5	$ResI_3 \longrightarrow ResI + I_2aq$	N/A[a]
6	$ResI + H_2O \longrightarrow ResOH + H^+ + I^-$	N/A
7	$H_2O \longrightarrow H^+ + OH^-$	1.00E-14
8	$CO_2 + H_2O \longrightarrow H_2CO_3$	N/A
9	$H_2CO_3 \longrightarrow HCO_3^- + H^+$	4.30E-7
10	$HCO_3^- \longrightarrow CO_3^{=} + H^+$	5.60E-11

[a]. These constants are not available, the ones with ResI represent the ion exchange equilibria of the MCV resin.

Reactions 2 and 3 are not important as the concentrations of I_3^- and H_2OI^+ are normally insignificant in PW. However, reaction 1 produces HOI, H^+, and I^- in amounts sufficient to give PW a 5.75 pH and provide equivalent amounts of I^- and HOI. Figure 2 shows the relationship of these species to the amount of I_2 added to pure water. If the incoming water is much above pH 7 it can divert a large portion of I_2 to HOI and I^-. In pure water the amount of dissolved CO_2 will determine the pH by reactions 8 and 9, Table 2 and Figure 3. However, in treated water the usual levels of CO_2 are 100 fold below that of I_2 and the H_2CO_3/HCO_3^- ratio is controlled by the I_2 reactions.

Excess I^-

If I^- is present in the water in concentrations greater than available from the above reactions, the solution is considered to have "excess I^-". A major portion of the I^- in water treated with the regular MCV is "excess I^-", released from the resin by ion exchange reaction 7, Table 2. It is accompanied by equivalent amounts of H^+, which lowers the pH to about 5.3. Other sources of excess I^- are reactions which reduce I_2 to I^- and usually produce H^+ at the same time.

Two reactions that may be important in the PW systems are: 1) Microbial reduction of I_2 by iodine resistant bacteria, (perhaps they are using it as an energy source?). 2) The oxidation of reactive chromium or other atoms of stainless

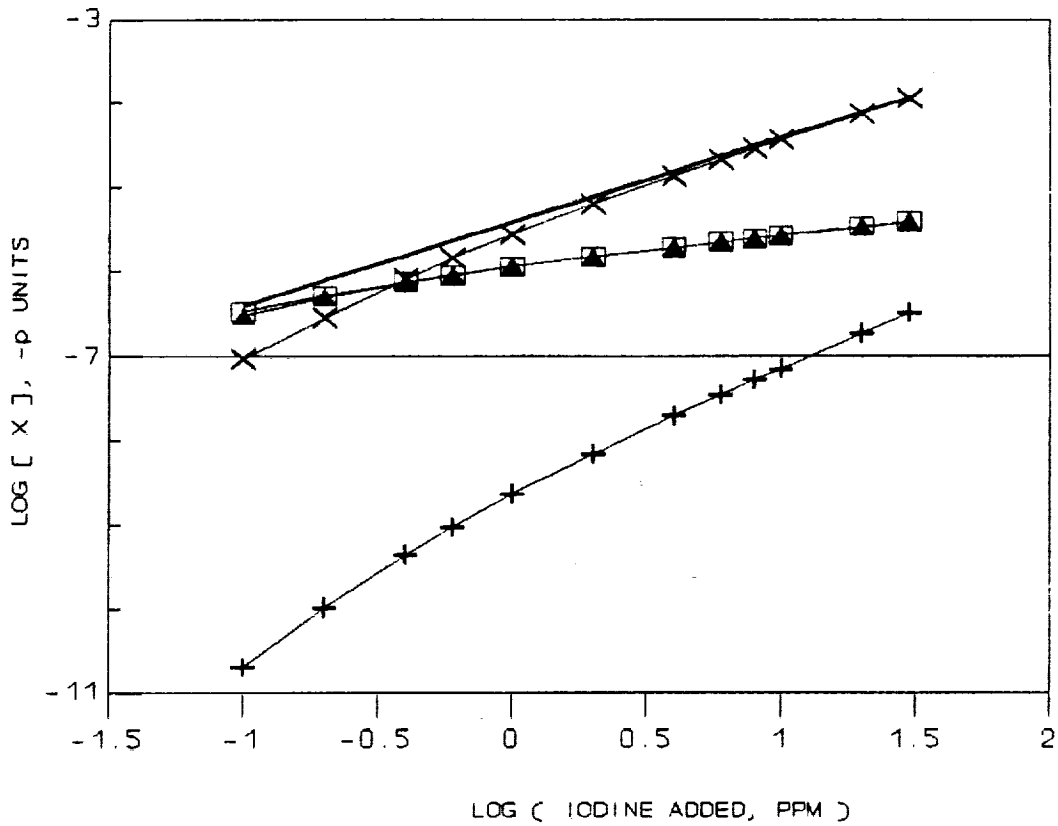

Figure 2.- Concentrations of ions from I_2 added to pure water. Legend: ----- I_2added; --X-- I_2; --[]-- -pH; --▲-- HOI and I^-; --+-- I_3^-.

steel in the PW system. This reaction, if it occurs, must be slow at room temperature, but possibly becomes important at higher temperatures. However no unusual amounts of Cr are seen in I_2 treated water, even though Fe, Ni, and Cr have been observed in untreated water in the BTB[a]. This might imply that an I_2 oxidation could be part of a metal passivation process leading to thicker oxide coatings, but also producing more H^+ and I^-.

Silver Iodide

The formation and stability of silver iodide (AgI) plays a key role in the operation of the EC-MCV for removal of iodine species. As mentioned earlier, the effect of the AgI thickness on the rate I_2 reacts with the underlying silver needs investigation, for the thickness can approach 40 μm in 90 days. Also important is the durability of the surface, as flaking of the AgI would interfere with recycling electrodes and could contaminate the PW. Finally, the increased solubility of the AgI with temperature may be important as the output water will often be heated prior to iodine removal.

However, Figure 4 shows that even at 100 C the Ag is still below the 50 ppb limit.

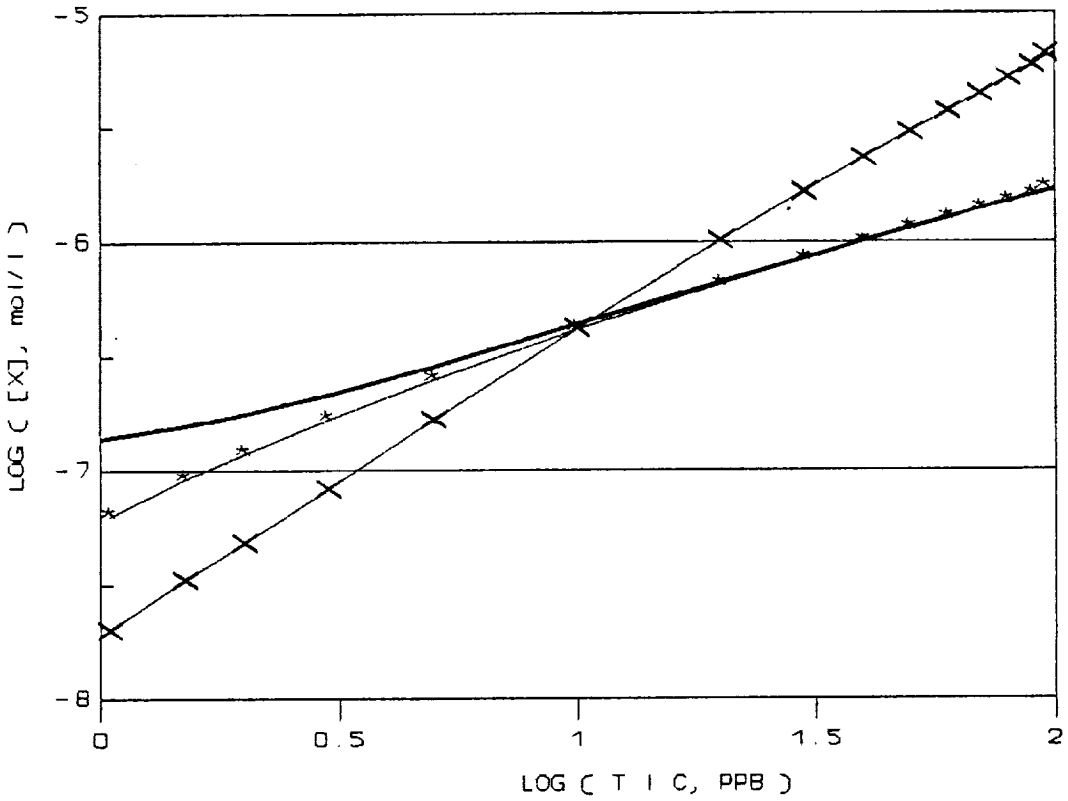

Figure 3.- Concentration of chemical species in pure water from dissolved CO_2 (reported as TIC). Legend: ----- H^+; --*-- HCO_3^-; --x-- H_2CO_3.

Redox Reactions and Electrode Potentials

Reduction and oxidation chemistry is at the heart of the generation and removal of I_2 by the EC-MCV and the significant reaction are given in Table 3. A negative cell potential indicates an electrolysis reaction controlled by an applied current or voltage. The more positive a value is the more "spontaneous" the reaction.

Included in the table are several reactions involving oxygen that may be important to the EC-MCV operation. In the iodine removal mode, without oxygen, the values for reactions 2 and 4 show that Ag reacts very vigorously with I_2, while it requires electrolysis condition with a voltage greater than 0.31 volts to remove I^-. Note, while Ag has only the slightest tendency to react with O_2 alone, in the presence of I^- it has a very positive potential to form AgI! This could solve all the problems of "excess I^-" removal without

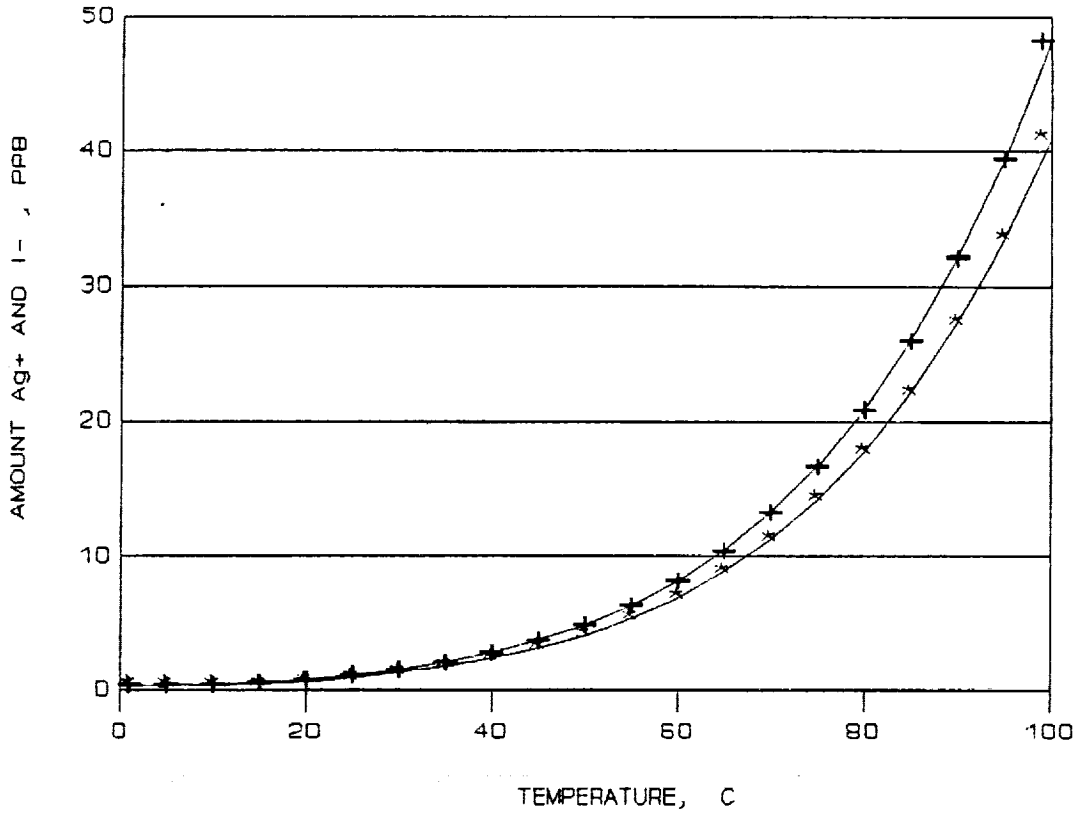

Figure 4.- The effect of temperature on the amounts of Ag^+ and I^- released by silver iodide surfaces. Legend: --*-- Ag^+; --+-- I^-.

electrolysis, just add oxygen. BUT, this idea must be tested experimentally, for O_2 reactions are notorious for having very slow kinetics even when the thermodynamics are very favorable. On the other hand, silver and iodine reactions have catalytic activity, so hopefully the reaction will proceed. Reaction 5 also indicates that oxygen in solution would be helpful in reforming I_2 from I^-, but this reaction is known to be slow unless catalyzed by near ultraviolet light.

Oxygen Problem

In the iodine addition mode, reactions 6 and 7 indicate that the controlled current generation of I_2 occurs before O_2 and the process may require less than 1 volt applied to the cell. However, reaction 8 presents another problem, any oxygen dissolved in the input water will be reduced very easily and the applied current will not reduce AgI to Ag and I^- until all the oxygen is reduced. Thus, for the EC-MCV to work as planned, the source of water must be free of oxygen, like that from the STS fuel cells. However, in this situation oxygen is not available to help remove excess I^-. One

TABLE 3.- IMPORTANT OXIDATION/REDUCTION REACTION IN THE OPERATION OF THE EC-MCV. EXPECTED CELL POTENTIALS ARE LISTED FOR ANTICIPATED CONCENTRATIONS OF REACTANTS AT 25 C.

	CELL POTENTIAL		
IODINE REMOVAL MODE	STD[a]	EXPECTED[b]	
1 $4\ Ag + O_2aq \longrightarrow 2\ Ag_2O$	0.102	0.060	0.006
2 $2\ Ag + I_2aq \longrightarrow 2\ AgI$	0.767	0.617	
3 $O_2aq + 4\ H^+ + 4\ Ag + 4\ I^- \longrightarrow 4\ AgI + 2\ H_2O$	1.424	0.753	0.699
4 $2\ H^+ + 2\ Ag + 2\ I^- \longrightarrow 2\ AgI + H_2$	0.152	-0.310	
IN SOLUTION			
5 $O_2aq + 4\ H^+ + 4\ I^- \longrightarrow 2\ I_2aq + 2\ H_2O$	0.657	0.136	0.017
IODINE ADDITION MODE			
6 $2\ AgI \longrightarrow I_2aq + 2\ Ag$	-0.767	-0.617	
7 $4\ AgI + 2\ H_2O \longrightarrow O_2aq + 4\ H^+ + 4\ Ag + 4\ I^-$	-1.424	-0.753	-0.699
8 $O_2aq + 4\ H^+ \longrightarrow O_2aq + 4\ H^+$	0.000	0.053	-0.267

[a]. Reactants at unit activity, but O_2aq and I_2aq are based upon theoretical 1 molar solutions, and not saturated solutions at unit activity[7,8].

[b]. First entry for O_2 saturation (1.29 mM), second for 10 ppb O_2, other species: I_2 3 ppm, pH 5.3, and I^- 4.8 μM.

solution is to electrolytically remove O_2 before iodination and afterward add it back by going thru the other half of the electrolytic cell. Another solution for the Space Station with oxygen in the water is to use the regular MCV and then remove the I_2 and excess I^- aided by the O_2 (if that reaction works) with a MCV unit filled with silver shot. This system would preclude recycling the iodine directly.

ANALYTICAL CHEMISTRY

Routine chemical and physical testing of the PW is needed to insure its quality and proper operation of the iodination system. The high purity of the PW, as typified by the BTB analyses, presents problems and challenges for analytical chemistry, especially when they will be compounded with the space environment. A review of the results the Water and Food Analysis Lab (WAFAL), NASA at Johnson Space Center, have obtained for the BTB during its year of operation are impressive[a]. Using Ion Chromatography, Atomic Absorption, and Total Organic Carbon analyses they are now able to analyze for nearly all anion and cations expected in the PW, or are of concern. They have been able to get closure on the equivalents of charged ions at the ppb level and also excellent agreement with the water conductivity. However, these methods may be difficult to implement within the limitations of orbital flight and microgravity.

To monitor the performance of the iodination of PW one needs to know the total amount of iodine added, and the amounts of I_2, I^-, CO_2 and H^+. As found from the BTB results, the common potentiometric technique for pH is not accurate in low conductivity water[a]. However, in fairly pure systems conductivity gives a very good measure of pH as the H^+ contributes 82 % to the conductivity below pH 7 and the other ions all have similar equivalent conductances[9]. Ion Selective Electrodes (ISE) in general will have the same problems as pH electrodes unless buffers are added to increase conductivity. Conductance techniques should be adaptable to ISE[10] for ion measurements in these "pure" water systems and development of these methods should be supported.

The determination of I^- has been a problem for WAFAL as the photometric method depends on the H^+ and I_3^- measurements, both of which where inaccurate. A technique that removes the active iodine species with metallic silver after measuring I_2 photometrically is being developed to measure the residual I^- without interference[a]. From these data all the iodine species can be calculated accurately. It also appears feasible to carry out these same iodine measurements automatically using cathodic stripping voltammetry[11].

Oxygen is one important component of the PW system that is not currently being measured. It should be measured at several locations in the system, as its concentrations may reflect the degree of microbial growth. The oxygen data would also be important for the proper operation of a EC-MCV and if excess oxygen or one of its reactive derivatives (ozone, superoxide or hydrogen peroxide) were injected as adjuncts for microbial control.

SUMMARY

An electrochemical method (EC-MCV) for controlling the iodine disinfectant in potable water for NASA's space operations has been proposed. The factors affecting the design and performance of the unit have been analyzed. This showed that it would be feasible to construct a recyclable unit in a small volume that will operate in either an iodine removal or addition mode. The EC-MCV should remove active iodine species rapidly from PW, but the rapid delivery rates at end-use may make complete removal of excess I^- difficult under some conditions. Its performance change with AgI buildup needs to be investigated, as this controls the time for recycling the unit. The EC-MCV has advantages over the passive MCV currently in use, as it would allow precise control of the I_2 level and would not introduce excess I^- to the water. The presence of oxygen in the EC-MCV needs to be investigated as it could affect the efficiency of I_2 addition and excess I^- removal.

REFERENCES

1. Space Station Program Definition and Requirements Document. NASA SST 30000. Rev D., 1987, Table 2-34.

2. Bard, A. J.; and Faulkner, L. R.: Electrochemical Methods. John Wiley & Sons, 1980, p. 129.

3. Sawyer, D. T.; and Roberts, J. L. Jr.: Experimental Electrochemistry for Chemists. John Wiley & Sons, 1974, p. 68.

4. Shrader Analytical and Consulting Laboratories Report of Analytical Services: Space Lab 3 ARS Humidity Condensate. SL 12352, 1985.

5. Burger, J. D.; and Liebhafsky, H. A.: Therodynamic Data for Aqueous Iodine Solutions at Various Temperatures. Analytical Chemistry, vol. 45, 1973, pp. 600-602.

6. Lange, N. A.: Handbook of Chemistry. Handbook Publishers (Sandusky, OH), 1956, pp. 1198-1204.

7. Latimer, W. M.: Oxidations Potentials. Prentice-Hall, 1938, pp. 293-317.

8. Skoog, D. A.: Principles of Instrumental Analysis, third edition. Saunder College Publishing, 1985, pp. A25-A27.

9. Skoog, D. A.: Principles of Instrumental Analysis, third edition. Saunder College Publishing. 1985, p. 706.

10. Holler, F.J.; and Enke, C. E.: Conductivity and Conductometry. Laboratory Techniques in Electroanalytical Chemistry, P. T. Kissinger, and W. R. Heineman, eds., Marcel Dekker, 1984, pp. 263-264.

11. Heineman, W. R.; Mark, H. B.; and Wise, J. A.: Electrochemical Preconcentration. Laboratory Techniques in Electroanalytical Chemistry, P. T. Kissinger and W. R. Heineman, eds., Marcel Dekker, 1984, p. 502.

OVERTRAINING AND EXERCISE MOTIVATION: A RESEARCH PROSPECTUS

Final Report

NASA/ASEE Summer Faculty Fellowship Program--1989

Johnson Space Center

Prepared By:	Anthony C. Hackney, Ph.D.
Academic Rank:	Assistant Professor
University & Department:	University of North Carolina Exercise Physiology Laboratory Department of Physical Education, Exercise and Sport Sciences Chapel Hill, NC 27599-8700
NASA/JSC	
Directorate:	Space and Life Sciences
Division:	Medical Sciences
Branch:	Biomedical Laboratories
JSC Colleague:	Pat Santy, M.D. Steve Siconolfi, Ph.D.
Date Submitted:	September 22, 1989
Contract Number:	NGT44-001-800

ABSTRACT

The problem of exercise "overtraining" has recently become one of great interest to professionals in the field of human performance assessment. Quite obviously, the ultimate goal of the training process is to improve physical performance. However, excessive training can result in the opposite effect, that is, a performance decline and an impairment in the functional work capacity of the body. Research indicates that both psychological as well as physiological disturbances are quite common in overtrained individuals (32, 33, 34). For example, psychological changes include increased levels of depression, fatigue, and a lack of motivation (34, 45, 51). Similarly, impairment of the physiological function of the cardiovascular, metabolic, and endocrine systems also have been found (3, 8, 12, 13, 14).

Some similarities may be found in the psychological and physiological states of crew members exposed to extended space flight and overtrained individuals. Therefore, the possibility exists that the crew members subjected to extended missions in space may develop over stressed or overtrained or both states during their flights. If such states do develop within the crew members, mission performance may be impaired.

With these points as a background, the intent of this prospectus is to address potential research directions that NASA may consider viable and of a mutual interest to this investigator. A clear framework by which to begin discussion of research topics is needed, therefore working definitions of "overtraining" and "exercise motivation" are presented. Subsequently, a proposed conceptional model of how exercise overtraining and motivation interact is presented. In support of the proposed model is brief literature review of relevant areas. Potential research projects are presented and discussed.

INTRODUCTION

A major concern in the space program has been the detrimental effects of prolonged space flight on the physiological functions of the human body (28, 39, 40). Biomedical research from Skylab and Salyut indicated prolonged exposure to space flight results in cardiovascular deconditioning, bone mineral loss, muscular atrophy, and fluid shifts (28, 39). These changes appear to be the physiological consequences of exposing the body to zero gravity and a reduction in the typical level of earth bound activity. Exercise training is a proposed requirement to attenuate these effects on the body's systems while the astronauts are in space. In addition to this exercise training during space flight, many other physical as well as mental demands (i.e., mission operations) will be made of the astronauts. Potentially, the combination of exercise training and demanding work requirements (e.g., isolation) could lead to a over stressed stated in the astronauts. The latter issue, psychological stress of the astronauts, is becoming an increasingly important concern. Specifically, future NASA space missions will be of greater duration and crew make-up will become more heterogeneous (i.e., multi-national) in nature. These combined stressors could lead to adverse coping strategies or negative group interaction, both which could endanger the success of the mission.

For example, psychological changes include increased levels of depression, fatigue, and a lack of motivation (34, 45, 51). Similarly, impairment of the physiological function of the cardiovascular, metabolic, and endocrine systems also have been found (3, 8, 12, 13, 14).

Furthermore, the motivation to continue exercising frequently diminishes when the over stressed states occur (10,11, 33). This lack of motivation (i.e., exercise adherence) has been reported by the Soviet Union for their cosmonauts on a number of the extended duration space missions (Salyut and Mir) (36). As exercise adherence becomes reduced, muscle strength and bone mass losses would be accelerated in the zero gravity of space. These latter effects could act in a synergistic fashion with the others stressors associated with space flight to further augment the performance decline of the crew members. Work examining the interaction of exercise training, over stressed states, and exercise motivation seems warranted as NASA enters an era where the duration of space missions are lengthened such as the Extended Duration Orbiter, Space Station Freedom, Lunar Base, and Mars projects.

WORKING DEFINITIONS

Initially, this investigator wishes to propose a simplistic model dealing with overtraining and exercise motivation. It is suggested that overtraining be viewed as the process leading to a state of being overtrained (or over stressed) which should be considered a response. This response state will be termed staleness. It should be noted, however, within the research literature the name given to the response state due to overtraining varies somewhat. The term "overtrained" (6, 51) or "overtraining syndrome" (32) frequently appear in the physiological research, while int he psychological research the terms "staleness" 934) or "burn-out" (50) have been used more prevalently. To prevent difficulty in the semantics of terms, it is proposed than the following working definitions be used to separate and clarify the terms.

OVERTRAINING - an abnormal extension of the physical training process with the results culminating in the state of staleness. Therefore, in this paper the term overtraining will be viewed and used only in the context of "a process".

STALENESS - a state in which the individual has difficulty maintaining a standard training regimens and can no longer achieve previous performance results (i.e., a consistent lack of performance improvement and/or a progressive decline in performance). This term can be defined as "the response" to the overtraining process. The most common sign and symptoms of individual who have progressed to the state of staleness are listed in Table 1 (3, 34).

TABLE 1.

Psychological	Physiological
Apathy	Muscle Pain or Soreness
Heavy Feeling	Performance Decline
Low Motivation	Retarded Recovery After Exertion
Lethargy	Weight Loss
Mood Changes	Lymphadenopathy
Withdrawal	Drawn Appearance
Altered Perception	Appetite/Sleep Loss

EXERCISE MOTIVATION - a series of qualities and characteristics displayed by an individual doing exercise training which affects their exercise experience in such a fashion that it may aid or distract from the person's adherence/compliance to their training regime (10, 11). For

example, factors associated with motivation as reported by Dishman and Ickes (11) are: willpower, organization, determination, persistence, apathy, lethargy, diligence, dependability, and commitment.

PROPOSED CONCEPTUAL MODEL

A conceptual model of the training process and exercise motivation, based upon the preçeding working definitions as well as available research findings, is presented in Figure 1. The basic premise or this model is the "stimulus - response" paradigm. In Figure 1, section A - B represents a normal exercise training response (1, 5, 18). As a training stimulus is applied (i.e., loads are increased) and the body adapts and improves, positive psycho-physiological responses occur. However, if too much of a stimulus occurs (i.e., overtraining) negative responses develop. This response is depicted in section C. Section D of Figure 1 represent a detraining or undertraining scenario (i.e., lack of enough of a training stimulus) Which also results in negative responses. However, this aspect of the model is not addressed currently since it is not entirely within the purpose of this prospectus. Figure 2 attempts to summarize some of the interactions for psychological and physiological stimuli and responses within the model.

EXPERIMENTAL PROTOCOLS TO INDUCE OVERTRAINING

It is proposed that the initial step in conducting research into the area of overtraining/staleness/motivation should involve the development of a experimental tool. That is, currently a standardized protocol or prescription for induced overtraining does not exist. The development of a standardized experimental procedure or manipulation is essential if successive studies analyzing the various psycho-physiological aspects of overtraining, staleness, and exercise motivation are to be conducted.

Existing Protocols

In the research, two basic approaches have been reported for studying individuals subjected to overtraining: 1) "expo facto", and 2) experimental. In the former, investigators have evaluated subject characteristics after self-reporting of indicators suggestive of overtraining (9, 12, 27, 30, 32). In these studies no controls as to training load had been employed and in many cases evaluations of training regimes are highly anecdotal. Conversely, the experimental methodology has involved investigator manipulation of the training load to

FIGURE 1

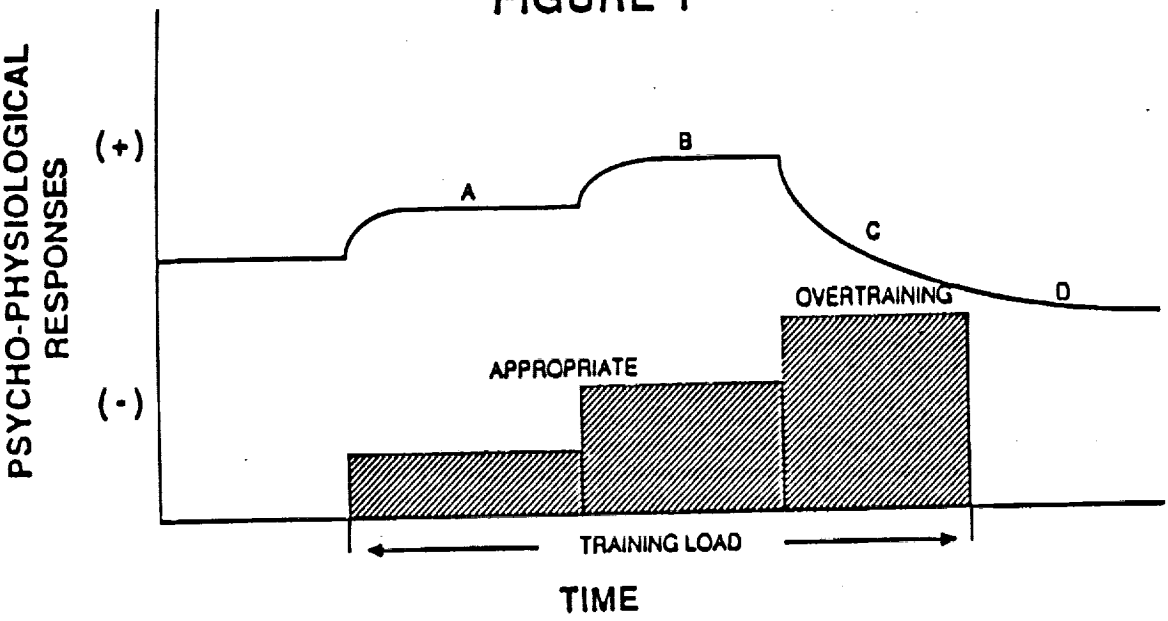

FIGURE 2

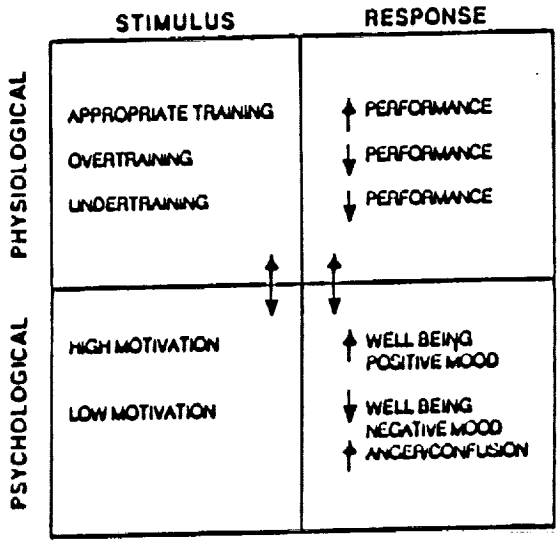

produce overtraining and induce staleness. Within the intent of this prospectus, the methodology of the experimental studies are of a more applicable nature; therefore; only the experimental studies will be discussed.

The literature suggest that the overtraining process involves increases in the amount of daily work requirements (i.e., training volume) for the exercising individual. These work requirements can be in the form of absolute work (training volume) performed as well as evaluations in the intensity of work performed (1, 18).

It would appear increases in absolute amounts of training volume (i.e., total work performed [= frequency x duration x intensity of exercise]) have been the major means of inducing overtraining. The degree of training volume increases have varied from 50% up to 370% of the amount the subjects performed prior to the experiments beginning (8, 13, 31, 40, 41, 52). This large range in volume increases seems to be influenced by several factors; 1) the initial fitness levels of the subjects, 2) the amount of pre-experiment training being performed, and 3) the time-frame in which the investigators are subjecting the individual to the overtraining stimulus. Primarily, the larger increases in training loads were found in those studies submitting their subjects to relatively short periods of overtraining (10 to 14 days) (8, 13, 31). Conversely, lower increases in absolute training load were associated with studies of extended duration (approximately 4 weeks or greater) (37, 41, 48, 53). The type of training associated with these studies has tended to be of a combined variety (continuous duration and intermittent activities) and has involved cycling, swimming, or running as an exercise modality (8, 13, 31,37, 41, 48, 52). Principally, in designing the set-up of these studies the investigators have attempted to mimic a program that a competitive individual may encounter during the course of their training.

Almost all the experimental studies also have attempted to manipulate the intensity at which the overtraining individuals were working. However, the manipulation of this variable has been typically to a much smaller degree than that of the total volume of work performed. In the majority of the studies the training intensities were maintained at relatively moderate to high levels (65 to 94% of maximal capacity) (8, 13, 31,37,41,48, 53). The one exception to this was the study performed by Sharp and Hackney (47). In this investigation, the subjects were required to perform repeated weekly training sessions (>30 % total training volume) involving intermittent bouts of exercise at supra-maximal work (125-175% of maximal capacity). This training intensity, while high, is not outside of the range that competitive athletes perform in training practices.

Generally, the overtraining protocols have manipulated training volume with either a rapid (10-14 day) or slow (3-4 months) onset of supra-normal training loads. There is no evidence to suggest that the variety of psychological and physiological responses to these ends of the overtraining continuum (see next section) differ. However, rapid on-set protocols may introduce an acute stress responses in the body which could potentially interfere with experimental interpretation. A protocol employing a moderate amount of time (4 weeks) for introducing a training overload presents a means to avoid this potential problem. Furthermore, work from our laboratory indicates that staleness characteristics are manifested significantly by 4 weeks and are relatively unchanged by additional overtraining (6 weeks) (25, 38, 47, 48).

Psycho-Physiological Findings

Psychological disturbances have frequently been reported for overtrained and stale individuals (6, 33, 34,51). The research suggest that mood disturbances may increase in a progressive manner with step-wise increases in training load (34, 35, 41). Therefore, several investigator (35, 41) have hypothesized that this relationship is dose-dependent, and reductions in training load should be accompanied by improved mood states. However, the current prospective research findings are inconclusive as to whether such a relationship exist.

Some specific mood alterations reported in response to overtraining and staleness have been increased levels of depression, anger, and fatigue (35, 41). Typically, these behavioral states have been assessed by the "Profile of Mood States" (POMS) test. Another measure from the POMS also found to be elevated due to overtraining is the composite indicator, global mood state (35, 41). Studies by Morgan et al. (33, 35) indicate that a person's perception of their "general state of well-being" declines as overtraining occurs. Furthermore, as well-being declines the perception of exercise difficulty (i.e., rating of perceived exertion) increases (34, 35). Research evidence suggest that as these behavioral changes take place an individual's self-motivation decreases and this facilitates a reduction in the adherence to their training regime (44, 45).

Physiologically, one of the most common complaints of the overtrained athlete is muscle soreness and chronic muscle fatigue (6, 12, 25, 35, 51). Serum levels of creatine kinase (muscle tissue damage marker) show concomitant increases that mirror that of the reported cases of muscle soreness (4, 12). These creatine kinase changes suggest that the subjective soreness increases have a physiological basis in muscle tissue damage. Some researchers have reported declines in muscle

function coinciding with the increased complaints of soreness (44, 45, 52). In a study by Ness (38) subjects performed the "Wingate" anaerobic power test (indicative of muscular power) at 2 week intervals during 8 weeks of intensive training. It was found that the subjects who complained of severe muscle soreness showed a lack of power improvement after the initial 4 weeks of training. This response occurred even though the subjects received a continuous anaerobic training stimulus throughout the study. Similarly, Hakkinen and associates (26) have reported that overtrained subjects do not show improved muscular strength development even with exposure to an appropriate training stimulus. Coinciding with these changes in muscle function in the Hakkinen study were lowered serum testosterone-cortisol ratios (anabolic vs catabolic status). This finding of a reduced testosterone-cortisol ratio during the overtraining process has also been reported by several other investigators (23, 24, 25, 56). Additionally, numerous studies have found elevated resting serum and salivary coritsol levels during overtraining (25, 41, 53, 56). Concomitant with the elevations in cortisol have been increases in serum and urinary urea nitrogen levels (protein breakdown byproduct) (25, 30). These urea nitrogen changes are reflective of an increased catabolic state in overtraining subjects (15). Also research indicates that the rate of nitrogen loss can result in a chronic negative nitrogen balance in the overtraining athlete (25, 54).

Barron and colleagues (3) have evaluated hormone responses to insulin induced hypoglycemia challenges in ultra-marathoners with and without diagnosed staleness. The ultra-marathoners displaying staleness showed reduced ability to release growth hormone, adrenocorticotropin hormone, and cortisol as compared with the control ultra-marathoners. After a four week rest period the endocrine function of the stale ultra-marathoners was found to improve and approach that of the control marathoners. The authors concluded these hormonal findings imply a state of pituitary-adrenal gland "exhaustion" may be associated with overtraining and have physical and psychological effects. Several preliminary reports have suggested the changes in testosterone levels and pituitary function associated with overtraining may produce an impairment in reproductive capacity (2, 22, 23, 24); however, the findings are currently inconclusive and can not suggest a disruptive relationship exist.

The cardiovascular system also displays a series of perturbations due to overtraining. Progressive increases in the resting heart rate and systolic blood pressure have been reported in overtraining individuals (9, 14). Several researchers have speculated that these changes in resting cardiovascular measures are due to enhanced neuroendocrine influences (14, 20), however, an exact mechanism for the changes remains uncertain. The research is somewhat

contradictory concerning overtraining effects on the cardiovascular function during exercise, primarily with respect to oxygen uptake capacity. Foster et al. (17) has shown a declining capacity, while Stray-Gundersen et al. (53) as well as Costill et al. (8) have demonstrated slight, but non-significant increases in oxygen uptake capacity during overtraining. In each of these studies an appropriate training stimulus was being applied such that improved oxygen uptake capacity should have occurred (1). Several investigators have found overtraining produces what is termed "sport anemia" (13, 19, 59). Others, however, have failed to demonstrate marked changes in hematological measures during overtraining (8, 31, 47, 48). These latter results are supported by Wishnitzer and associates (58) who evaluated bone marrow cellularity, bone marrow hemosiderin, hemoglobin, and serum ferritin levels in overtrained and healthy runners. A higher degree of bone marrow hypocellularity was found in the overtrained than in the healthy runners (54 % vs 66 %); however, all other measures were similar between the groups and within normal acceptable physiological ranges.

Costill et al. (8) have reported lower muscle glycogen levels were observed in overtrained athletes who exhibited staleness. Costill has proposed that this finding may be the result of inadequate dietary carbohydrate ingestion. That is, reduced carbohydrate intake results in lowered muscle glycogen levels, thereby reducing energy substrate availability and impairing energy metabolism (7, 46, 57). This in turn results in the reduced performance found in stale athletes. Suppressed lactate profiles (blood lactate levels in response to a fixed workload) are also found in the overtraining athletes. This indirectly supports Costill's theory as the suppressed profiles could be due to muscle glycogen depletion (1, 49).

Another common anecdotal reported symptom of individuals subjected to overtraining are increased numbers of head colds and respiratory infections (16, 27, 42, 45, 51). Total lymphocyte counts, salivary immunoglobulin A (IgA), helper T, and suppressor T levels/function have all been reported suppressed during period of overtraining (21, 29, 37, 43, 55). However, at this time since very little experimental work has been performed evaluating how overtraining affects the immune system the implication of these findings is uncertain.

FUTURE PROJECTS AND RECOMMENDATIONS

The completion of this pilot project and the refinement of an experimental protocol to produce overtraining and induce staleness presents many avenues for future joint as well as separate research projects such as; 1) Overtraining Threshold - is there a threshold level of training load at which overtraining starts to develop and can it accurately be

identified in individuals. Such information would be helpful in the establishment of exercise prescriptions; 2) Exercise Motivation Strategies - can motivation strategies be identified in overtraining individuals who develop staleness (responders) and those who do not (non-responders). This information could be useful in behavioral modulation to prevent staleness from occurring; 3) Social Intervention and Overtraining - if non-responders associate with responders during the overtraining process do the responders develop non-responder coping strategies (i.e., become less likely to become stale). This has potential implication in the selection of crew make-up; and 4) Recovery from Overtraining and Staleness - the steps and methods that are necessary to recovery from overtraining or staleness is uncertain. Such information could be help in the determination of the recovery time necessary between missions.

The intent of preparing this prospectus was to stimulate discussion of research relative to human health and well-being with prolonged exposure to microgravity. Historically, problems with microgravity exposure and space flight have been addressed in a retroactively fashion. The issue of "exercise overtraining and motivation" as a research topic is being presented in a proactive fashion. That is, planned space missions have a high potential risk for inducing the problems discussed within this prospectus. Hopefully, appropriate planning and measures can be taken prior to such problems developing. If research can take place to examine this issue early and extensive enough there can be an elimination for "quick or stop-gap" measures in the future.

REFERENCES

1. Astrand, P.O., & Rohdahl, K. (1977). Textbook of work physiology: Physiological basis of exercise. New York: McGraw-Hill, 141-199.

2. Ayers, J.W.T., Komesu, Y., Romani, T., & Ansbacher, R. (1985). Anthropometric, hormonal, and psychologic correlates of semen quality in endurance-trained athletes. Fertility and Sterility, 43, 917-921.

3. Barron, J.L., Noakes, T.D., Levy, W., Smith, C., & Millan, R.P. (1985). Hypothalmic dysfunction in overtrained athletes. Journal of Clinical Endocrinology and Metabolism, 60, 803-806.

4. Byrnes, W.C., & Clarkson, P.M. (1986). Delayed onset muscle soreness and training. In F.I. Katch, & P.S. Freedson (Eds.), Clinics in sports medicine (pp. 605-614). Philadelphia: W.B. Saunders.

5. Costill, D.L. Carbohydrates for exercise: dietary demands for optimal performance. International Journal of Sports Medicine. 9: 1-18, 1988.

6. Costill, D.L. (1986). Detection of overtraining. Sportsmedicine Digest, 8(5), 4-5.

7. Costill, D.L. (1984). Energy supply in endurance activities. International Journal of Sports Medicine. 5: 19-21.

8. Costill, D.L., Flynn, M.J., Kirwan, J.P., Houmard, J.A., Mitchell, J.B., Thomas, R.S., & Park, S.H. (1988). Effects of repeated days of intensified training on muscle glycogen and swimming performance. Medicine and Science in Sport and Exercise, 20, 249-254.

9. Czajkowski, W. (1979). A simple method to control fatigue in endurance training. In P.V. Komi (ed.), Exercise and sport biology (pp. 207-212). Champaign, IL: Human Kinetics.

10. Dishman, R.K., & Gettman, L.R. (1980). Psychobiologic influences on exercise adherence. Journal of Sport Psychology. 2: 295-310.

11. Dishman, R.K., & Ickes, W. (1981). Self-motivation and adherence to therapeutic exercise. Journal of Behavioral Medicine. 4(4): 421-438.

12. Dressendorfer, R.H., & Wade, C.E. (1983). The muscular overuse syndrome in long-distance runners. The Physician and Sportsmedicine, 11(11), 116-130.

13. Dressendorfer, R.H., Wade, C.H., & Amsterdam, E.A. (1981). Development of pseudoanemia in marathon runners during a 20-day road race. Journal of the American Medical Association, 246, 1215-1218.

14. Dressendorfer, R.H., Wade, C.E., & Scaff, J.H. (1985). Increased morning heart rate in runners: a valid sign of overtraining? The Physician and Sportsmedicine, 13(8), 77-86.

15. Dolny, D.G. & Lemon, P.W.R. (1988). Effect of ambient temperature on protein breakdown during prolonged exercise. Journal of Applied Physiology, 64, 550-555.

16. Eberhardt, A. (1970). Resistance against infections with intensive training and overtraining. Sport Wyzycnowy Warszawa, 8, 40-45.

17. Foster, C., Pollock, M., Farrell, P., Maksud, M., Anholm, J., & Hare, J. (1982). Training responses of speed skaters during a competitive season. Research Quarterly for Exercise and Sport, 53, 243-246.

18. Fox, E.L., Bowers, R.W., & Foss, M.L. (1988). The physiological basis of physical education and athletics (4th ed.). Philadelphia: Saunders.

19. Fredrickson, L.A., Puhl, J.L., & Runyon, W.S. (1983). Effects of training indices on iron status of young cross-country runners. The Journal of Sports Medicine and Physical Fitness, 15, 271-276.

20. Galbo, H. (1983). Hormonal and metabolic adaptation to exercise. New York: Thieme-Stratton Inc.

21. Green, R.L., Kaplan, S.S., Rabin, B.S., Stanitski, C.L. & Zdziarski, U. (1981). Immune function in marathon runners. Annals of Allergy, 47, 73-75.

22. Griffith, R.B., Dressendorfer, R.H., & Fullbright, C.O. (1988). Effects of overwork on testosterone, sperm count and libido. Medicine and Science in Sport and Exercise, 20 (Suppl. 2), S39.

23. Hackney, A.C., & Sinning, W.E. (1986). The effects of wrestling training on reproductive hormones. Medicine and Science in Sport and Exercise, 18, 196.

24. Hackney, A.C., Sinning, W.E., & Bruot, B.C. (1988). Reproductive hormonal profiles of endurance-trained and untrained males. Medicine and Science in Sport and Exercise, 20, 60-65.

25. Hackney, A.C., Sharp, R.L., Runyan, W.S., Kim, Y. & Ness, R.J.(1988). The effects of combined aerobic training on post-exercise nitrogen excretion. Proceedings of the 7th International Biochemistry of Exercise Conference. Canadian Journal of Sport Science, 13, 14P.

26. Hakkinen, K., Parkarinen, A., Alen, M., & Komi, P.V. (1985). Serum hormones during prolonged training of neuromuscular performance. European Journal of Applied Physiology, 53, 287-293.

27. Hollman, W., & Hettinger, T. (1980). Sportmdizin, arbeits und trainings-grundlagen. F.K. Schattawer and Stuttgart, 549-552.

28. Johnson, R.S., & Dietlein, L.F. (1977). Biomedical Results From Skylab. NASA Scientific and Technical Information Office, Washington, D.C.

29. Keast, D., Cameron, K., & Morton, K.R. (1988). Exercise and the immune response. Sports Medicine, 5, 248-267.

30. Kindermann, W. (1986). Das uebertraining-ausdruck ciner vegetativen fehlsteuering. Deutsche Zeitschrift fur Sportmedizin, H8, 139-145.

31. Kirwan, J.P., Costill, D.L., Flynn, M.G., Mitchell, J.B., Fink, W.J., Neufer, P.D., & Houmard, J.A. (1988). Physiological responses to successive days of intense training in competitive swimmers. Medicine and Science in Sport and Exercise, 20, 255-259.

32. Kupiers, H., & Keizer, H.A. (1988). Overtraining in elite athletes. Sports medicine, 6, 79-92.

33. Morgan, W.P. (1979). Negative addiction in runners. The Physician and Sportsmedicine, 7(2), 57-70.

34. Morgan, W.P., Brown, D.R., Raglin, J.S., O'Connor, P.J., & Ellickson, K.A. (1987). Psychological monitoring of overtraining and staleness. British Journal of Sports Medicine, 21, S50.

35. Morgan, W.P., Costill, D.L., Flynn. M., Raglin, J., & O'Connor, P.J. (1988). Mood disturbances following increased training in swimmers. Medicine and Science in Sport and Exercise. 20: 408-414.

36. Moroz, O., & Zagalskily, L. (1989). Psychological support experts view social interaction of cosomnauts. Literaturnava Gazeta. 4: 10.

37. Neisler, H.M., Bean, M.H., Pittington, J., Thompson, W.R., & Johnson, J.T. (1989). Alteration of lymphocyte subsets and endocrine response during 42 days of competitive swim training. Medicine and Science in Sport and Exercise, 21, S110.

38. Ness, R.J. (1988). Effects of protein intake on physiological adaptations to training. Unpublished master's thesis. Iowa State University.

39. Nicogossian, A.E., & Parker, J.F. (1982). Space Physiology and Medicine. NASA Scientific and Technical Information Office, Washington, D.C.

40. Nicogossian, A.E. (1977). The Apollo-Soyuz Test Project: Medical Report. NASA Scientific and Technical Information Office, Washington, D.C.

41. O'Connor, P.J., Morgan, W.P., Raglin, J.S., Barksdale, C.M., & Kalin, N.H. (1989). Selected psychoendocrine responses to overtraining. Medicine and Science in Sport and Exercise, 21, S50.

42. Peters, E.M., & Bateman, E.D. (1983). Ultramarathon running and upper respiratory tract infections. South African Journal of Medicine, 64, 582-584.

43. Raglin, J.S., & Morgan, W.P. (1989). Development of a scale to measure training-induced distress. Medicine and Science in Sports and Exercise. 21: S50.

44. Rowland, T.W. (1986). Exercise fatigue in adolescents: diagnosis of athlete burnout. The Physician and Sportsmedicine, 14(9), 69-77.

45. Ryan, A.J., Burke, E.R., Falsetti, H.L., Frederick, E.C., & Brown, R.L. (1983). Overtraining of athletes. The Physician and Sportsmedicine, 11(6), 93-110.

46. Scharf, M.B., & Barr, S. (1988). Craving carbohydrates: a possible sign of overtraining. Annals of Sports Medicine, 4, 19-20.

47. Sharp, R.L., & Hackney, A.C. (1988). Effects of a protein supplement on adaptations to combined aerobic and anaerobic training. Medicine and Science in Sports and Exercise. 20: S3.

48. Sharp, R.L., Ness, R.J., Hackney, A.C., & Runyan, W.S. (1989). Compatability of aerobic and anaerobic adaptations to training in males. Medicine and Science in Sport and Exercise, 21, S76.

49. Sharp, R.L., Vitelli, C.A., Costill, D.L., & Thomas, R. (1984). Comparison between blood lactate and heart rate profiles during a season of competitive swim training. Journal of Swimming Research, 1, 17-20.

50. Silva, J. Psychological profiles of athletes with overtraining syndromes. Presentation at the national meeting of Association for the Advancement of Applied Sports Psychology. Nausha, NH, 1988.

51. Stamford, B. (1983). Avoiding and recovering from overtraining. The Physician and Sportsmedicine, 11(10), 180.

52. Standish, W.D. (1984). Overuse injuries in athletes: a perspective. Medicine and Science in Sport and Exercise, 16, 1-7.

53. Stray-Gundersen, J., Videman, T., & Snell, P.G. (1986). Changes in selected objective parameters during overtraining. Medicine and Science in Sport and Exercise, 18(Suppl. 2), 54.

54. Tarnopolsky, M.A., MacDougall, J.D., & Atkinson, S.A. (1988). Influence of protein intake and training status on nitrogen balance and lean body mass. Journal of Applied Physiology, 64, 187-193.

55. Tharp, G.D., & Barnes, M.W. (1989). Reduction of immunoglobin-A by training. Medicine and Science in Sport and Exercise, 21, S109.

56. Urhasen, A., Kullmer, T., & Kindermann, W. (1987). A 7-week follow-up study of the behaviour of testosterone and cortisol during the competition period in rowers. European Journal of Applied Physiology, 56, 528-533.

57. Vollsted, N.K., & Sejersted, O.M. (1988). Biomechanical correlates of fatigue. European Journal of Applied Physiology, 57, 336-347.

58. Wishnitzer, R., Berrebi, A., Hurwitz, N., Vorst, E., Eliraz, A.(1986). Hypocellularity and overtraining. The Physician and Sportsmedicine, 14(7), 86-100.

59. Yoshimura, H. (1961). Adult protein requirements. Federation Proceedings, 20, 103-110.

RESEARCH IN HUMAN PERFORMANCE RELATED TO SPACE: A COMPILATION OF THREE PROJECTS/PROPOSALS

Final Report

NASA/ASEE Summer Faculty Fellowship Program--1989

Johnson Space Center

Prepared By:	Scott M. Hasson, Ed.D., P.T.
Academic Rank:	Assistant Professor
University & Department:	University of Texas Medical Branch Department of Physical Therapy Galveston, TX 77550
NASA/JSC	
Directorate:	Space and Life Sciences
Division:	Man Systems/Medical Sciences
Branch:	Crew Station/SD5
JSC Colleague:	Mavis Fujii, M.D.
Date Submitted:	September 20, 1989
Contract Number:	44-001-800

ABSTRACT

Scientific projects have been developed in order to maximize performance in space and assure physiological homeostatis upon return. Three projects that are related to this common goal were either initiated or formulated during the Faculty Fellowship Summer Program. The projects were entitled: 1) Effect of simulated weightlessness (bed rest) on muscle performance and morphology; 2) Effect of submaximal eccentric muscle contractions on muscle injury, soreness and performance: A grant proposal; and 3) Correlation between isolated joint dynamic muscle strength to end-effector strength of the push and pull EVA ratchet maneuver. The purpose of this report is to describe each of these studies in greater detail.

EFFECT OF SIMULATED WEIGHTLESSNESS ON MUSCLE PERFORMANCE AND MORPHOLOGY

S. Siconolfi, S. Carter, V. Edgerton, M. Fujii, M. Greenisen, B. Harris, J. Hayes, J. Herbison, M. Jaweed (Study initiated 7/22/89; to be completed 10/9/89).

HYPOTHESES

The following hypotheses will be investigated during 7 days of bedrest:

1. There will be significant decreases in muscle performance of upper and lower extremity flexors and extensors.

2. There will be a significant decrease in muscular electrical activity.

3. There will be measurable muscle atrophy in the vastus lateralis muscle without significant alterations in contractile protein and metabolic enzymes.

INTRODUCTION

Prolonged immobilization and bed rest are believed to have qualitative similarities to weightlessness (7). Limb immobilization and bed rest have been demonstrated to produce skeletal muscle atrophy and decreased muscle performance (2). Histological techniques have been utilized to further document atrophy in both Type I and II muscle fibers (3). In addition, electromyographic (EMG) activity decreases with chronic immobilzation (5).

The purpose of this study will be to examine the effects of simulated weightlessness (bed rest of 7-days length) on muscle performance and morphology. It is hoped that the results of this study will aid to develop exercise countermeasures to combat muscular detraining.

METHODS

Subjects

Twelve healthy subjects will be recruited and undergo an Air Force Class III physical examination and treadmill exercise stress test. Subjects will be in the age group of 30-50 years old without cardiovascular disease.

Procedures

Three days prior to bed rest the subjects will be tested for concentric and eccentric isokinetic muscle strength. Electromyographic activity (EMG) will also be evaluated during muscle strength testing. Muscle strength and EMG testing will be repeated 24-hours later for test/re-test reliability. The subjects will have a needle muscle biopsy taken on the non-dominant leg the day of admittance for bed rest. Subjects will have seven days of complete bed rest with the second biopsy taken on the seventh day. Subjects then will be re-evaluated for muscle strength and EMG on the seventh day with measures repeated 24-hours later. Subjects will return at 1 and 2 week time periods for re-assessment of muscle strength and EMG.

Muscle Testing and EMG

Muscle performance will be evaluated each day utilizing the Biodex dynamometer (Biodex Corp., Shirley, NY). Concentric and eccentric maximum torque of the elbow, shoulder, trunk, knee and ankle flexors and extensors will be taken. The subject will be placed in the Biodex unit so that the axis of the specific joint tested will be directly in line with the axis of the goniometer. Prior to specific joint muscle testing the subject will perform 3 submaximal and 1 maximal warm-up repetitions at the designated testing velocity (elbow, shoulder, and trunk = 75 degrees/sec; knee and ankle = 30 degress/sec). The subject will be instructed to give maximum efforts for each repetition and informed to flex and extend the body segment through the entire available range as forcefully as possible for the 3 repetitions. Data will be collected on the dominant side with 5-minutes of rest between each joint tested. EMG signals will be recorded by means of Ag/AgCl electrodes placed over the belly of each tested muscle group in a bipolar configuration with the site marked for identical placement on later trials. A reference electrode will be placed over a bony prominance (clavicle for upper extremity and trunk; head of fibula for lower extremity. The muscles studied for the elbow joint will be biceps brachii and triceps brachii; for shoulder anterior deltoid and latissimus dorsi; for trunk rectus abdominus and erector spinaii; for knee vastus lateralis and biceps femoris; and for ankle anterior tibialis and gastrocnemius. Electrode placement will be preceded by abrasion and cleansing of the skin surface to reduce source impedence to less than 3000 ohms. During each contraction raw EMG signals will be amplified (Gould, band-pass 3-1000 Hz) recorded at a rate of 1250 Hz and stored on tape for further computer analysis (Ariel System). Signals will be processed for signal amplitude (IEMG) (10).

Morphology

Needle muscle biopsies of the vastus lateralis will be taken using sterile technique. Enzymatic analyses will consist of measuring succinate dehydrogenase, glycerophosphate dehydrogenase, myofibrillar ATPase, and myosin ATPase. In addition, the cross sectional area of the biopsy will be analyzed to determine changes of actual myofiber size.

Statistical Analyses

A two-factor factorial design will be employed to determine the effects of ambulatory status, time of measurement, and their interaction on muscle performance, EMG and muscle morphology. A two-way ANOVA, adjusted for repeated measures across time of measurement (split plot) will be utilized with significance established at $p<0.05$.

EFFECT OF SUBMAXIMAL ECCENTRIC CONTRACTIONS ON MUSCLE INJURY, SORENESS AND PERFORMANCE: A GRANT PROPOSAL

S. HASSON, M. FUJII, M. GREENISEN, B. PATTEN, W. BARNES, AND J. WILLIAMS

(Initial proposal submitted for Summer Faculty Fellowship Grant; Resubmission to NASA targeted for 12/89-with planned start of 2/90)

HYPOTHESES

The following hypotheses will be investigated immediately, 24 and 48-hours after eccentric knee extension exercise bouts of low and high load:

1. There will be no decreases in muscle performance following low load eccentric exercise, but significant decreases will occur following high load eccentric exercise.

2. There will be no change in EMG activity for any of the quadriceps muscles following low load eccentric exercise. However, EMG activity will significantly increase for rectus femoris and decrease for vastus lateralis and medialis following high load eccentric exercise.

3. There will be no change in muscle creatine kinase and muscle morphology following low load eccentric exercise. There will be an elevation of muscle creatine kinase and signifcant alteration in muscle and conncetive tissue indicating damage following high load eccentric exercise.

4. There will be no muscle soreness perception of the quadriceps musculature following low load eccentric exercise, but significant muscle soreness perception will occur following high load eccentric exercise.

INTRODUCTION

Muscle weakness and atrophy occured after exposure to a zero-gravity environment during the Skylab missions (16). Concentric exercise programs were employed to neutralize these detrimental changes. However, most functional movements at one-g require both concentric and eccentric muscular contractions. At zero-g eccentric contractions of the lower and upper limbs may occur less frequently since weight-bearing is minimized in this environment. Upon return to a one-gravity environment after extended zero-gravity habitation, mission specialists may have difficulty performing normal dynamic functional activities requiring eccentric contractions of large lower limb muscle groups (i.e. stand to sit, sit to supine, and many deceleration functions of the lower limb segments during ambulation and stair decent). In addition, there is some cause for concern of potential muscle injury when eccentric contractions are required again. This concern arises from data on deconditioned patients who unexpectedly performed eccentric contractions during stair decent resulting in quadriceps muscle rupture at the musculotendinous junction (13, 14). Eccentric muscle contractions produce an equal amount of force with less active motor units, thus greater force per tissue area than concentric contractions. This is one explanation as to why micro-injury, macro-injury and muscle soreness occur at musculotendinous junctions when "unaccustomed" eccentric contrac-

tions are performed (1, 6, 15). Earlier data suggests that submaximal eccentric loads (60-80% of body weight) for the lower extremities does not initiate muscle soreness (8). However, little research has been performed to determine at what level of eccentric load (percent of body weight) may be noninjurious and yet provides sufficient eccentric stimulus to delay connective tissue weakening.

The purpose of this investigation will be to determine: 1) A dose-response curve of eccentric loads at various percents of body weight on indices of muscle damage and performance.

METHODS

Subjects

Twelve healthy subjects will participate in this investigation. All subjects will be male (non-smokers) ages 20-45 that will be recruited from the Houston/Galveston community by the Health Screening Facility of the Medical Sciences Division in Building 37. The subjects will not have had experience in weight-training nor have had any orthopaedic or neurological limitations of the knee joint (i.e. ligamentous surgery, Rheumatoid Arthritis of Osteoarthritis). All subjects will undergo an Air Force Class III physical examination and will be familiarized with the experimental procedures and possible risks involved, and asked to provide informed consent.

Procedures

On each test day subjects will report to the laboratory in a fasting condition. On the first session subjects will be randomly assigned to two treatment conditions (% body weight for eccentric load); one for each leg (1 limb low percent 60, 70 or 80%, and the other limb high percent 90, 100 or 110%) therefore an N of 4 limbs for each experimental condition. Immediately after baseline muscle force, plasma creatine kinase, electromyographic activity (EMG), and soreness data are collected the subjects will perform the eccentric exercise bout at the desired experimental load. The exercise bout will consist of 10-minutes incorporating 150 eccentric muscle contractions of the quadriceps. Immediately after the conclusion of the exercise bout subjects will have the opposite leg go through the same procedure, but at a different experimental condition. At the conclusion of both experimental exercise bouts the limbs will be evaluated for muscle force production, creatine kinase, EMG and muscle soreness perception. Subjects will return to the laboratory 24-hours and 48-hours post exercise, and will be evaluated again for force production, creatine kinase, EMG and muscle soreness. In addition, at 24-hours subjects will have a muscle biopsy excised.

Muscle Testing, EMG and Muscle Soreness

Force production will be evaluated at 2 velocity settings using a Lido isokinetic dynamometer (Loredan Co., Davis, CA). The velocities of the maximum contractions will be 60 degress/second and 180 degrees/second. In addition, maximum knee extension isometric force (MVC) with knee joint stabilized at 60 degrees of flexion will be measured. The subject will be placed in the Lido unit so that the axis of the knee joint is directly in line with the axis of the goniometer. Prior to the knee joint muscle testing the subject will perform 5 submaximal repetitions at the designated

testing velocities. The subjects will be instructed to give maximum efforts for each repetition. Data will be collected at the high velocity (180 deg/sec) for 20-repetitions on both knee joints with 15-minutes of rest before data collection at the low velocity (60 deg/sec) for 5-repetitions. MVC measures will follow isokinetic knee joint testing after an additional 15-minutes of rest. Three MVC measures will be taken on each leg with a rest period of 3-minutes between contractions.

Areas over the mid-belly of rectus femoris, distal head of vastus medialis and proximal head of vastus lateralis will be prepared by abrasion and cleansing with alcohol to reduce source impedence to less than 3 Kohms. All areas will be marked so that identical sites will be used on subsequent testing. Raw EMG signals will be amplified, recorded at a rate of 1024 Hz, digitized and stored on hard disk for further computer analysis (Ariel Motion Analysis System) during MVC maneuvers. Mean power frequency and root mean squared will be computed by means of full wave rectification and fast Fourier transformation of raw EMG data (11).

A polyurethane sheet marked with a grid of intercepts 2cm apart, used as soreness test sites, will be attached to the anterior thigh with the skin marked to insure constant positioning in subsequent tests. A round-ended metal probe (2mm diameter at tip) will be attached to a load cell (SensorMedics Model UL4-50) and a strain gauge (Gould-Statham Model UTC3). The load cell/strain gauge instrument is interfaced to the R511A SensorMedic dynagraph via a voltage/pulse/pressure coupler (SensorMedics Model 9853A) and to an 8-channel A/D board (Metrabyte DASH-8) and IBM 286 computer. The amplified force signal will be displayed and recorded on the hard disk of the computer for further analysis. At each test site, a gradually increasing force will be applied up to a maximum of 50 Newtons of pressure. The subject will be asked to verbally indicate when the sensation of pressure changed to discomfort. The amount of force will then be recorded via computer. If no indication of discomfort is reported up to 50 Newtons, soreness will not be considered to be present at the site. A standard pattern of testing will be performed in order to insure complete evaluation of the entire quadriceps muscle (9).

Muscle Enzymes and Morphology

Muscle creatine kinase will be evaluated from plasma samples. Histochemical analyses will be performed on muscle tissue removed via open muscle biopsy of the proximal head of vastus lateralis of both legs. Analyses will include trichrome, ATPase at pH 9.4, NADH-TR, succinate dehydrogenase and glycerol-3-phosphate dehydrogenase to document myofibrillar and/or connective tissue damage. Tissue samples will be analysed visually for damage using electron microscopy.

Statistical Analyses

A two-factor factorial design will be employed to determine the effects of the experimental conditions, time of measurement and their interaction on muscle performance, EMG, muscle morphology, muscle enzymes and perception of muscle soreness. A two-way ANOVA, adjusted for repeated measures across time of measurement (split-plot) will be utilized with significance established at $p<0.05$.

CORRELATION BETWEEN ISOLATED JOINT DYNAMIC STRENGTH TO END-EFFECTOR STRENGTH OF THE PUSH AND PULL EVA RATCHET MANEUVER

S. HASSON, A. PANDYA, S. WEI, T. DEVERE, M. GREENISEN, AND B. WOOLFORD

(Initial pilot data [2 cases] begun 7/89 with proposed study to begin 10/89 to 6/90).

HYPOTHESES

1. There will be a significant correlation between isolated joint maximum torque production and the EVA ratchet push/pull maneuver when adjusted for lean body mass of subject and ratio of EMG of primary muscle groups comparing both activities.

2. The predicted maximum torque production for the EVA ratchet maneuver will be highly correlated to actual measured EVA ratchet torque production.

INTRODUCTION

Development of an accurate predictive computer equations for graphical display and animation of EVA maneuvers requires establishment of a dynamic maximum muscle strength data base (4). The purpose of this project was to develop a protocol and mathematical equation to predict end-effector strength of a common EVA activity (push/pull ratchet maneuver) utilizing isokinetic isolated joint upper extremity muscle performance and lean body mass measures. The project was broken down into three portions for the initial 2 case studies: 1) Determination of end-effector strength and electrical myographic (EMG) activity of contributing muscles during a simulated ratchet tightening and loosening maneuver; 2) Determination of isokinetic isolated upper extremity joint maximum strength and EMG activity during varying angular velocities; and 3) Determination of lean body mass. Following completion of data collection an initial regression equation will be developed to predict end-effector strength from isolated joint maximum torque, EMG activity of contributing muscle, and lean muscle mass of the subjects. Following successful completion of the case studies; a data base of 80 subjects will be performed.

METHODS

Subjects

Eighty healthy subjects will be participate in this investigation. Approximately 40 males and 40 females without extensive weight training experience and orthopaedic limitations of the upper extremity will be recruited from the Houston/Galveston community by the principal investigator. All subjects will undergo an orthopaedic screening of the upper quarter by a certified Physical Therapist and will be familiarized with the experimental procedures and possible risks involved, and asked to provide informed consent.

Procedures and Instrumentation

Determination of End-Effector Strength, Angular Velocity and EMG During a Simulated EVA Ratchet Tightening and Loosening Maneuver

Specific NASA requirements for tightening and loosening bolts for shuttle bay doors with an EVA ratchet wrench have been established at 25 foot-pounds of torque requiring 5 loosening or tightening maneuvers. Simulation of this task can be accurately performed by utilizing a dynamometer which is able to apply a constant (isotonic) load for a ratcheting maneuver (Lido Multi-Joint Testing Unit, Loredan Biomedical, Inc., Davis, CA).

On day one the subject will perform the ratchet tightening and loosening maneuvers. The subject will be seated and trunk restraints will be applied to minimize trunk movement/muscle substitutions during the trials. Before each trial the subject will perform 3 submaximal repetitions at a low resistance (5 ft-lbs). The subject will then perform 5 maximum repetitions receiving strong verbal encouragement. The subject will perform 3 loosening and 3 tightening trials determined randomly with 5-minutes of rest between trials. Torque and angular velocity are determined during the ratchet maneuver by the Lido dynamonmeter. In addition, the tightening and loosening maneuvers will be filmed and segment/angular velocities will be determined for the elbow and shoulder joint by the Ariel Motion Analysis System. EMG activity will be measured during the tightening maneuver by isolating and recording signals from the primary movers of the shoulder and elbow joints (latissimus dorsii - shoulder extension and biceps brachii - elbow flexion); and the loosening maneuver (anterior deltoid - shoulder flexion and triceps brachii - elbow extension). Raw EMG signals will be recorded from Ag/AgCl surface bipolar electrodes (Pre-Amplifier Electrodes - Motion Control, Inc Salt Lake City, UT) located over the muscle belly at a rate of 1024 Hz, digitized, and stored on disk for further computer analysis (Advanced Logic 386 with Metrabyte Dash 16 A/D board). Signals will be processed for frequency content (mean power frequency [MPF]) via 512-point fast Fourier transformation, and for signal amplitude (root mean squared [RMS]) (11).

Determination of Isolated Isokinetic Muscle Strength and EMG Activity at Varying Angular Velocities

In order to predict end-effector maximum torque for any given upper extremity activity the isolated shoulder, elbow and wrist joints must be evaluated for maximum torque (Lido Multi-Joint Testing System, Loredan Biomedical, Inc Davis, CA) and EMG over the entire available range of motion, and at varying angular velocities (30 deg/sec upto 240 deg/sec). On days 2 through 5 the subject will be evaluated for shoulder abduction/adduction; shoulder internal/external rotation; shoulder flexion/extension; elbow flexion/extension; elbow (forearm) pronation/supination; Wrist ulnar deviation/radial deviation; and wrist flexion/extension. The subject will be seated for elbow and wrist testing while shoulder testing will be performed in the supine position. Each joint will be stabilized with velcro straps to minimize muscular substitutions and extraneous movement. During each testing day, 2 of the 7 joint movements will be selected randomly and evaluated. The testing protocol will consist of performing 3 submaximal contractions at the test velocity followed by 5 maximal repetitions. The subject will have 3-minutes of

rest, and the procedure will be repeated until all 8 velocities are evaluated. The order of velocity presentation will be randomized. Once one joint movement has been fully evaluated, 15-minutes of recover will be given before the next joint movement is tested. Four successive test days will be scheduled to accomidate all seven joint movements and allowing 24-hours of recovery between test sessions.

Determination of Lean Body Mass

Lean body mass will be determined utilizing the 1990B Bio-Resistance Body Composition Analyzer (Valhalla Scientific, El Cajon, CA). The subject will have the skin on the dorsum of the hand/wrist and foot/ankle prepared by abrasion and vigorous alcohol rub. Lead I electrodes will be placed on the dorsal surface of the right wrist bisecting the styloid processes of the fadius and ulna, and on the distal metacarpal of the index finger of the same hand. The second set of electrodes (Lead II) will be placed on the dorsal surface of the right ankle bisecting the medial and lateral malleoli, and on the first distal metatarsal of the same foot. The subjects will be placed in a supine position and asked to refrain from moving. Low amperage direct electrical current is generated, delivered into the subjects body at the proximal electrode and detected by the distal electrode. The difference between the charge introduced and detected is described as the bioelectric impedance. A close relationship has been established between lean body mass and electric current conductance (12). This procedure will require 15-minutes to perform.

Statistical Analyses

The relationship between end-effector maximum muscle strength and isolated joint maximum muscle strength (after lean body mass is accounted for and EMG activity for primary muscle groups is compared between the two tasks) will be determined by least-squares regression techniques. Regression equations will be developed for isolated joint maximum muscle strength curves (position to predict strength) at all 8 speeds, to predict push/pull end-effector task strength at any given angle.

SUMMARY

Exploration of space can be divided into stages of ascent, orbit, and egress. Physiological changes take place at each stage. One major concern with extended missions is the negative adaptations to a zero-gravity environment (16). Physiological measurements following SkyLab Missions suggested a decrement in muscle and bone tissue. Results from SkyLab data were instrumental in: 1) Developing further studies on effect of simulated weightlessness on muscle function; and 2) Developing exercise protocols to counteract the negative affects of zero-gravity adaptations.

Another area of concern with extended missions is performance of tasks within the shuttle or space station. Computer software programs have been developed to perform simulated tasks, prior to actual performance in mock-up or true space environment. Accurate information given to the computer model results in better task simulation.

The studies described in this report are derived to answer or clarify questions on human performance during and upon completion of space travel. The results from these studies will assist NASA in programming safe and productive missions in the near future.

REFERENCES

1. Armstrong R: Mechanisms of exercise induced delayed onset muscular soreness: A brief review. Med Sci Sports Exerc 16: 529-538, 1984.

2. Booth FW: Effect of limb immobilization on skeletal muscle. J Appl Physiol 52: 1113-1118, 1982.

3. Booth FW, Kelso JR: Effect of hind-limb immobilization on contractile and histochemical properties of skeletal muscle. Pfluegers Arch 342: 231-238, 1973.

4. Chaffin DB, Freivalds A, Evans SM: On the validity of an isometric biomechanical model of worker strengths. IIE Transactions 19: 280-288, 1987.

5. Fischbach GD, Robbins N: Changes in contractile properties of disused soleus muscles. J Physiol London 201: 305-320, 1969.

6. Friden J, Kjorell U, Thornell L: Delayed muscle soreness and cytoskeletal alterations. An immunocytological study in man. Int J Sports Med 5: 15-18, 1984.

7. Greenleaf JE: Physiological responses to prolonged bed rest and fluid immersion in humans. J Appl Physiol 57: 619-633, 1984.

8. Hasson S, Barnes W, Hunter M, Williams J: Therapeutic effect of high speed voluntary muscle contractions on muscle soreness and muscle performance. J Orthop Sports Phys Ther 10: 499-507, 1989.

9. Hasson S, Wible C, Reich M, Barnes W, Williams J: Dexamethasone iontophoresis: Effect on delayed muscle soreness and muscle function. Med Sci Sports Exerc (In Press).

10. Hasson S, Williams J, Henrich T, Gadberry W: Viewing low and high wave length light: Effect on EMG activity and force production during maximal voluntary handgrip contraction. Physiotherapy Canada 41: 32-35, 1989.

11. Hasson S, Williams J, Signorele J: Fatigue induced changes in myoelectric signal characteristics and perceived exertion. Can J Spt Sci 14: 99-102, 1989.

12. Jackson AS, Pollock ML, Graves JE, Mahar MT: Reliability and validity of bioelectrical impedance in determining body composition. J Appl Physiol 64: 529-534, 1988.

13. Keogh P, Shanker SJ, Burke T, O'Connell RJ: Bilateral simultaneous rupture of the quadriceps tendons. Clin Orthop 234: 139-141, 1988.

14. Larsen E, Lund PL: Ruptures of the extensor mechanism of the knee joint. Clin Orthop 213: 150-153, 1986.

15. Newham D, McPhail G, Mills K, Edwards R: Ultrastructural changes after concentric and eccentric contractions of human muscle. J Neurol Sci 61: 109-122, 1983.

16. Thornton WE, Rummel JA: Muscular deconditioning and its prevention in space flight. In Johnston RS, Deitlein LF (eds): Biomedical Results of Skylab. Washington, DC, US Government Printing Office, pp. 191-197, 1977.

THE DEVELOPMENT OF EXPERTISE ON AN INTELLIGENT TUTORING SYSTEM

Final Report

NASA/ASEE Summer Faculty Fellowship Program--1989

Johnson Space Center

Prepared By:	Debra Steele Johnson, Ph.D.
Academic Rank:	Assistant Professor
University & Department:	University of Houston Department of Psychology 4800 Calhoun Houston, TX 77204
NASA/JSC	
Directorate:	Mission Support
Division:	Mission Planning and Analysis
Branch:	Technology Development and Applications
Section:	Artificial Intelligence
JSC Colleague:	Robert T. Savely
Date:	August 14, 1989
Contract Number:	NGT 44-001-800

ABSTRACT

An initial examination was conducted of an Intelligent Tutoring System (ITS) developed for use in industry. The ITS, developed by NASA, simulated a satellite deployment task. More specifically, the PD (Payload Assist Module Deployment)/ICAT (Intelligent Computer Aided Training) System simulated a nominal Payload Assist Module (PAM) deployment. The development of expertise on this task was examined using three Flight Dynamics Officer (FDO) candidates who had no previous experience with this task. The results indicated that performance improved rapidly until Trial 5, followed by more gradual improvements through Trial 12. The performance dimensions measured included performance speed, actions completed, errors, help required, and display fields checked. Suggestions for further refining the software and for deciding when to expose trainees to more difficult task scenarios are discussed. Further, the results provide an initial demonstration of the effectiveness of the PD/ICAT system in training the nominal PAM deployment task and indicate the potential benefits of using ITS's for training other FDO tasks.

INTRODUCTION

Intelligent Tutoring Systems (ITS's) have been developed for a variety of tasks, ranging from geometry to LISP programming.[1] However, many of these systems have been used primarily for research purposes and have not been widely used in academic or industrial settings. An examination is needed of an ITS developed for use in an industrial setting. More specifically, an examination is needed of the development of expertise on an ITS in an industrial setting.

BACKGROUND ON PD/ICAT

Recently, an ITS was developed at NASA simulating the deployment of a specific type of satellite. Researchers at NASA developed the PD (Payload Assist Module Deployment)/ICAT (Intelligent Computer Aided Training) system.[2,3] The task selected for this ITS was unique in that it required highly specialized skills and required extensive training using traditional OJT (On the Job Training) methods. The population (i.e., FDO's) performing this task were also unique in that they tended to be well-educated and highly motivated. The PAM deployment task is one of many tasks (e.g., Ascent, Entry, Perigee Adjust, Rendezvous, IUS Deployments) performed by Flight Dynamics Officers (FDO's) working in the Mission Control Room. The training period for certifying a FDO ranges from two to four years. Due to the high costs and time required for training, researchers at NASA were charged with investigating tools to more quickly and economically train FDO's. The PAM deployment task was selected for ITS development in part because it was of moderate difficulty compared to other FDO tasks. In addition, PAM deployments were very common at that time, so training on this task was likely to be immediately useful to a FDO (although the frequency of PAM deployments has declined more recently). Moreover, the PAM deployment task had components common to several other FDO tasks, so training on this task was expected to transfer in part to performance on other FDO tasks.

The PD/ICAT system included a domain expert (i.e., an expert model), a trainee model, a training session manager, a scenario generator, and a user interface.[2] The domain expert contained information on how to perform the task. The task was described by a sequence of required and optional actions. However, it was necessary to build some flexibility into the sequence because several alternative sequences were equally acceptable for subsets of the actions. The knowledge type could be described as "flat procedural", that is, as requiring procedural knowledge without requiring subgoaling.[4] Because the PAM deployment task was a highly procedural task, the domain expert was constructed as a set of procedures. To model the trainee, the system used an overlay model and a bug library.[4] The system assumed the trainee model was similar to the expert model, but with some procedures missing. Further, the trainee model enabled the identification of incorrect procedures through the bug library. It is important to note that although the expert and trainee models were built as a set of procedures, extensive declarative knowledge was required to understand and perform those procedures. The training session manager interpreted the student's actions and reported the results in system (statement of action taken) messages or provided coaching in tutor (error, hint, or help) messages. Moreover, as recommended by other researchers,[5,6] the training session manager provided feedback at each step in the action sequence and provided different levels of help or hints depending on the frequency of specific errors. Information from the training session manager was also

incorporated into the student's performance record. Thus, the trainee model and training session manager together performed the major functions of student modelling: updating the level of student performance, providing information to the tutor, and recording student performance.[7] The training scenario generator was used to expose the student to scenarios of varying difficulty. Lastly, the user interface enabled the student to interact with the system to obtain, enter, and/or manipulate information and complete actions.

DEVELOPMENT OF EXPERTISE ON THE PD/ICAT SYSTEM

The experts identified a total of 57 actions (38 required; 19 optional) to perform the PAM deployment task. These actions were performed in sequence although some subsets of actions could be performed in varying orders. In addition, the experts identified 83 display fields to check on 8 different displays. Some actions were performed more than once (e.g., anchoring an ephemeris); similarly, some of the displays were viewed more than once (e.g., the Checkout Monitor display). Performance improvement was defined in terms of increasing performance speed, completing task actions in sequence, requiring less help, and checking displays fields identified as important by the experts. These performance dimensions provided a means for examining the development of expertise on the task. Other researchers[8,9,10] have similarly described the development of skill or expertise in terms of increasing performance speed and decreasing errors. More specifically, the declarative phase of skill acquisition involves acquiring knowledge about the task. Performance at this phase tends to be slow and error-prone. The knowledge compilation phase of skill acquisition involves using declarative knowledge to build procedures for performing the task. In this phase, performance speed increases and errors are reduced as productions are built and refined.

The purpose of the current project was to map the development of expertise on the PD/ICAT task. The data collected would provide an initial examination of how efficiently novices learned from the PD/ICAT system and enable recommendations for further refinements to the software. To accomplish this, the novices' performance on various dimensions was mapped across task trials and patterns of performance examined.

METHOD

Subjects and Procedure

Three novices performed 12 task trials on the PD/ICAT. The novices were Flight Dynamics Officer (FDO) candidates. None had previous experience with Payload Assist Module (PAM) deployments. Experience with other integrated simulation tasks ranged from a minimum of 12 hours of observing IUS (Inertial Upper Stage) Deployments to a maximum of 48 hours of observing IUS Deployments plus more than 60 hours observing and participating in other integrated simulations (e.g., Deorbit Preparation, Entry, Ascent, Perigee Adjust, Rendezvous).

Each novice agreed to work 15-20 hours on the task in approximately 3-hour blocks spaced over a few weeks. However, due to work and other constraints, each novice had a different schedule of work sessions. Also, novices performed multiple task trials in a single work session after the initial task trials (i.e., after 3 to 5 trials, depending on the novice).

Novices were asked to read the section on PAM deployments in the Spin-Stabilized Deployment section of the Procedures Manual prior to coming to their first session. At the first session novices were shown an example of the screen display and told how to use the keyboard and the mouse to enter and manipulate task information. They were asked to "think out loud" as they performed the first task trial, that is, to describe what they were doing. In addition, the novices were invited to give their comments about the task interface and to ask questions as they performed the task. Their description of their actions, comments, and questions were tape recorded. All comments on the interface and questions about the task were noted by the researcher. However, only questions about the mechanics of the task were answered. No information was provided about which actions to perform at various points in the task. The novices were also told that their comments about the interface would be discussed with the task experts and the PD/ICAT programmers. Following each session, novices were shown a computer-generated feedback report describing their performance, their comments and questions were noted, and the next work session was scheduled. They were asked to "think out loud" again for Trials 3 and 9 (Trial 8 for one subject who was available for only 11 trials). On all other trials, the novices performed the task without having their comments tape recorded. Their comments and questions were noted by the researcher, usually at the end of the task trial.

The 12 task trials were completed in 5-6 work sessions. Following the last work session, the novices were asked to complete two short, paper and pencil tests. First, novices were asked to sort a list of all task actions into the proper sequence as quickly and accurately as possible. Second, novices were asked to identify information fields on screen displays as quickly and accurately as possible. Printed copies of each screen display were provided on which novices circled or checkmarked information fields they thought they were supposed to check during the PAM deployment task. Two of the novices completed these tests 7 days after and one novice 12 days after their last work session. Finally, novices were debriefed and thanked for their participation.

Measures

Performance measures were collected by the computer during task performance. The performance measures collected for each trial were: trial time, number of actions completed, number of errors, number of help requests, and number of display fields checked. Trial time referred to the time required (in minutes) to complete a task trial. Number of actions completed referred to the number of actions (with or without errors) completed by the novice rather than by the Training Session Manager. (The PD/ICAT system was structured such that when the novices made three consecutive errors while attempting to complete an action, the Training Session Manager used the domain expert to complete the action.) Number of errors was the sum of three types of errors: the number of actions performed in an incorrect sequence, typographical errors (i.e., inputs the computer was unable to interpret), and optional (but recommended) actions which were not performed by the novice. Number of help requests was the sum of two types of help requests: the number of times novices requested more information from a tutor message following an error and the number of requests for explanations of the current or last step of the task.

Finally, number of display fields checked was the sum of the checks made on 8 unique screen displays, some viewed multiple times (see Table 1). The maximum score was 83 display checks. Data was not available for one other display (Detailed Maneuver Table 1) because the computer did not correctly record the number of

display fields checked. Viewing any display was an optional (but recommended) action. (The PD/ICAT system was structured such that configuring and viewing each display constituted two separate actions. A display could be configured without being viewed.) The recommended sequence and frequency of viewing different displays was determined by experts and incorporated into the PD/ICAT software. The Vector Comparison Display, however, was the only display not viewed as often as recommended by the experts. Rather than penalize the novices for failing to check displays fields on a display they failed to view, an average score was calculated. The score for the Vector Comparison Display was calculated as the average number of display fields checked each time the display was viewed (e.g., the score was 5 if the novice viewed the display twice and checked 4 and 6 fields on the first and second viewings, respectively).

TABLE 1.- DESCRIPTION OF SCREEN DISPLAYS AND DISPLAY CHECKS.

Display	# of Times Viewed	# of Display Fields to Check
Vector Comparison*	3	7, 6, 6
Trajectory Digitals	1	2
Checkout Monitor	4	9, 9, 9, 9
Trajectory Profile Status**	2	7, 7
Detailed Maneuver Table 2	1	7
Weight Gain/Loss Table	1	3
Supersighter	1	9
FDO Deploy Comp	1	12

*An average score was used calculated from the 3 viewing opportunities.
**Only the score for the 2nd viewing opportunity was used. Data was not correctly recorded by the computer for the 1st viewing opportunity.

Additional performance measures were collected using the paper and pencil tests administered after the task trials. Three performance measures were collected on the sorting task. Sorting time referred to the time (in minutes) required to sort the sequence of actions. Unacceptable reversals referred to the number of actions sorted in incorrect sequences. Acceptable reversals referred to the number of actions sorted in a sequence regarded by the experts as an acceptable alternate sequence of actions. Two performance measures were collected from the display checking task. Checking time referred to the time (in minutes) required to check display fields on the 8 displays listed in Table 1. Number of display checks recalled was the sum of the fields checked on these 8 displays.

RESULTS

To examine how efficiently the novices learned the PD/ICAT task, their data was plotted for each performance measure. As discussed below the data indicated rapid performance improvements until Trial 5 and more gradual further improvements

through Trial 12. A logarithmic function was used to describe the data in each measure.

As shown in Figure 1, the trial time required to perform the task decreased rapidly until Trial 5. Further performance speed improvements were more gradual. In Trial 1 only one novice completed the task and required 195 minutes. The mean trial time was approximately 46 minutes by Trial 5 and decreased to approximately 26 minutes by Trial 12. The data was described by a logarithmic function ($Y = 233.95 * X^{-.83}$, $R^2 = .87$). Interestingly, the novices who were unable to complete the task in the initial task trials demonstrated a performance pattern similar to that shown by Novice 1. Two novices failed to complete the task during the first 3-hour session, and 1 novice failed to complete the task until the third session. However, these novices demonstrated trial times similar to Novice 1 by Trial 5. Finally, the data indicates that the instruction to "think out loud" while performing the task slows performance speed. The time required to perform the task increased in Trial 3 for Novice 1, in Trial 8 for Novice 2, and in Trial 9 for Novices 1 and 3.

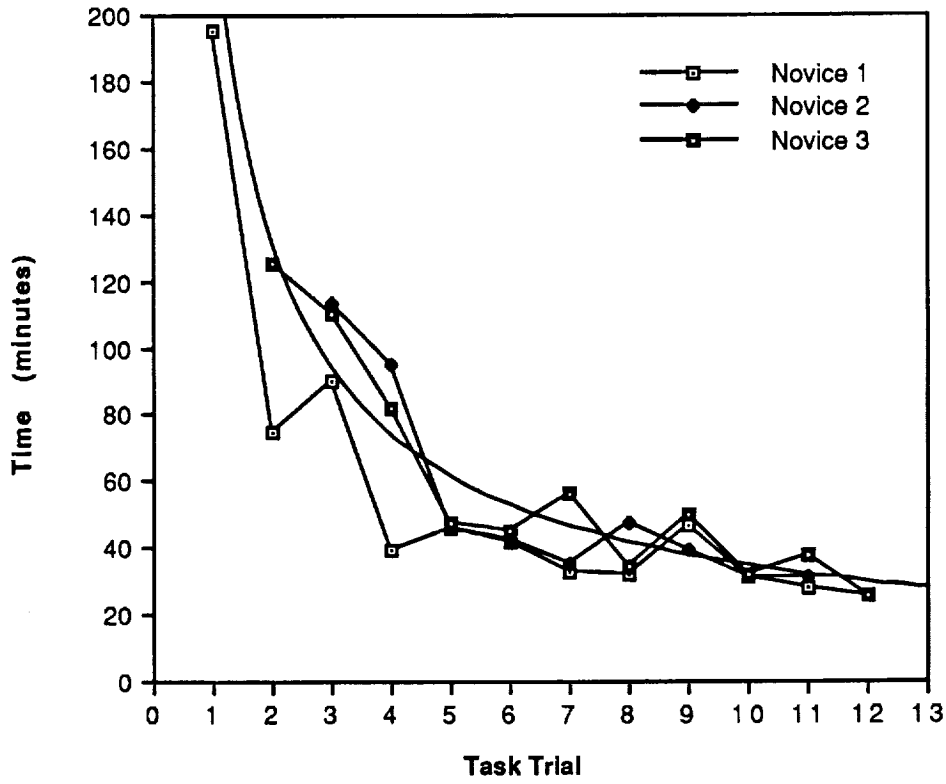

Figure 1.- Performance speed in Trials 1 through 12.

Number of actions completed also demonstrated rapid performance improvements until Trial 5 and then gradual further improvements. A logarithmic function (Y =

34.49 * $X^{.22}$) accounted for 63% of the variance (see Figure 2). In Trial 1, Novice 1 completed 43 actions out of the 57 possible actions. The remaining 14 actions were completed by the Training Session Manager, using the domain expert. Novices 2 and 3 completed only 28 and 26 actions, respectively. An additional 5 actions were completed by the Training Session Manager. Thus, Novice 1 completed 75% of the actions he attempted and Novices 2 and 3 completed 85% and 84% of the actions they attempted. However, one should note that Novices 2 and 3 completed or attempted to complete only 60% of the possible actions during Trial 1 while Novice 1 completed or attempted to complete all possible actions. The novices completed a mean of 52.33 actions in Trial 5 and a mean of 53.67 actions in Trial 12. Further, the novices completed at least 96% of the actions they attempted in Trial 5 and at least 98% in Trial 12. None of the novices attempted to complete more than 55 actions. Thus, novices chose not to perform at least 2 of the optional actions in every trial.

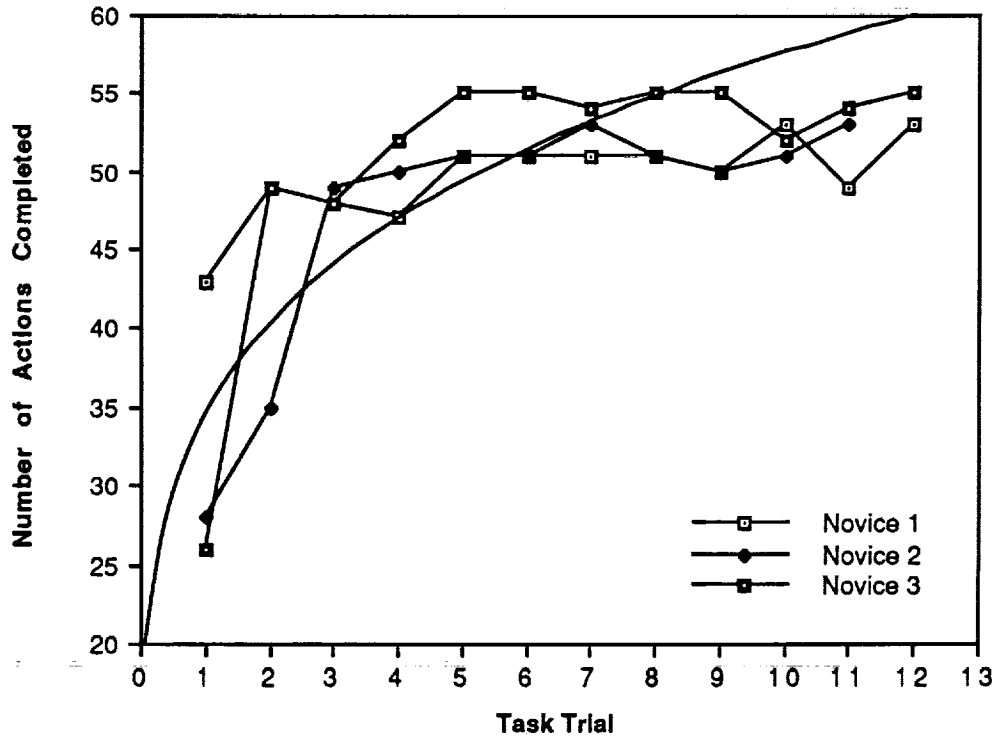

Figure 2.- Number of actions completed in Trials 1 through 12.

Number of errors demonstrated a similar pattern of performance. A logarithmic function (Y = 40.46 * $X^{-1.00}$) accounted for 69% of the variance (see Figure 3). In Trial 1, the novices made a mean of 24 errors. Novice 1, however, made .54 errors/action attempted while Novices 2 and 3 made .58 and .87 errors/action attempted, respectively. By Trial 5, the novices made a mean of 4.33 errors and

further reduced their errors to a mean of 3.5 by Trial 12. Thus, by Trial 5 the novices made a mean of only .08 errors/action attempted. By Trial 12, further performance improvements resulted in a mean of only .06 errors/action attempted.

Similar to other performance measures, number of help requests demonstrated rapid reductions from Trial 1 to Trial 5, but there were few help requests following Trial 5. A logarithmic function ($Y = 46.44 * X^{-1.58}$) accounted for 91% of the variance (see Figure 4). (Note: The data in Figure 4 reflect a transformation of [X + 1] to enable a logarithmic function to be fit. Data reported in the text are in their original, untransformed units.) However, the novices showed much greater variability in their help requests than in other performance measures, especially in Trials 1 and 2. In Trial 1, the number of help requests ranged from 7 to 32 requests. The number of help requests varied even more in Trial 2, ranging from 1 to 49 requests. By Trial 3, however, the novices made similar numbers of requests with a mean of 7.33 requests. In Trial 5, the novices made a mean of .67 help requests and only one help request was made from Trial 8 through 12.

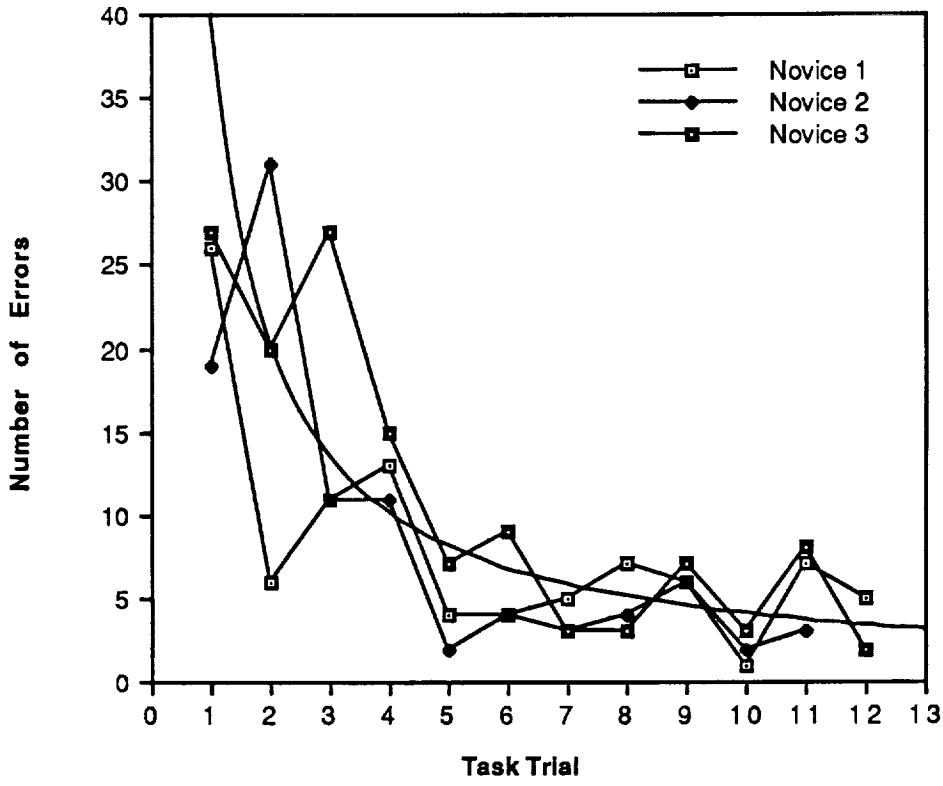

Figure 3.- Number of errors made in Trials 1 through 12.

Finally, number of display fields checked demonstrated rapid performance improvements from Trial 1 to Trial 5 and more gradual improvements through Trial

12. A logarithmic function ($Y = 25.94 * X^{-.50}$) accounted for 70% of the variance (see Figure 5). In Trial 1, the novices checked a mean of 10.33 display fields. However, only Novice 1 had the opportunity to check all 83 display fields because the other two novices did not complete the task in Trial 1. Thus, Novice 1 checked 13% of the appropriate display fields. Novice 2 checked 12% of the 34 display fields he viewed, and Novice 3 checked 59% of the 27 display fields he viewed. Although Novice 3 checked a higher percentage of display fields than the other novices, it is not clear that he understood which fields should be checked. He may have checked numerous fields because he was unsure which were important. The task software did not record checks of any display fields other than those identified as important by the experts. Thus, following Trial 1, the novices were instructed to check only those fields they considered important in each display. In Trial 5, the novices checked a mean of 69.22 fields which was 80% of the identified display fields. By Trial 12, the novices checked a mean of 79.89 fields, checking 96% of the identified fields.

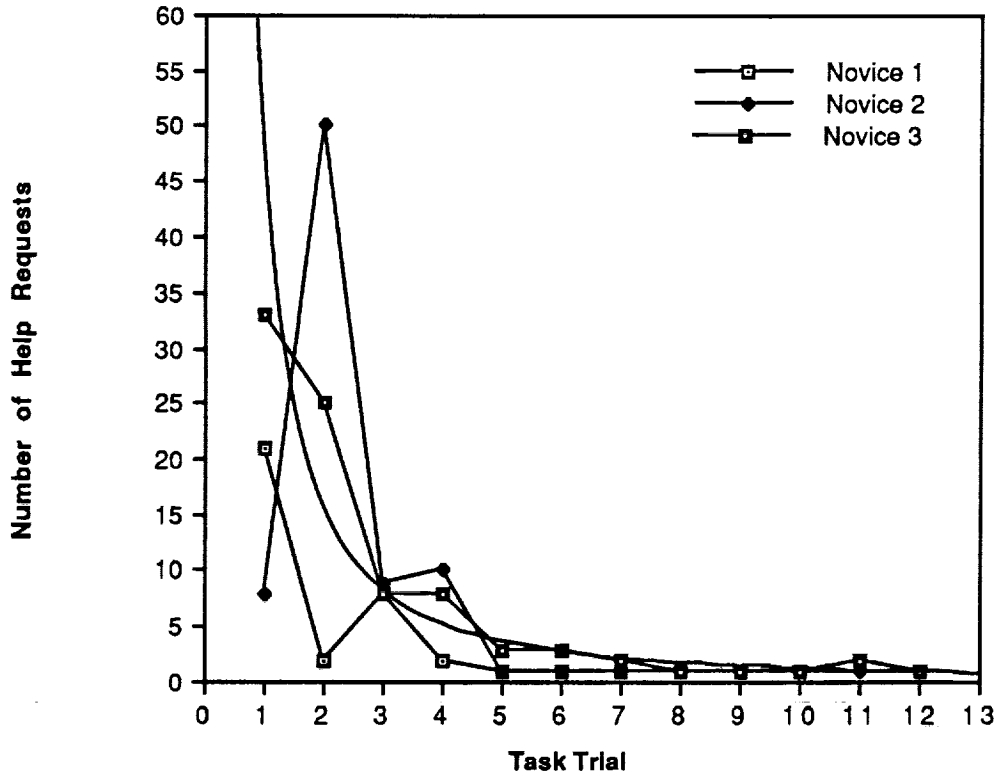

Figure 4.- Number of help requests in Trials 1 through 12.

The results from the two paper and pencil tests were examined to determine whether the novices knew the correct sequence of actions in the task and whether they knew which display fields were important to check, as identified by the experts. The

results of the sorting test indicated that Novices 2 and 3 required 17.08 and 17.92 minutes, respectively, to sort the task actions into the correct sequence. These two novices made 5 and 2 reversals, respectively, in how they sequenced the actions, but both reversals reflect alternate sequences regarded as acceptable by the experts. Novice 1 required 29.25 minutes to sort the task actions and made 4 acceptable and 3 unacceptable reversals. Of the 3 unacceptable reversals, one action was placed too soon, a second action too late, and the third action omitted from the task sequence. Thus, Novices 2 and 3 were able to correctly sort the task actions even after a 7-day delay. However, Novice 1 made 3 errors in sorting the task actions after a 12-day delay.

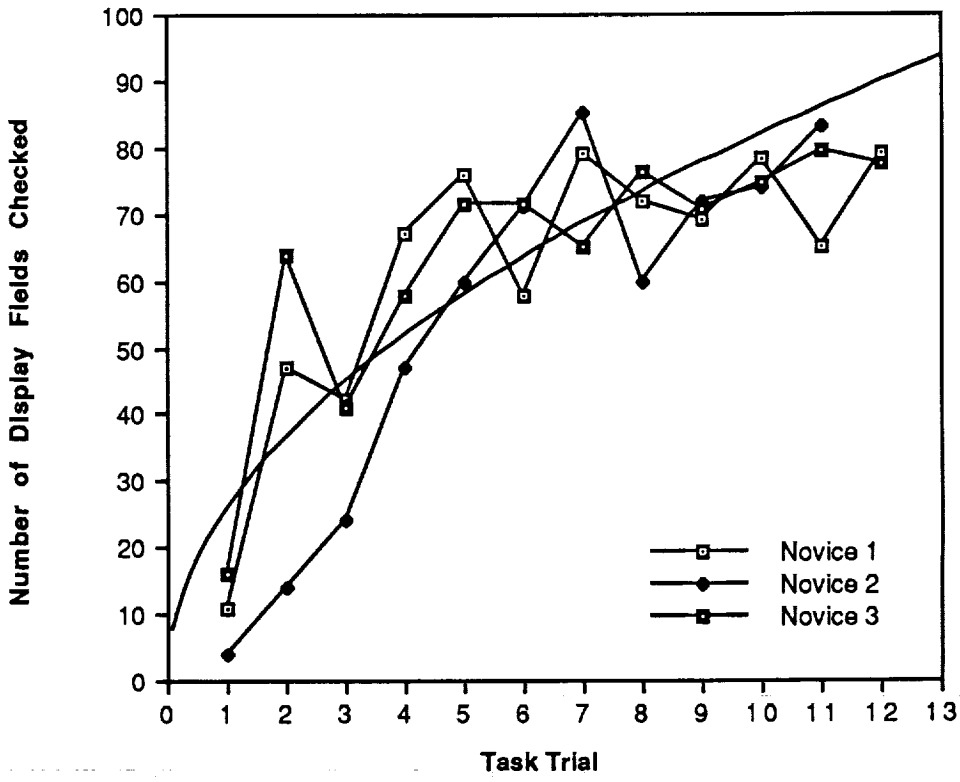

Figure 5.- Number of display fields checked in Trials 1 through 12.

The results of the display checking task indicated that the novices required between 3.18 and 6.58 minutes to complete the task. They checked between between 62 and 68 display fields, with a mean of 64.33. Of the total fields checked, between 40 and 51 (with a mean of 44.67) of the display fields were those identified as important by the experts. Thus, the novices checked 77% of the 58 identified display fields. However, the novices also checked between 17 and 22 (with a mean of 19.67) display

fields not identified as important. This indicated that 31% of the fields the novices checked were not identified as important by the experts.

DISCUSSION

The results indicated that performance improved most rapidly from Trial 1 to Trial 5 on the PD/ICAT task. Additional task trials showed smaller, more gradual improvements. This suggests that the novices had developed effective procedures for performing the task by Trial 5. Additional task trials enabled the novices to refine these procedures, increasing performance speed and decreasing errors. If the goal is to train the novices to perform this specific task version as efficiently as possible, additional practice in Trials 6 through 12 may be warranted. However, the novices performed only the nominal PAM deployment task on the PD/ICAT. They also need to learn how to deal with problems that can occur during a PAM deployment, e.g., an OMS (Orbital Maneuvering Subsystem) propellant leak. So, given the smaller improvements following Trial 5, it may be reasonable after Trial 5 to expose the novices to more problematic PAM deployment scenarios.

Prior to making this decision, though, criteria should be identified for each performance dimension. That is, one needs to identify acceptable levels of performance in terms of time (in minutes) required to complete a task trial, number of completed actions (both required and optional), number of errors made, number of help requests, and number of display fields checked. These criteria, rather than a trial number, could then be used to determine when to expose a novice to a more difficult task scenario.

The results of the two tests administered after task performance indicated that the novices were able to recall the appropriate sequence of task actions a week after performing the last task trial, although there may be some decrements in recall for delays of more than a week. Similarly, the novices recalled 77% of the display fields to check after a week delay. However, decisions also need to be made here regarding 1) how many display fields should be recalled and 2) the potential benefits or costs of checking display fields not identified as important by the experts. In the nominal PAM deployment task the novices performed, no costs were associated with checking fields other than those identified. One needs to determine under what conditions it is acceptable and perhaps even desirable to check additional display fields. Experts may need to rank order the importance of checking different displays.

Finally, a few comments on the task interface are needed. These comments are based on comments and problems reported to the researcher by the novices. First, the novices experienced difficulty in beginning the task during Trial 1. All three novices were unsure what the first step should be. Consequently they received multiple error messages and may have become frustrated. To alleviate this problem, it may be appropriate to provide novices with additional information prior to performing Trial 1. This information could be in the form of task instructions, an example of the task sequence performed by the computer as the novice observes, or perhaps step by step help in completing the task sequence in the first task trial.

Second, the novices reported that some displays should be accessible at any point in the task. The PD/ICAT task as currently designed allows the novice to request displays only at specific points in the task. The novices' report should be clarified with experts and modifications made to the software to either provide novices with greater access to displays or more explanation about why they should or should not need to view a display at a specific point in time.

Third, all three novices had difficulty interpreting the error messages provided. Further refinements of the PD/ICAT task should include improvements in the tutoring (i.e., error messages) provided.

Finally, more consideration needs to be given to the data collected from novices' task performance. Observing the novices performing the task indicated that they often attempted to perform actions out of sequence, primarily in the initial task trials. However, while the PD/ICAT software currently records whether an action has been completed and number of errors associated with that action, no record is made of the specific sequence in which the actions were attempted. Further refinements to the software should enable the recording of sequencing information. Similarly, the current PD/ICAT software records only checks of identified display fields. Thus, a possible task strategy for a novice would be to check every field in a display to ensure that the machine recorded s/he had checked the important fields. A future enhancement of the software should include recording all display fields checked and perhaps providing information to the novice on why the identified fields are important to check.

CONCLUSIONS

Novices can efficiently learn to perform the PD/ICAT task which simulates a nominal PAM deployment. Additional work is needed to more clearly identify performance criteria and expand the PD/ICAT software to include more problematic PAM deployment scenarios. Finally, refinements are needed to improve the tutoring (error messages) provided and to assist the novice in performing the first task trial. The generally positive results of this project provide an initial demonstration of the effectiveness of the PD/ICAT software in teaching novices a nominal PAM deployment task and indicates the potential benefits of future refinements and expansions of the PD/ICAT software.

REFERENCES

1. Wenger, E. (1987). Artificial Intelligence and Tutoring Systems. Los Altos, CA: Morgan Kaufmann.

2. Loftin, R. B. (1987). A General Architecture for Intelligent Training Systems. Final Report, NASA/ASEE Summer Faculty Fellowship Program, Johnson Space Center, Contract No. 44-001-800.

3. Wang, L., Baffes, P., Loftin, R. B., & Hua, G. (1989). An intelligent training system for space shuttle flight controllers. Proceedings of the 1989 Conference on Innovative Applications of Artificial Intelligence.

4. VanLehn, K. (1988). Student modelling. In M. C. Polson & J. J. Richardson (Eds.), Foundations of Intelligent Tutoring Systems. Hillsdale, NJ: Erlbaum, 55-78.

5. Burton, R. R. & Brown, J. S. (1982). An investigation of computer coaching for informal learning activities. In D. Sleeman & J. S. Brown (Eds.), Intelligent Tutoring Systems. NY: Academic Press, 79-98.

6. Reiser, B. J., Anderson, J. R., & Farrell, R. G. (1985). Dynamic student modelling in an intelligent tutor for LISP programming. Proceedings of the 9th International Joint Conference on Artificial Intelligence (Vol. 1, pp. 8-14).

7. Biegel, J. E., Interrante, L. D., Sargeant, J. M., Bagshaw, C. E., Dixon, C. M., Brooks, G. H., Sepulveda, J. A., & Lee, C. H. (1988). Input and instruction paradigms for an intelligent simulation training system. Proceedings of the 1st Florida Artificial Intelligence Research Symposium (pp. 250-253).

8. Anderson, J. R. (1985). Cognitive Psychology and its Implications (2nd Edition). NY: W. H. Freeman.

9. Chi, M. T. H., Glaser, R. , & Rees, E. Expertise in problem solving. In R. J. Sternberg (Ed.), Advances in the Psychology of Human Intelligence (Vol. 1). Hillsdale, NJ: Erlbaum, 7-76.

10. Stevens, A., Collins, A., & Goldin, S. E. (1982). Misconceptions in students' understanding. In D. Sleeman & J. S. Brown (Eds.), Intelligent Tutoring Systems. NY: Academic Press, 13-24.

NASA
National Aeronautics and Space Administration

REPORT DOCUMENTATION PAGE

1. Report No.	2. Government Accession No.	3. Recipient's Catalog No.
NASA CR 185601		

4. Title and Subtitle	5. Report Date
NASA/ASEE Summer Faculty Fellowship Program--1989 Volume 1	December 1989
	6. Performing Organization Code
7. Author(s)	8. Performing Organization Report No.
William B. Jones, Jr. and Stanley H. Goldstein, Editors	
9. Performing Organization Name and Address	10. Work Unit No.
Texas A&M University College Station, TX 77843	11. Contract or Grant No. NGT 44-001-800
12. Sponsoring Agency Name and Address	13. Type of Report and Period Covered
National Aeronautics and Space Administration Washington, D.C. 20546	Contractor Report
	14. Sponsoring Agency Code

15. Supplementary Notes

16. Abstract

The 1989 Johnson Space Center (JSC) National Aeronautics and Space Administration (NASA)/ American Society for Engineering Education (ASEE) Summer Faculty Fellowship Program was conducted by Texas A&M University and JSC. The 10-week program was operated under the auspices of the ASEE. The program at JSC, as well as the programs at other NASA Centers, was funded by the Office of University Affairs, NASA Headquarters, Washington, D.C. The objectives of the program, which began nationally in 1964 and at JSC in 1965, are (1) to further the professional knowledge of qualified engineering and science faculty members; (2) to stimulate an exchange of ideas between participants and NASA; (3) to enrich and refresh the research and teaching activities of participants' institutions; (4) to contribute to the research objective of the NASA Centers

Each faculty fellow spent at least 10 weeks at JSC engaged in a research project commensurate with his/her interests and background and worked in collaboration with a NASA /JSC colleague. This document is a compilation of the final reports on the research projects performed by the faculty fellows during the summer of 1989. Volume 1 contains reports 1 through 13, and Volume 2 contains reports 14 through 26.

17. Key Words (Suggested by Author(s))	18. Distribution Statement
	Unclassified - Unlimited

19. Security Classification (of this report)	20. Security Classification (of this page)	21. No. of pages	22. Price
Unclassified	Unclassified	338	NTIS

For sale by the National Technical Information Service, Springfield, VA 22161-2171

JSC Form 1424 (Rev Aug 89) (Ethernet Jan 88)
U.S. Government Printing Office:1989-761-014/00212